POLITECNICO DI TORINO

MASTER's Degree in
Biomedical Engineering

Politecnico
di Torino

MASTER's Degree Thesis

Computational search for putative inhibitors of MAP-tau hyperphosphorylation in Alzheimer's disease

Supervisors
Prof. Jacek Adam Tuszynski

Candidate
GIULIA NELLI

March 2023

Abstract

Alzheimer's disease (AD), which has no known cure, is currently the most common neurodegenerative disease. Since the average age of the global population is constantly rising, AD is also recognized as one of the diseases with the quickest rate of growth. The loss of memory and executive functions is a hallmark of AD. This disease is characterized by aggregation of microtubule-associated protein tau and βamyloid peptides, which are components of neurofibrillary tangles (NFTs) and amyloid plaques, respectively. It has been demonstrated that one of the primary factors contributing to the development of AD is the aggregation of the microtubule-associated protein tau (MAPT), which was found to promote microtubule instability. This aggregation originates from the hyperphosphorylation of protein tau, which reduces its ability to bind to microtubules. The aim of this study is to identify potential inhibitors useful to reduce protein tau hyperphosphorylation and prevent the progression of Alzheimer's disease. The first phase of this project involved researching the function and structure of the tau protein, with a focus on potential phosphorylation sites. Tau is phosphorylated during both healthy and pathological activities. It has been observed that protein tau has roughly 80 possible phosphorylation sites, and that over 50% of these sites are phosphorylated in the AD brain. By conducting this research, it was possible to identify the enzymes responsible to the phosphorylation of each of these sites, 17 different enzymes have been identified. After that it was possible to begin a thorough investigation into potential inhibitors useful to lowering the activity of these enzymes. As a result, each enzyme's possible inhibitors were found. The metabolites of each of these inhibitors have been identified by using the comprehensive computational tool Biotransformer (Djoumbou-Feunang et al., 2019). The focus of the study's final phase was to determine whether these inhibitors and their metabolites could inhibit the previously identified enzymes directly into the brain, due to this crucial quality, understanding how phosphorylation enzymes are expressed in various tissues and organs was essential for selecting the best inhibitors that would effectively produce the desired effect. The ability of each compound to cross the blood brain barrier was evaluated using ADMET software by analyzing the values of the BBB Filter and the LogBB, with a focus on any potential violations of Lipinski's rule of 5. The best inhibitor among those identified for each enzyme under test could be selected using the values of the elements described above. The results of this study will enable further exploration of the inhibitors' potential to prevent the hyperphosphorylation of tau protein from setting off the chain of events that results in the onset of Alzheimer's disease.

Tables of contents

Chapter 1

Alzheimer's disease

The most prevalent neurological illness in the world is Alzheimer's disease which it is also classified as one of the leading causes of death for individuals over 65. Age is the factor that contributes most to the development of AD, despite the fact that both genetic and environmental factors play a part. Given the rising average population age, Alzheimer's disease is predicted to affect an increasing number of people each year. The typical symptoms of Alzheimer's disease are memory loss in the early stages, but as the disease develops, other symptoms such as anxiety, rage, petulance, sadness, sleeplessness, and delusions start to appear. Alzheimer's Disease is characterized by loss in cerebral function as neurons begin to die. Clinical signs are seen in the brain region affected by Alzheimer's disease as a result of impaired neuronal transmission. Gross atrophy of the affected areas is the outcome of this loss, including degeneration in the temporal and parietal lobes, as well as portions of the frontal cortex and cingulate gyrus. Due to the progressive nature of this disease which leads to a severe cognitive decline, it is possible to identify four different stages of Alzheimer's disease based of the severity of the symptoms: (Calabrò et al., 2021)

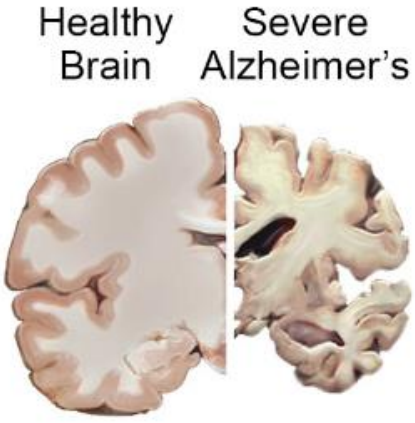

Figure 1 Comparison of slices of healthy and pathological brain. (Source: www.nia.nih.gov)

- **Preclinical**: in this phase no severe symptoms are present, the subject in this stage presents mild memory loss without a major impairment in their daily activities. The entorhinal cortex and then the hippocampus begin to undergo the first pathological changes in the brain during this stage (Calabrò et al., 2021).

- **Mild Alzheimer Disease**: cognitive signs are present throughout this stage. Combined with memory loss, there is an inability to remember new information followed by impairment in problem-solving, judgment and executive function. The

affected subjects also show personality changes, mood swings and loss of spontaneity with states of confusion and disorientation. At this point, the cerebral cortex is affected by pathological changes (Calabrò et al., 2021).

- **Moderate Alzheimer Disease**: the symptoms severity increase, the damage spreads to the areas of the brain responsible for language, reasoning and sensory processing, this leads to language disorders and impairment of visuo-spatial skills. In this phase individuals have troubles identifying their own loved ones (Calabrò et al., 2021).

- **Severe Alzheimer Disease**: The subjects entirely lost their independence during this stage. The entire cortex area has been damaged. The affected individuals' cognitive abilities decline to their lowest level, and additional systemic symptoms such as dyspraxia (difficulty performing learned motor tasks), olfactory dysfunction, sleep disturbances, and extrapyramidal motor signs like dystonia, akathisia, and parkinsonian symptoms start to manifest (Calabrò et al., 2021).

In Alzheimer's disease the development of amyloid plaques and neurofibrillary tangles seems to be the primary causes of the loss of neurons' ability to function. The amyloid plaques are extracellular formations consisting in an aggregation of amyloid-β peptides while neurofibrillary tangles are fibrillary structures in neurons formed by an aggregation of protein Tau (Stefanoska et al., 2022). These two types of aggregations have been the primary targets for defining a potential treatment for Alzheimer's since the disease was first examined. In recent years, special attention has been placed on the study of βamyloids plaques and how to prevent them, unfortunately without great success, as a result, the focus has also shifted to the investigation of the role played by protein tau in the progression of this disease (Zhang et al., 2022). Several research are currently being conducted to learn how to stop or slow down the growth of these agglomerations, and the study for this thesis is founded directly on this concept.

The role of protein Tau

A group of neurodegenerative disorders known as tauopathies are characterized by an abnormal concentration of phosphorylated tau protein in the human brain. Many

clinicopathological disorders, including Alzheimer's disease, have been linked to tauopathy. A series of post-translational changes that can be applied to tau can reduce the protein's structure, function, turnover, or even cause multimeric aggregation. These alterations also include acetylation, methylation, nitration, glycosylation, and sumoylation in addition to phosphorylation (Muralidar et al., 2020). Because post-translational phosphorylation is regarded as a defining feature of all tauopathies, it is still the change of tau that has been the subject of most of the research. One of the main factors contributing to the development of Alzheimer's disease has been identified as the protein Tau, specifically its hyperphosphorylation. Protein Tau is an intrinsically disordered protein that, by its direct interaction with tubulin dimers, is most strongly linked to the stabilization of cytoskeletal and mitotic microtubules (MTs). Microtubules are hollowed cylinders formed by the combination of α and β-tubulin heterodimers, in a roughly 1:1 ratio. They are roughly 40% identical and 63% homologous, which makes α and β-tubulin monomers quite similar to one another. There are 450 amino acid residues total in a tubulin monomer, and each one is somewhat different from the others. The cytoskeleton of the cell, which is made up primarily of micro-tubules and is crucial for intracellular movement, signaling, and cell division, is a structural component of the cell. Each tubulin protein consists of a well-defined globular domain (core) and a disorganized, negatively charged C-terminal tail (CTT), which is a target for numerous post-translational changes (PTMs) (Marien et al., n.d.). Tau plays a crucial role in controlling axon outgrowth and preserving the integrity and trafficking of axonal cytoskeleton (Giovinazzo et al., n.d.). For a long time, it was believed that Tau's only job was to keep MTs stable. Therefore, more recently, the emphasis has switched to its capacities to regulate the MTs dynamics rather than stabilize them (Limorenko & Lashuel, 2022). It is crucial to emphasize that although the protein Tau plays a healthy role in the brains, the development of this horrific disease is caused by hyperphosphorylation of the

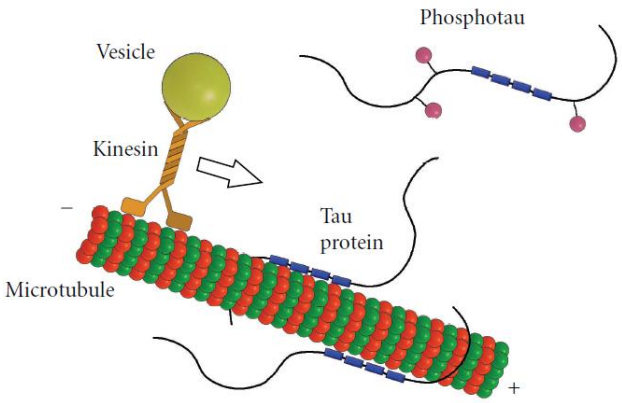

Figure 2 Normal function of tau protein. The phosphorylation of tau (pink balls) regulates its activity to bind to microtubules and can affect axonal transport (Kolarova et al. 2012) .

protein tau and subsequently aggregation of them in tangles. In healthy brains, protein Tau is bound to microtubules and has a specific amount of phosphate molecules attached to it; however, in AD brains, this system is altered, resulting in an unnatural increase in the phosphorylation. The hyperphosphorylation leads to the tau molecules' detachment from the microtubules. Altered protein Tau have a propensity to organize into paired helical filaments, which then congregate into intractable neurofibrillary tangles. This aggregation causes neurotoxicity by altering the cytoskeletal architecture, axonal transport, and mitochondrial respiration, among other ways. Transport of nutrients and other crucial chemicals inside neurons is inhibited by tau tangles. When the disease advances, they spread throughout the brain like plaques, starting close to the entorhinal cortex, moving to the hippocampus, and eventually covering the cerebral cortex (Ricci et al., 2021). Although research indicates that the tau protein plays a crucial part in the progression of Alzheimer's disease, which makes it an ideal candidate to discovery and development a drug to slow the disease's progression, the molecular and cellular mechanisms that triggers tau protein misfolding and aggregation and promote the development of tauopathies in the brain are still unknown.

Chapter 2

Tau structure

The microtubule-associated protein tau's role is to facilitate microtubule stabilization and assembly, which are regulated by the level of phosphorylation in the protein. According to gene expression data, tau expression is highest in the frontal and occipital cortices, followed by white matter, although its level is much lower in the putamen and cerebellum. Tau protein is encoded by the microtubule associated protein tau (MAPT) gene on chromosome 17 via 11 exons, which are subject to alternative splicing of exons 2, 3, and 10 (Kolarova et al., 2012; Limorenko & Lashuel, 2022). Exon 2 and exon 3 encode two distinct 29 aminoacid N-terminal domains; their presence or absence determines whether the isoform is 0N, 1N, or 2N. Exon 10 specifies the alternate splicing of the second microtubule-associated binding repeat (MTBR), which distinguishes between the 3R and 4R tau isoforms. 3R tau isoforms contain the first, third, and fourth MTBR, while 4R tau isoforms contain all four MTBR. The inclusion or absence of these exons results in six main isoforms of tau: 0N3R, 1N3R, 2N3R, 0N4R, 1N4R and 2N4R (Xia et al., 2021). The expression levels of the six major tau isoforms differs considerably in the adult human brain: ~40% of all isoforms are 0N isoforms, ~50% are 1N isoforms, and ~10% are 2N isoforms. In the brain, expression of the 3R and 4R isoforms is roughly equal. The ratio of protein tau isoforms containing 3 or 4 MT-binding repeats is disturbed in individuals diagnosed with Alzheimer's disease(Limorenko & Lashuel, 2022; Xia et al., 2021), which is known as a 3R+4R tauopathy (Zhang et al., 2022). The six isoforms will consequently also have various length, with the shortest (0N3R) consisting in 352 amino acids and the longest (2N4R) being 441 amino acids long.

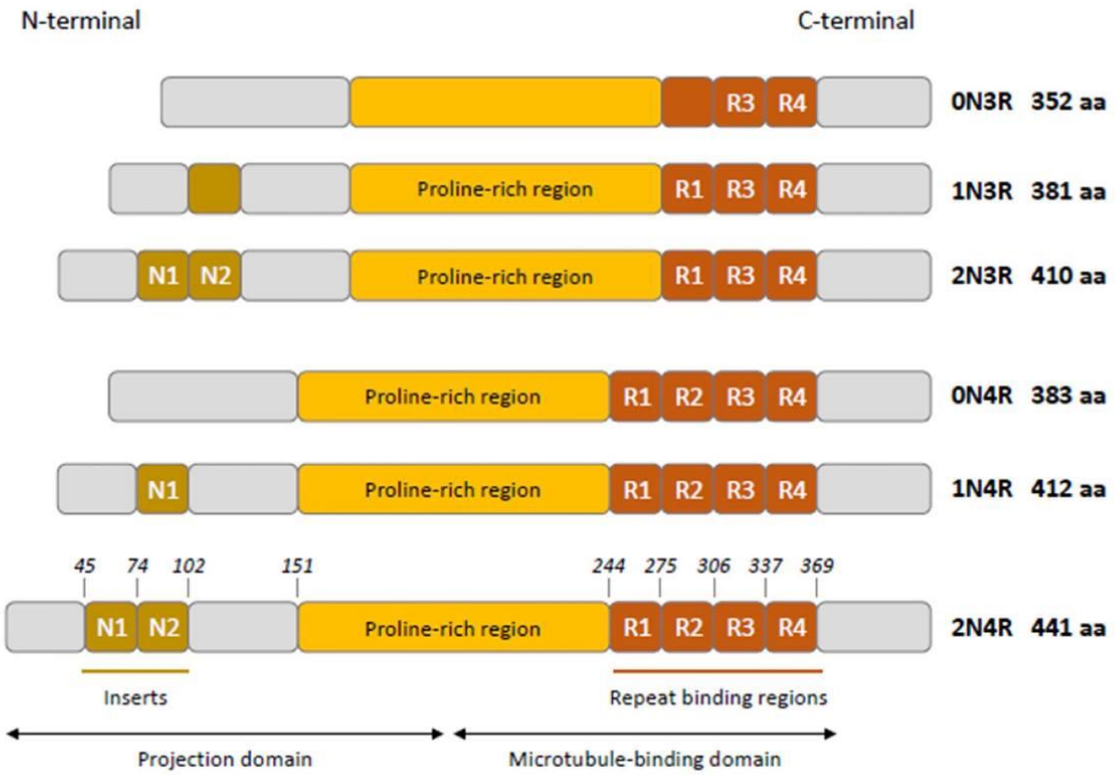

Figure 3. Schematic representation of tau isoforms in human adult brain (Duquette et al. 2012).

Full-length tau is a dipole with distinct domains that have the opposing charge at physiological pH. Its proline-rich domain (pI = 10.3) and the microtubule-binding domain (MBD) (pI = 9.8) are positively charged, whereas its acidic N-terminal domain (pI = 4.0) is negatively charged (Rogowski et al., 2021). The MTBR is typically positively charged to facilitate the interaction with microtubules that are naturally negatively charged, which is desirable because the primary function of the tau protein is to bind to microtubules. The tau protein's negative charge increases upon phosphorylation, which weakens the protein's bond with microtubules. Tau can become phosphorylated at particular sites as a result of imbalances in tau kinase and phosphatase activity, which increases tau's propensity to separate from microtubules. The formation of bigger protein aggregates, filament assembly, and bundling of paired helical filaments (PHF) into neurofibrillary tangles (NFT), can result in cellular neurotoxicity, all of which are more likely to occur when tau is abnormally dissociated.

Tau phosphorylation site

The phosphorylation of tau is present in both physiological and pathological processes, as was previously noted in the section concerning the role of protein Tau. It is yet unknown what mechanism causes protein tau to become hyperphosphorylated (Tan et al., 2021). On its longest isoform (441 amino acids), protein tau was reported to include roughly 80 possible serine, threonine, or tyrosine phosphorylation sites. The predominance of these phosphorylation sites is found in the proline-rich region and C-terminal extremity, close to the microtubule binding region (MTBR). In healthy conditions at least 30 tau phosphorylation sites have been reported, in contrast to the AD brain where approximately 45 phosphorylated sites have been identified, meaning that almost 50% of all phosphorylable residues have been phosphorylated. By examining the phosphorylation sites of full-length tau, researchers identified two phosphorylation clusters at the start of the second and third repetition domains of the Microtubule-binding domain, two hexapeptides, 275VQIINK280 and 306VQIVYK311, which are known to be involved in the formation of the β-sheet structure during tau aggregation (Cehlar et al., 2021; Song et al., 2021). In the early stages of AD, tau phosphorylation causes this particular domain's overall charge to flip from positive to negative. Phosphorylation of C-terminal residues tend to increase tau's aggregation, while additions of negative-charge bulky phospho-groups to the N-terminal domain or MTBR tend to decrease it. Mid-domain phosphorylation, on the other hand, tendS39 to be highly context-dependent when it comes to modulating tau's aggregation. The majority of the possible sites have been found close to the MTBR in the proline-rich region and at the C-terminal end of the tau protein molecule. These discrepancies in phosphorylation sites between the C-terminal and N-terminal imply that the regulation of MT binding considerably depends on the location of the phosphorylation site it self. It is essential to recall that the sum of many phosphorylation sites influences tau's bidirectional control of the physiologic MT regulation. As afore mentioned, the tau protein contains phosphorylation sites throughout all of it, but they are particularly concentrated between the C-terminal and the N-terminal. The placement of the site is crucial, since it determines what will cause the tau protein to be phosphorylated. The phosphorylation sites' locations and associated functions are shown in the examples below. S262, S293, S324 and S356, which are found on the R1, R2, R3 and R4 domains, are examples of phosphorylation sites that are

not a part of Proline-rich region and C-terminal. The N-terminal phosphorylation sites T175/T176/T181 mostly prevent tau aggregation. Moreover, the proline-rich region contains three phosphorylation sites, S202/T205/S208, that are sufficient to cause tau self-aggregation without the use of an exogenous aggregation inducer (Song et al., 2021). S422 tau protein exhibits a strong effect on aggregation, which may be related to the conversion of tau monomer from inert to seed-competent form because of increased accessibility of these residues. S422 tau protein exhibited increased aggregation in the presence of both metal ions and heparin inducers. All brain regions showed enhanced oligomerization in response to specific phosphorylation events (S198, S199, and S416), suggesting that phospho-sites control tau aggregation as AD neurodegeneration progresses(Song et al., 2021). All five tyrosine residues, three N-terminal residues (Y18, Y29, and Y197), or just one tyrosine residue (Y310) in the MTBR were phosphorylated, and this significantly decreased Tau aggregation. Another analysis revealed that full-length Tau easily produced fibrils in vitro when the mid-domain residues S202, T205, and S208 were hyperphosphorylated by kinases, but not S262. Tau's ability to aggregate was only slightly boosted by the phosphorylation of the mid-domain area residues T181, S199, S202, T205, T212, S214, T217, T231, or S262. It was discovered that increasing cAS”CDKTau aggregation by changing serines to glutamines mimicked phosphorylation at sites S396 and S404. In vitro Tau aggregation was significantly boosted by the enzymatic phosphorylation of C-terminal residues S396, S404, S409, or S422 alone or in combination with the mid-domain residues. According to other research, tau phosphorylation at T231 or S262 can actually prevent MT interactions from happening (Xia et al., 2021). Increased MT binding results from site-specific tau phosphorylation at other sites, such as S208, which suggests that the phosphorylation site plays a key role in controlling MT binding. In addition to microtubules binding, tau's capacity to encourage MT assembly and control MT dynamic stability can be diminished by phosphorylation at T231, S262, S396, or S404 (Xia et al., 2021). Axonal transport can be impacted by the effects of MT modulation since tau phosphorylation at Y18 regulates tau's inhibition of motor proteins like kinesin-1 and is generally a protective mechanism that encourages normal axonal trafficking. On the other hand, S422 phosphorylation has a general inhibitory effect on both anterograde and retrograde axonal transit. The propensity for phosphorylation at T231, S235, and S262 in tau from AD brains appears to be correlated with clinical AD progression (Wegmann et al.,

2021). It is possible to detect large amounts of basal phosphorylation of tau at a number of locations, especially S262, S356, and S396, that most likely controls physiologic tau-tubulin interaction and tau protein localisation (Bao et al., 2021). Yet, it has been discovered that some tau phosphorylation sites are substantially enriched in disease but absent throughout brain development or in people with cognitively normal aging. Particularly, the fetal brain and cognitively healthy adults lack phosphorylation of tau at S422 almost entirely. Early on, in the development of AD, significant increases in tau phosphorylation at S422 are recorded, and the loss of cholinergic neurons and cognitive decline are correlated with the number of tau-S422-immunopositive neurons (Bao et al., 2021). Determining the kinases responsible for tau's pathological S422 phosphorylation may therefore help find prottbkmising treatment targets.

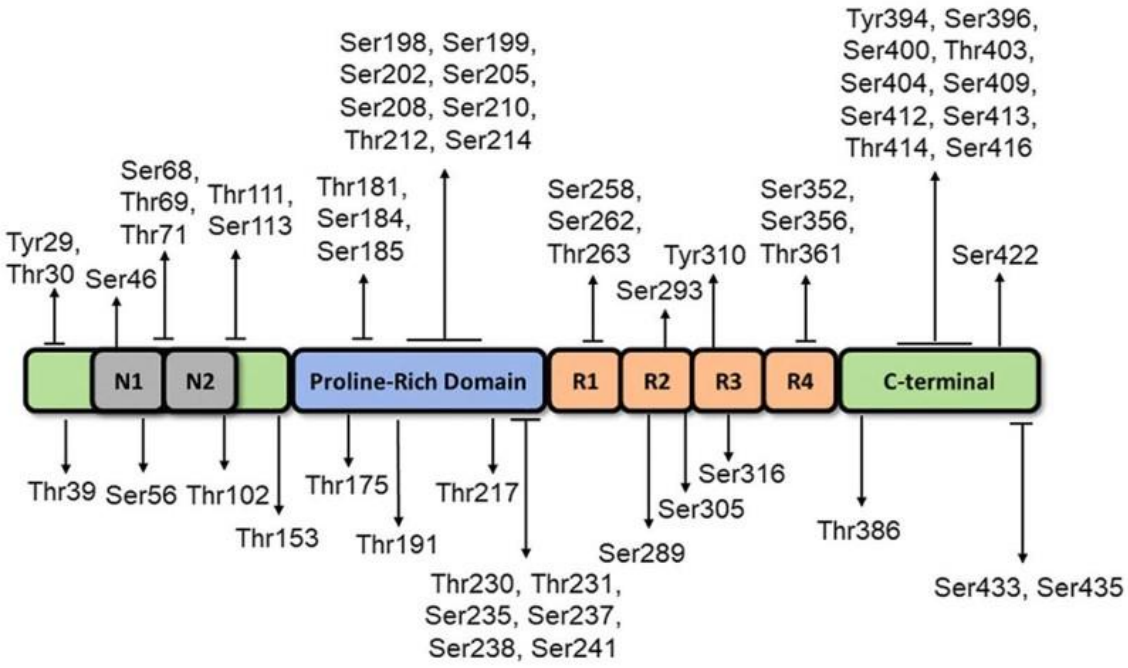

Figure 4 Schematic representation of phosphorylation sites of protein tau (Xia et al. 2021).

As was already explained in the study, the phosphorylation of tau is a healthy process, but when it becomes excessive and leads to hyperphosphorylation and a pathological condition can be identified. According to these two situations, it is possible to classify the phosphorylation sites in four different categories as it is shown on the next table (Martin et al., 2013).

Table 1 List of each phosphorylation sites found in healty brain and AD brain.

Sites only found in AD brains	Sites found in AD and control brains	Sites found in physiologic conditions	Putative sites
Y18	S46	T17	T30
S68	T181	Y29	S61
T69	S198	T39	T63
T71	S199	T50	S64
S113	S202	T52	T76
T123	T205	S56	S129
T153	T212	T95	S137
T175	T217	T101	Y310
T184	T231	T102	T319
S185	S235	T111	T377
S191	S396	S131	
Y197	S400	T135	
S208	S404	T149	
S210	S412	T169	
S214	S413	S195	
S237	S416	T220	
S238		S241	
S258		T245	
S262		T263	
S289		S285	
S356		S293	
Y394		S305	
T403		S316	
S409		S320	
S422		S324	
T427		S341	
S433		S352	
S435		T361	
		T373	
		T386	
		T414	

Chapter 3

Tau phosphorylation is regulated by a delicate balance between tau kinase and phosphatase activities, abnormal tau phosphorylation and subsequent aggregation in Alzheimer's disease might result from upregulated tau kinases or downregulated tau phosphatases, but these two possibilities are not mutually exclusive. Kinases are members of the enzyme class known as "transferases", since they transfer the phosphate group from high-energy donor molecules, like ATP or GTP, to specified substrates (Martin et al., 2013). All kinases share a common catalytic center, which is where the phosphorylation event takes place. Its functionally active region has a fixing site where is kept the substrate to be phosphorylated and an ATP/GTP binding pocket. Phosphate transfer takes place when the energy donor and the substrate are attached to the kinase. A phosphate group is retained in some kinases' autoregulation loops so they can function without an energy source. The regulation of kinase activity can take place through post-translational modifications like phosphorylation (provided by ATP or GTP), interaction of the kinase catalytic subunit with other molecules or other subunits (for multimeric kinases), which can modify the kinase's specificity, and by kinase distribution intracellularly (according to its localization in the cell a kinase can exert different effects). One of the methods for reversing tau phosphorylation is to inhibit particular tau kinases. There are three primary kinds of protein kinases (PKs) that phosphorylate tau: proline-directed protein kinase (PDPK), non-proline directed protein kinase (NonPDPK), and tyrosine protein kinases (TPK) (Muralidar et al., 2020). As an alternative method for lowering tau phosphorylation, protein phosphatase activation has also been suggested, particularly in the context of the critical brain tau phosphatase (PP2A). Yet, because PP2A contains several regulatory subunits and a wide range of substrate specificities, it is challenging to target the right group at the right time and place (Yadikar et al., 2020). The distribution of an enzyme is essential for determining whether it is a reasonable target for this study. The distributions of the enzymes in question have been obtained by consulting the website *"The human protein Atlas"*. Thanks to the *"Protein Data Bank"* (PDB) it was possible to determine whether or not the crystalline structures of the enzymes under study are currently known. Additionally, research was done on the website *"Kegg-Pathways"* for

each enzyme to determine how involved they were in other physiological processes. The following paragraphs show the identified crystalline structures.

CaMKII

CaMKII is a non-proline-directed protein kinase. It is composed of 4 isozymes: α, β, γ and δ. CaMKII is activated as a result of calcium/calmodulin interaction, which encourages autophosphorylation at threonine 286 for the α subunit and at threonine 287 for the β, γ and δ subunits (Martin et al., 2013). N-methyl-daspartic acid (NMDA) receptor is binded by CaMKII that has been phosphorylated at threonine (which is targeted by memantine). Threonine 306 and 307 have inhibitory phosphorylation sites that prevent calcium/calmodulin binding. Serines 131, 214, 262, 356, 416 and threonines 135, 212 are the locations where CaMKII phosphorylates tau, however five of these sites are observed to be phosphorylated in AD brains (Martin et al., 2013). CaMKII is expressed in neurons with NFT in AD brains. These findings imply that CaMKII inhibitors might be useful in the creation of AD treatment options. The CaMKII enzyme is widely distributed throughout the body's tissues and organs. It is widely present in the brain, but it is also found in the endocrine tissue, the respiratory system, the digestive tract, the liver, the kidneys and the bladder, in male and female tissues and in smaller amounts in muscles, close to the digestive tract, in bone marrow and in lymphoid tissues.

Figure 5 Crystal structur of human CaMKII (Source:PDB)

CDK5

CDK5 is a proline-directed protein kinase (PDPK). CDK5 works with its co-activator named p39/p35 and p29/p25. The monomeric form of CDK5 is inactive as an enzyme without this interaction. P39 shares around 57% of homology with p35 and is expressed during fetal development. When p35 is expressed, p39's expression gradually declines. CDK5 activity is only present in neurons as a result of the nervous system-specific

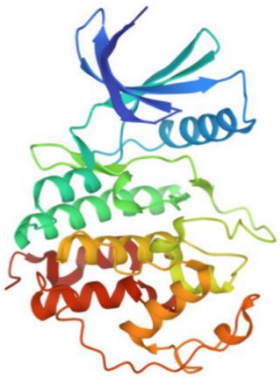

Figure 6 Crystal structure of human CDK5 (Source:PDB)

distribution of its activators, p35 and p39 (Martin et al., 2013). The central nervous system (CNS) development depends on CK5, which also controls synaptic functions, neuritic outgrowth, vesicular transport, and the dynamic cytoskeleton of neurons. CDK5 is controlled by the inhibitory phosphorylation of threonine 14 and serine 159, and the activating phosphorylation of tyrosine 15. C-Abelson (c-Abl), which connects CDK5 and c-Abl, targets tyrosine 15 for phosphorylation, and c-Abl-binding adaptor protein (Cables) amplifies this process. To stop the development of the CDK5/p25 hyperactive complex, CDK5 phosphorylates p35 at serine 8 and threonine 138. This inhibits the conversion of p35 to p25. The more stable proteins p25 and p29 are created by the proteolytic processing of the proteins p35 and p39 by calcium-dependent calpains. The CDK5/p25 complex, the most active version of CDK5, has the power to accelerate tau phosphorylation and cause neurodegeneration. In the brain of people with AD, all 11 of the sites on tau that CDK5 phosphorylates are found to be phosphorylated. The p25/p35 ratio and level of the hyperactive complex CDK5/p25 are both elevated in AD brains. These studies show that CDK5 is a potentially effective treatment target for AD (Martin et al., 2013). The body's CDK5 enzyme is found in a variety of tissues and organs, with the brain and male tissues having the highest concentrations of it. It is also found in smaller amounts in the endocrine system, the respiratory system, the gastrointestinal tract, the liver, the pancreas, the kidneys and bladder, on female tissues, close to the digestive tract, the skin, bone marrow and non-lymphoid tissues. CDK5 is involved in four different pathways, in particular on: Alzheimer's disease, axon guidance, cocaine addiction and pathways of neurodegeneration (multiple disease).

CK1α-1δ-1ε-2

CK1 and CK2 are non-proline-directed protein kinases (non-PDPK). CK1 has 7 isoforms but only α/δ/ε isoforms are involved in AD. By kinase activity, CK1 and CK2 control the microtubule dynamics. In AD brains, 25 of the 46 tau phosphorylation sites that CK1/2 phosphorylates are observed to be phosphorylated. Because of their numerous phosphorylation sites, CK1/2 are potential therapeutic targets for the treatment of AD

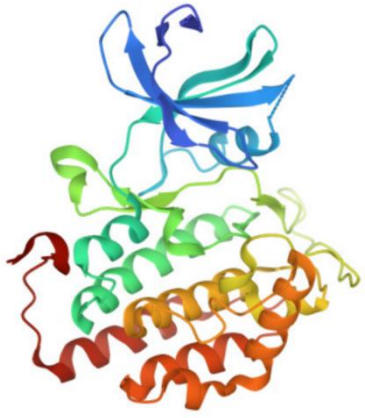

Figure 7 Crystal structure of human CK1ε (Source:PDB)

(Martin et al., 2013). Casein kinases control pathways involved in apoptosis and survival. Fas/CD95-induced apoptosis is accelerated by inhibiting the CK1α, δ and CK2 isoforms. CK1 and CK2 are members of the Wnt/ β-catenin pathway, but only CK1α/1δ/1ε isoforms phosphorylate -catenin at serine 45, encouraging its movement into the nucleus and, consequently, the transcription of genes essential for cell survival. This phosphorylation at serine 45 is required for GSK3β to prime β-catenin by phosphorylating it at threonine 41, serine 37, and serine 33. CK1 co-localizes with NFT in AD brains, and levels of all CK1 isoforms are elevated (Martin et al., 2013). The distribution of the various CK1 and CK2 isoforms is not uniform; it has been discovered that δ isoform and CK2 are significantly expressed in the brain while α and ε isoforms are only moderately expressed. These enzymes are all widely expressed throughout the body in general. CK2 and the isoforms of CK1 are involved in various pathways, but in humans, these are primarily associated in the pathways of Alzheimer's and other neurodegenerative diseases.

DYRK1A/2

DYRK1A and DYRK2 are non-proline-directed protein kinases. Among 6 isoforms of DYRK, only DYRK1A and DYRK2 seem to be involved in AD. The only gene responsible for encoding DYRK1A is found in the 21q22.2 locus, which is part of the crucial portion of chromosome 21 associated with Down syndrome. As the majority of Down syndrome patients acquire SP and NFT, this may be pertinent to AD (Martin et al., 2013). Tau and the transcription factor cAMP Response Element Binding (CREB), which are important in learning and memory neural processes, are phosphorylated by DYRK1A and DYRK2 (AD patients develop memory loss). Their autophosphorylation is self-catalyzed by DYRK within an autoregulation loop at the YXY motif of the catalytic domain. DYRK behave as serine/threonine kinases after this autophosphorylation. The serine 202, threonine 212, and serine 404 sites on tau are phosphorylated by DYRK1A overexpression in vitro and in a

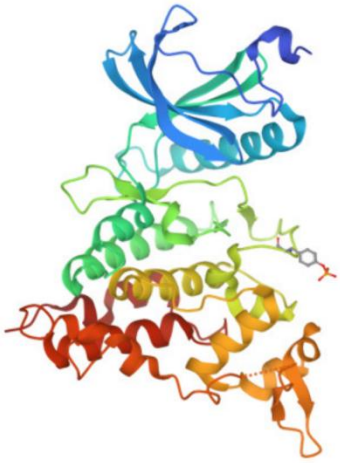

Figure 8 Crystal strucutre of human DYRK1A (Source:PDB)

transgenic mouse model, and all of these sites were discovered to be phosphorylated in AD brains. Tau phosphorylation by DYRK1A or DYRK2 at threonine 212 may start at serine 208 by GSK3 (by the priming process). Instead, DYRK1A promotes tau exon 10 alternative splicing, which is known to control the proportion of cells that enter apoptosis. The response to DNA damage is the only function of DYRK2 in apoptosis. DYRK1A mRNA levels are elevated in AD brains. The treatment of AD and Down syndrome may both benefit greatly from DYRK, or at the very least DYRK1A, targeting (Martin et al., 2013). The protein expression levels of the two isoforms, DYRK1A and DYRK2, in the brain are both approximately moderate. Both enzymes are commonly distributed throughout the body, with a higher degree of expression in the kidneys, liver, female tissues, bone marrow, and lymphoid tissues, near the digestive tract and at the level of the gastrointestinal tract.

ERK1/2

ERK1/2 is a proline-directed protein kinase (PDPK). ERK1/2 isoforms control cell division, growth, proliferation, and apoptotic cell death. They share 83% homology. Dual phosphorylation of threonine 202 and tyrosine 204 for Erk1 and threonine 184 and tyrosine 186 for ERK2 activates ERK1/2. The prolyl-isomerization site on tau is one of the 16 places where Erk1/2 phosphorylates tau; serines from the R1-R4 domains are excluded. 15 phosphorylated locations on tau are phosphorylated by ERK1/2 in AD brains. It's interesting to note that the cytoskeleton toxin paclitaxel, which is also used as an anticancer medication, causes ERK activation, tau phosphorylation, and then apoptosis. ERK1/2 activity is elevated in AD brains with aberrant tau phosphorylation. ERK may play a role in the pathophysiology of AD and may be a useful treatment target for AD, but still, because it is implicated across several different pathways, it is challenging to identify a drug that is effective exclusively for AD. The two isoforms of ERK, ERK1 and ERK2, are both widely expressed in the brain, as well as in the digestive system, the pancreas, the kidneys and the bladder, in female and male tissues, connective tissues, bone marrow and lymphoid tissues.

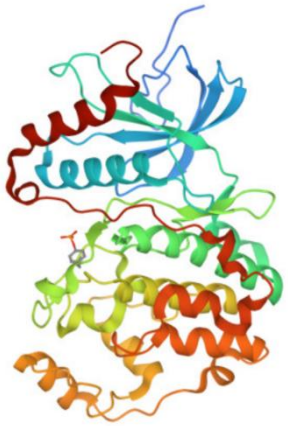

Figure 9 Crystal structure of human ERK1 (Source:PDB)

GSK3β

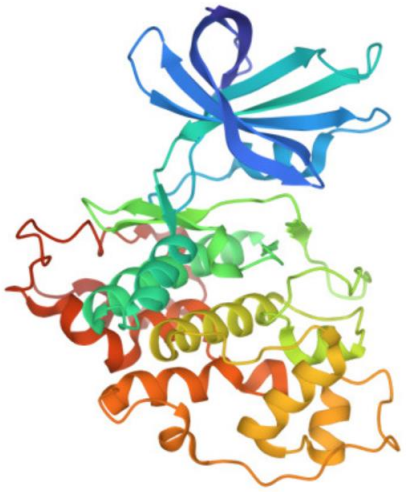

Figure 10 Crystal structure of human GSK3β (Source:PDB)

GSK3β is a proline-directed protein kinase (PDPK). Although two Glycogen Synthase Kinase-3 isoforms α and β are encoded by different genes, they share about 85% sequence homology. Alternative GSK3β isoform splicing of exon 8A generates two isoforms β1 and β2 differing by the presence of 13 amino acid insert between leucine 303 and valine 304 in β2 isoform. β2 isoform accounts only for 15% of total GSK3β and displays a reduced activity on tau phosphorylation compared to the β1 isoform. β2 isoform is found in neuronal soma while β1 isoform is found both in neuronal soma and in axons (Martin et al., 2013). GSK3 was initially discovered as a player in the glycogen metabolism. GSK3 has also been linked to oncogenesis, brain processes, cell proliferation, embryonic development, apoptosis, and immune response pathways. GSK3β can phosphorylate at least 26 Tau residues between serine and threonine. For the GSK3 isoform, phosphorylation at serine 21 (for GSK3α isoform) and at serine residues 9 and 389 (for GSK3β isoform) decreases GSK3 activity, whereas phosphorylation at tyrosine 279 (for GSK3α isoform) and tyrosine 216 (for GSK3β isoform) increases GSK3 activity. Protein kinases such as protein kinase cAMP-dependent (PKA), protein kinase B (PKB), protein kinase C (PKC), p70S6K/p85S6 kinase, and p90-ribosomal S6 kinase can all catalyze the phosphorylation of GSK3. Both Akt/PKB and MAPK (p38 and Erk1/2) cause the activation of P70S6K/p85S6 kinase and p90-ribosomal S6 kinase, respectively (Martin et al., 2013). A process known as "substrate priming," which is carried out by priming kinases, is required for a substrate to be effectively phosphorylated by GSK3 at a location 4 amino acids upstream of the phosphorylation site targeted by GSK3. Tau is a superior substrate for GSK3β after substrate priming. Only two proteins are exempt from priming: axin and β-catenin. GSK3β phosphorylates tau at 42 different sites, and AD brains include phosphorylation at 29 of those sites. Lithium, a GSK3β inhibitor, reverses both processes caused by tau hyperphosphorylation and neurodegeneration in transgenic

mice with overexpressed GSK3. Moreover, GSK3β overexpression results in apoptotic cell death in cell lines, indicating that tau phosphorylation by GSK3β can be harmful. GSK3β has recently been shown to play a crucial function in AD. Many pieces of evidence show that GSK3, particularly GSK3β, connects Aβ to tau disease. A peptide promotes GSK3β activity, tau phosphorylation, and apoptotic neuronal death in cultured rat hippocampus neurons. Increased GSK3β activity has been shown to contribute to memory impairment, tau hyperphosphorylation, hippocampal neurodegeneration, inflammatory response, increased production of Aβ, and decreased acetylcholine synthesis in animal models (a cholinergic deficit is observed in AD) (Martin et al., 2013). It is interesting to note that tau proteins mediate the learning deficits and hippocampus atrophy caused by GSK3. GSK3β co-localizes with NFT in AD patients, and the frontal cortex of AD brains include more active GSK3β (phosphorylated at tyrosine 216). GSK3β is a prospective therapeutic target for tauopathies like AD because of the rise in GSK3β activity in AD brains and its role in the acceleration of tau pathology. The enzyme GSK3β is expressed on average in the brain, although it is more abundantly expressed in the gastrointestinal system, the kidneys and bladder, male tissue, bone marrow, and lymphoid tissues.

JNK

c-Jun N-terminal kinases (JNK) is a Proline Directed Protein Kinases. JNK are expressed in the brain, where protein kinases like MKK4 or MKK7 can activate them while protein phosphatases like mitogen-activated protein phosphatases can inhibit them (MAPP). In AD brains, JNK phosphorylates tau at all 12 of its phosphorylation sites (Martin et al., 2013). JNK controls apoptosis in response to several stresses, including exposure to ultraviolet light, ionizing radiation, anticancer medications (such as cisplatin and etoposide), cytokines, and a lack of nerve growth factor (NGF). It is interesting to note that JNK, like p38, is activated after the cytoskeleton is disrupted, which induces apoptotic cell death. Activated and phosphorylated JNK are redistributed in the cell and co-localized with hyperphosphorylated tau proteins as AD

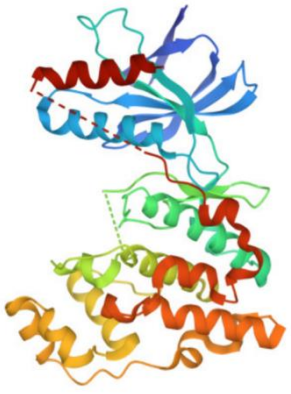

Figure 11 Crystal structure of human JNK (Source:PDB)

progresses. In AD, JNK are found in tau aggregation. A possible function for JNK in SP formation is suggested by the fact that activated JNK are also engaged in enhanced γ-secretase activity that results in Aβ buildup. JNK inhibition may therefore be a method of neuroprotection against AD (Martin et al., 2013). JNK are average expressed in the brain, but more heavily expressed in the gastrointestinal tract and in female tissue. It's crucial to remember that JNK participates in numerous distinct pathways.

P38

P38 is a proline-directed protein kinase. Under physiological circumstances, cytokine exposure or extracellular stress results in the dual phosphorylation of the TGY motif, which activates the p38 protein. P38's autophosphorylation also causes it to become active. At 21 potential tau phosphorylation sites, P38 phosphorylates tau. In the brains of AD patients, 15 of these sites, including S356 in the R4 domain and threonine 231, the location of tau prolyl-isomerization are phosphorylated. P38 also phosphorylates p53 and GSK3β in addition to tau (phosphorylation at serine 389) (Martin et al., 2013). P38 plays a role in oxidative, environmental, or chemical stress-induced apoptosis. It's interesting to note that cytoskeleton destabilization or Aβ causes p38 to become active during apoptotic cell death. The inflammatory response linked to AD may be mediated by P38. The p38 active form also co-localizes with NFT in AD brains. These results pointed to a potential role for p38 in the development of AD and imply that preventing tau pathology by inducing neuronal cell death may be an effective treatment for the disease (Martin et al., 2013). The enzyme P38 is highly expressed at the level of the brain, as well as in the gastrointestinal tract, liver, kidneys and bladder.

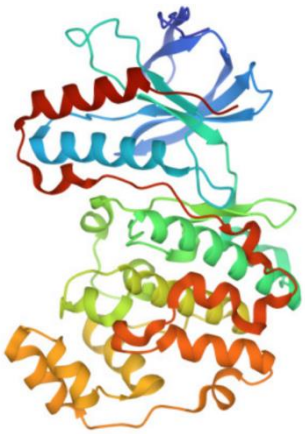

Figure 12 Crystal structure of human P38 (Source:PDB)

PKA

PKA is a non-proline-directed protein kinase. The tetrameric enzyme, PKA consists of two regulatory and two catalytic subunits. The terms R1α, R2α, R1β, and R2β refer to the four regulatory subunits, respectively (Martin et al., 2013). Intracellular cAMP stimulates the activation of PKA complexes. PKA substrates include Akt/PKB, PKC, tau, and GSK3 (inhibitory phosphorylation sites are at serine 21 and serine 9 for and α and β isoforms, respectively). A pro-apoptotic kinase is PKA. Adenylate cyclase activator forskolin causes tau hyperphosphorylation and impairs spatial memory. Tau becomes a more favorable substrate for GSK3 after PKA phosphorylates it (probably by promoting priming). 17 of the 25 tau sites phosphorylated by PKA that are targeted in AD brains. PKA catalytic subunit KO in Drosophila melanogaster impairs memory performance without affecting longevity. PKA proteins are active and co-localized in NFT in AD brains (Martin et al., 2013). PKA might therefore be considered a therapeutic target for AD. The brain and male tissues have a significant level of PKA expression, while the remaining tissues and organs have a moderate level of this protein expression.

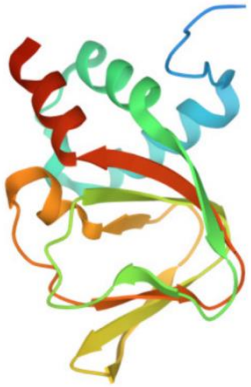

Figure 13 Crystal structure of human PKA (Source:PDB)

PKB

PKB is a non-proline-directed protein kinase. Akt1, Akt2, and Akt3 are other names for the PKB isoforms α, β, and γ, respectively. At T308 and S473, phosphorylation of PKB causes it to become active. The primary antagonistic regulator of the protein kinase B (PKB) pathway is phosphatase and tensin homolog deleted on chromosome 10 (PTEN). In addition to PKA, PKB also controls glycogen production by phosphorylating GSK3β at inhibitory sites (Martin et al., 2013). PKB overexpression enhances tau phosphorylation at threonine 212, serines 214, and 396 in Neuro-2A cells; all of these residues were discovered phosphorylated in AD brains. In contrast to PKA, however, PKB inhibits pro-apoptotic proteins such GSK3β, Bad, and 14-3-3 proteins

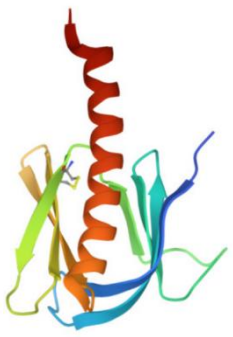

Figure 14 Crystal structure of human PKB (Source:PDB)

to support cell survival. PKB activity is reduced in the hippocampus of senescence-accelerated mouse prone 10 (SAMP10) mice. SAMP10 mice exhibit aging-related traits like emotional disorders, amyloidosis, brain atrophy, learning and memory difficulties, and other traits shown in people with neurodegenerative diseases (Martin et al., 2013). In light of this, PKB represents a possible therapeutic target for AD. Almost every tissue and organ in the body contains significant levels of the PKB enzyme.

PKC

PKC is a non-proline-directed protein kinase. PKC isoforms in mammals are classified into three groups: atypic PKC (ζ and λ/ι isoforms), novel PKC (δ, ε, η and θ isoforms), and classic PKC (α, βI, βII, and γ isoforms). These three groups' structures and sensitivity to their activators vary. Except for the βI and βII isoforms, which arise from alternative splicing, PKC are encoded by different genes. PKC consists of the domains C1, C2, C3, and C4. The activator and calcium binding functions of the C1 and C2 regulatory domains are respectively involved. The catalytic domains C3 and C4 oversee ATP and substrate binding as well as enzymatic activity (Martin et al., 2013). Traditional PKC are composed of 4 domains. Due to the absence of the C2 domain, novel PKC are insensitive to calcium ions. Except for phosphatidylserine, atypic PKC are resistant to traditional PKC inhibitors because they lack the C2 and part of the C1 domain. The activation loop, the turn motif, and the hydrophobic motif are the three S/T conserved domains where PKC is phosphorylated. Trans-phosphorylation and auto-phosphorylation control this process. Serines 258, 293, 324, and 352 are where PKC isoforms phosphorylate tau. In AD brains, just one of these locations (at serine 258) is observed to be phosphorylated. Furthermore, GSK3β is directly and indirectly inhibited by PKC, which lowers A levels and tau phosphorylation at serine 202, threonine 205, and amino acid 181 (Martin et al., 2013). PKC is discovered to be mildly expressed throughout the rest of the body, while it is significantly expressed in brain and endocrine tissues.

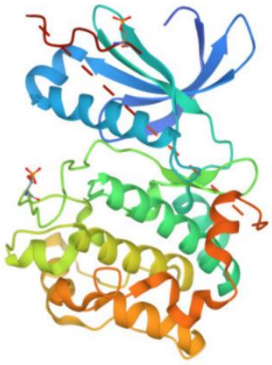

Figure 15 Crystal structure of human PKC (Source:PDB)

TTBK1

The protein tau-tubulin kinase 1 (TTBK1) is not proline directed (non-PDPK). The TTBK2 is a homolog of TTBK1, and it has divergent C-terminal domains (43% identity and 58% similarity) despite sharing highly comparable catalytic domains (88% identity and 96% similarity) (Bao et al., 2021). Because of its resemblance to TTBK2, TTBK1 is a difficult therapeutic target. There are two different genes that encode TTBK1 and TTBK2. TTBK2 is extensively expressed in the cerebellum (in Purkinje cells, in the granule cell layer), the hippocampus, and substance niagra, while TTBK1 is strongly expressed in cortical neurons and only at extremely low levels in other tissues. TTBK1/2 dose-dependently cause tau phosphorylation and tau aggregation into NFT in addition to tubulin phosphorylation. Ten sites on tau proteins are phosphorylated by TTBK1/2, and each of these ten sites is one that can be identified phosphorylated in AD brains (Martin et al., 2013). TTBK1 has been demonstrated to phosphorylate tau at serine residues 198, 199, 202, and 422 as well as at tyrosine 197 in vitro, locations that are also phosphorylated in AD PHFs, by partial phosphopeptide mapping. Only Ser199, Ser202, and Ser422 could be validated as TTBK1 substrates when co-expressed with tau in an intact cell culture. TTBK2 has been demonstrated to phosphorylate tau at Ser208 and Ser210 in vitro, both of which are located on AD PHFs (Lund et al., 2013). According to reports, the brain expresses TTBK1 specifically. Because of its apparent restricted expression to CNS neurons, TTBK1 seems to be a potentially appealing option for pharmacological inhibition. Additionally, TTBK1 is a serine/threonine and a tyrosine kinase with the capacity for dual phosphorylation. In vitro, TTBK1 was able to phosphorylate ten tau sites, including Tyr197. Tyrosine phosphorylation has been shown in PHF-tau, and it has been hypothesized that this is an early occurrence in PHF development. Only TTBK1 has been found to be able to phosphorylate Tyr197. It was shown that phosphorylation at S422 is of particular importance since it occurs in a variety of neurodegenerative diseases but is practically absent in adults with cognitive normal

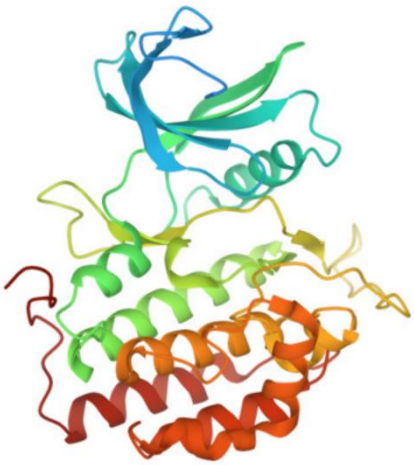

Figure 16 Crystal structure of human TTBK1(Source:PDB)

function (Bao et al., 2021). Knowing that practically all of the distribution of the enzyme TTBK1 occurs at the level of the brain, its suppression may be a very effective target for the purpose of this study.

Chapter 4

The research of potential compounds with the ability to block the hyperphosphorylation of the tau protein is founded on the identification of the aforementioned enzymes. Therefore, it would be perfect to find substances capable of inhibits the hyperphosphorylation of the tau protein and its potential aggregation, lowering or stopping the development of Alzheimer's disease, by identifying potential inhibitors of each enzyme outlined in the study. The qualities of each discovered inhibitor were then examined in detail. The “ChEMBL” and “Drugbank” databases have been used to identify potential primary targets of inhibitors and to establish if the compounds in the study were FDA-approved or if they are subject of clinical studies. It was possible to determine whether the crystal structures of the enzymes under research were published by consulting the PDB database. The comprehensive computational tool “BioTransformer” was then used to find the metabolites of each inhibitor. The inhibitors and their metabolites SMILES formula were then uploaded on the ADMET software which calculated the molecular weight of each compound , the BBB_Filter value, which indicates whether a substance can cross the blood-brain barrier, the LogBB, which is the logarithm of the brain-blood partition coefficient, and a score indicating the potential Lipinski's rule of five violations of the compound. The most often used parameter to estimate penetration of a chemical across the BBB is the ratio of the compound's concentration detected in the brain and the compound's concentration measured in the blood at steady state (Muehlbacher et al., 2011). This ratio, which is defined as LogBB (log[brain]/[blood]), at steady state estimates the overall amount of brain exposure. Compounds with LogBB > 0.3 have been shown to easily cross the BBB, while those with LogBB < -1 have been shown to have poor distribution in the brain (Carpenter et al., 2014; Vilar et al., 2010).

CaMKII inhibitors and their metabolites

Only one potential CaMKII inhibitor, KN93, was discovered (Martin et al., 2013), although the biotransformer allowed for the identification of ten different metabolites.

CDK5 inhibitors and their metabolites

Five potential inhibitors of CDK5 were discovered to exist: (R)-roscovitine, (R)-CR8, Olomoucine, Butyrolactone I, and Hymenialdisine (Martin et al., 2013). (R)-roscovitine, (R)-CR8 and Butyrolactone I have 10 metabolites each. 11 distinct metabolites are detected in Olomoucine. Only 3 different metabolites are detected in Hymenialdisine.(R)-roscovitine, or Seliciclib, is being tested in a phase II clinical investigation, this inhibitor's main targets include various Cyclin-dependent kinases, such as CDK1/2/7/9. Olomoucine's main targets include CDK5, but it is not a medication that the FDA has approved. Hymenialdisine has been identified as a potential CDK5 inhibitor because this enzyme is one of its main targets; however, the FDA has not approved this inhibitor. The databases used did not present the primary targets of (R)-CR8 and Butyrolactone I.

CK1α-1δ-1ε-2 inhibitors and their metabolites

For these enzymes, one potential inhibitor for CK1 and one for CK2 were reported (Martin et al., 2013). CK1 may be inhibited by IC261, which has 12 metabolites. A potential CK2 inhibitor, TBCA has 3 metabolites. Both TBCA and IC261 have not yet received FDA approval. Only the principal target of IC261—the Casein Kinase I isoform gamma 2—could be located in the databases.

DYR1A/2 inhibitors and their metabolites

Four distinct enzyme inhibitors were discovered (Martin et al., 2013). Hermine is one of the possible inhibitors which was found not to have any metabolites. The Pyrazolo 1,5-b inhibitor, which has 7 metabolites, was the second inhibitor under investigation. The third possible inhibitor for these enzymes is Aristolactam BII which presents 9 metabolites. ZDWX-25, which has 8 distinct metabolites, is the final inhibitor that might be of interest.

Of all possible inhibitors for DYR1A-2, none of them are FDA approved, only the primary target of Hermine was found, the Amine Oxidase [flavin-containing] A.

ERK1/2 inhibitors and their metabolites

Three potential inhibitors of ERK1-2 are available: FR-180204, PD98059, and U0126 (Martin et al., 2013). The first one present 5 metabolites, the second one 12 metabolites and the last one 5 metabolites. All the inhibitors of ERK1-2 are not FDA approved yet. Since no information was available in the databases, it was not possible to determine the primary target of these inhibitors.

GSK3β inhibitors and their metabolites

Since GSK3β is one of the enzymes that has been most thoroughly researched in relation to how Alzheimer's disease develops, many potential inhibitors have been discovered. There are twelve potential inhibitors known (Martin et al., 2013). Both lithium and hydrogen sulfite, two potential GSK3β inhibitors, lacking on metabolites. There are 15 distinct metabolites detected in Tideglusib. Another potential inhibitor for GSK3β, which has five metabolites, is Valproate. There are 11 distinct metabolites shown by ARN25068 (Demuro et al., 2022). 7 metabolites are shown by AR-A014418. There were found to be 11 metabolites in SB-216763. Only five potential metabolites for SB-415286 are listed. Seven distinct metabolites are shown in 6-BIO. There are 8 potential metabolites for 6-BIBEO. There are 12 metabolites in 6-BIDECO. Lastly, 6-BIMYEO has 15 distinct metabolites. Even if lithium is used for major depressive disorder, like bipolar disorder, the treatment of vascular headaches, and neutropenia, these treatments are not FDA approved. One of the main targets of this substance is GSK3β. Even hydrogen sulfite has not been approved by FDA. The only primary target of Tideglusib, which is currently in phase II of a clinical trial, has been identified as GSK3β. Although GSK3β is not one of the main targets for this inhibitor, valproate is FDA approved for treatment of bipolar disorders and epilepsy (Xia et al., 2021). The FDA has approved ARN25068, also known as Arnica Flower. AR-A014418 is not FDA approved but GSK3β is its primary target. SB-216763 and SB-415286 are not FDA-approved, and their main targets could not be determined. Although 6-BIO is not FDA-

approved, it has been acknowledged that GSBKβ is its main target. The information necessary on 6-BIBEO, 6-BIDECO, and 6-BIMYEO's approval status and suggested primary targets could not be established with the available database.

JNK inhibitors and their metabolites

It was established that JNK has two potential inhibitors (Martin et al., 2013). The first one, SP600125, displays 7 different metabolites, whereas AS601245 has 10 metabolites. The JNK is the primary target of SP600125, however it has not yet received FDA approval. The databases consulted did not contain information about AS601245.

P38 inhibitors and their metabolites

There are six distinct inhibitors that limit P38 (Martin et al., 2013). SB-239063 has 8 metabolites available. SB-203580 has 5 metabolites available. 10 metabolites are addressed by BIRB-769. There are no metabolites detected in Ginsenoside Rg1. MW181, presented 10 different metabolites while the inhibitor Trolox presented 7 different metabolites. The inhibitors SB-239063, SB-203580, Trolox, and MW181 are not FDA-approved, and the databases consulted does not report their primary target. A phase II clinical trial for BIRB-796 is now active, and its main target is the mitogen-activated protein kinase 14. Lastly, Ginosenoside Rg1 is not FDA approved, in the databases used, it was found that its primary target is the Solute carrier organic anion transporter family member 1B3.

PKA inhibitors and their metabolites

Only one potential inhibitor of PKA is reported, H-89 (Martin et al., 2013), which presents 15 potential metabolites. The FDA has not approved H-89. Its main targets are the Serine/Threonine Protein Kinase Haspin, cAMP-dependent Protein Kinase Catalytic Subunit Alpha, cAMP-dependent Protein Kinase Inhibitor Alpha, and the Interferon-induced, double-stranded RNA-activated Protein Kinase.

PKB inhibitors and their metabolites

Trifluoroacetate Hydrate Salt (Martin et al., 2013), the only potential inhibitor reported for PKB, does not have any metabolites. Trifluoroacetate Hydrate Salt is not FDA approved yet.

PKC inhibitors and their metabolites

PKC only identifies GF-109203X as a potential inhibitor (Martin et al., 2013), which presents 13 different metabolites. GF-109203X is not FDA approved. This inhibitor's primary targets are: Serine/Threonine-Protein Kinase Pim-1, Protein Kinase C Iota Type, and 3-phosphoinositide-dependent Protein Kinase 1.

TTBK1 inhibitors and their metabolites

The only possible inhibitor found for TTBK1 is called TTBK1-IN-2 (Martin et al., 2013) and presents 5 possible metabolites. It was impossible to determine whether it was FDA-approved or what its primary targets were based on the available sources.

Chapter 5

It was possible to determine which of the compounds under consideration are promising enough to warrant carrying out additional studies to validate their use against the development of Alzheimer's disease, using the values acquired from the analysis and research conducted. The decisions were based, in particular, on the BBB_Filter and LogBB values that were acquired as well as any potential Lipinski's rule of 5 violations by the compounds. In order to determine which of these would have a lower likelihood of blocking the enzyme in other regions of the body in addition to the brain, causing harm to the ill subject, special attention was also paid to the expression of target enzymes in the body.

Results of CaMKII inhibitors

Given the BBB_Filter value set by the ADMET software, the CaMKII enzyme inhibitor KN93 and its metabolites *(Figure A 1)* are not suitable for crossing the blood-brain barrier, however it should be noted that metabolites 7, 9, and 10 are able to accomplish this. It is uncertain whether or not these substances can be identified in the brain, according to the LogBB value, which shows that all of these substances are present in the LogBB hybrid band. Although it is important to note that the values of the various compounds varied slightly from the limit value of 500, almost all compounds break the Lipinski's rule on molecules having weights less than 500 Dalton *(Tables B 1)*. Overall, it can be said that this inhibitor and its metabolites are still acceptable study candidates, although they are not the most effective.

Results of CDK5 inhibitors

There are five potential inhibitors of the CDK5 enzyme *(Table B 2)*; the Olomoucine *(Figure A 4)* is the most promising one since the majority of its metabolites have high values, in spite of its low BBB_Filter value. The blood-brain barrier cannot be crossed by any of the remaining four potential inhibitors ((R)-roscovitine *(Figure A 2)*, (R)-CR8 *(Figure A 3)*, Butyrolactone I *(Figure A 5)*, and Hymenialdisine *(Figure A 6)*), and nearly all of their individual metabolites received low BBB_Filter values. All inhibitors have an intermediate

LogBB value, as do their metabolites. The inhibitor Hymenialdisine's metabolites also break the Lipinski's rules, particularly in regard to the quantity of hydrogen bond donors. The distribution of this enzyme in the body makes the research of it inhibitors particularly significant, together with the previous considerations, being that CDK5 is primarily expressed at the level of the brain as well as at the level of male tissues. This makes the CDK5 enzyme a prime candidate for the creation of a treatment.

Results of CK1α-1δ-1ε-2 inhibitors

Two potential inhibitors for the enzyme complexes CK1α, δ, and ε and CK2 have been identified. CK1 enzyme and its isoforms are inhibited by IC261 *(Figure A 7)* while CK2 enzyme is inhibited by TBCA *(Figure A 8)*. As almost all compounds have a high BBB_Filter value and only the inhibitor IC261's metabolite 7 has a low value, indicating that it cannot cross the blood-brain barrier, both inhibitors seem to be great options for the study. All of the substances under investigation had intermediate LogBB values. The TBCA inhibitor, in particular the logP value, is the only compound that demonstrates a breach of Lipinski's rules *(Table B 3)* . Contrary to the alpha and Epsilon isoforms of CK1, which are insufficiently expressed in the brain, both the delta isoform of the CK1 enzyme and the CK2 enzyme are significantly abundant there.

Results of DYRK1A/2 inhibitors

The four inhibitors of DYRK1A and DYRK2 do not violate any Lipinski's rules, and neither do any of their metabolites *(Table B 4)*. As all of the ZDWX-25 inhibitor's metabolites *(Figure A 11)* have low BBB Filter values, which indicate that they cannot cross the blood-brain barrier, it does not seem to be relevant for the study's objectives. The Harmine inhibitor has outstanding properties despite not having any metabolites, having a high BBB filter value, and an intermediate LogBB value. The inhibitor Pyrazolo 1,5-b and nearly all of its metabolites *(Figure A 9)*, with the exception of metabolite 5, have high BBB_Filter values and moderate LogBB values; the only metabolite with a superior LogBB value (LogBB>0,3) is metabolite 4. Ultimately, Aristolactam BII, which contains nine potential metabolites *(Figure A 10)*, is the most promising inhibitor. All of these substances can pass the blood-

brain barrier, and some of them, such as the Aristolactam BII itself and its metabolites 3, 4 have LogBB values that are greater than 0.3, making them good composites for further research. The central problem seems to be the low expression of the targeted enzymes at the level of the brain, which makes them a challenging target despite the outstanding results for inhibitors and metabolites.

Results of ERK1/2 inhibitors

There are three potential inhibitors of ERK1 and ERK2, but only the inhibitor PD98059 *(Figure A 13)* and almost all of its inhibitors appear to be able to cross the blood-brain barrier. Low BBB Filter values for FR-180204 *(Figure A 12)* and U0126 *(Figure A 14)* inhibitors and their metabolites demonstrate that these compounds cannot pass the blood-brain barrier. One of the Lipinski's rules is specifically violated by the inhibitor U0126 and its metabolites, whose exceed the predicted number of hydrogen bond donors *(Table B 5)*. Consequently, a potential future study should only take into account the best inhibitor, PD98059.

Results of GSK3β inhibitors

As was previously indicated, the enzyme GSK3β has the greatest number of inhibitors *(Table B 6; B 7; B 8)*. Lithium does not violate Lipinski's rules and has a high BBB Filter value and an intermediate LogBB value. On the other hand, hydrogen sulfite has an intermediate LogBB value and a low capacity to cross the blood-brain barrier. The Lipinski's rules are not violated by the inhibitor Tideglusib or any of its metabolites *(Figure A 15)*, all of which have intermediate LogBB values and high BBB Filter values. It should be noted that the inhibitor Tideglusib's LogBB value is quite close to the 0.3 threshold value. Except for metabolite 4, the valproate inhibitor and its metabolites *(Figure A 16)* cannot pass through the blood-brain barrier. All of these compounds have an intermediate LogBB value, and none of these violates any Lipinski rule. The inhibitor ARN25068 *(Figure A 17)* and almost all of its metabolites also have a poor ability to cross the blood-brain barrier; metabolites 4, 5, 9 and 11 are the exception. None of the compounds under study break Lipinski's rules, and they all have an intermediate value of LogBB. With the exception of metabolite 3, the inhibitor AR-A014418 and all of its metabolites *(Figure A 18)* have high Filter BBB values. None of

the intermediate LogBBs of the inhibitor or its metabolites break Lipinski's rules. With the exception of a few limited cases, all of the enzymes SB-216763 *(Figure A 19)*, SB-415286 *(Figure A 20)*, 6-BIO *(Figure A 21)*, 6-BIBEO *(Figure A 22)*, 6-BIDECO *(Figure A 23)*, and 6-BIMYEO *(Figure A 24)*, as well as all of their metabolites, have low BBB Filter values, indicating that none of these substances can pass across the blood-brain barrier. Except for metabolite 4 of the inhibitor 6-BIMYEO, which has a LogBB value of less than -1, almost all of these substances have an intermediate LogBB value. Last but not least, none of these enzymes or their metabolites violate any Lipinski's rules. As a result, the inhibitors Tideglusib and AR-A014418 are considered to be the most promising among all the candidates. It is important to note that Tideglusib has already being studied for a number of potential applications, including its potential to delay the progression of Alzheimer's disease.

Results of JNK inhibitors

SP600125 *(Figure A 25)* and AS601245 *(Figure A 26)* are two potential JNK inhibitors. The intermediate value of LogBB is shared by SP600125 and all of its metabolites. The remaining compounds have a low BBB Filter value in contrast to SP600125, metabolites 3, 4, and 5, which have high values. Because AS601245 and the majority of its metabolites have LogBB values lower than -1, they are less interesting for the study. None of the substances under investigation break any of Lipinski's rules *(Table B 9)*. The enzyme JNK is only moderately expressed at the level of the brain, regardless of the fact that SP600125 is the most promising inhibitor of the two.

Results of P38 inhibitors

As mentioned before, there are six potential inhibitors of the P38 enzyme *(Table B 10)*. The inhibitor SB-239063 *(Figure A 27)* and its eight metabolites do not break any Lipinski's rules, but they have different BBB Filter values. For example, while all eight metabolites of SB-239063 have low values, metabolites 1, 7, and 8 have high values, indicating that they can cross the blood-brain barrier. These compounds' LogBB values are all in the middle. Because SB-203580 *(Figure A 28)* and all five of its metabolites have low values for BBB Filter, further investigation of the aforementioned inhibitor is not desirable.

The same was discovered with the BIRB-796 inhibitor and its metabolites *(Figure A 29)*, which in addition to the inability of passing through the blood-brain barrier also violate a few of Lipinski's rules. The inhibitor Ginosenoside Rg1 has a LogBB value less than -1, is incapable of crossing the blood-brain barrier, and breaks three different Lipinski's rules. It also has no metabolites. Trolox and its metabolites *(Figure A 30)* also have a low Filter_BBB and LogBB values below -1. Together with SB-239063, the last inhibitor, MW181 *(Figure A 31)*, seems to be a promising subject for further study. It displays intermediate LogBB values along with its metabolites and does not break Lipinski's rules. The blood-brain barrier can be crossed by MW181, metabolites 1, 8, and 9, but not by the other metabolites, according to the BBB_Filter values. Due to its high protein expression in the brain and gastrointestinal system, the enzyme P38 may be a target of special interest.

Results of PKA inhibitors

According to the BBB filter values, the inhibitor H-89 *(Figure A 32)* and the majority of its metabolites are able to pass the blood-brain barrier, indicating that the molecule designated as an inhibitor for the PKA enzyme is appropriate for the study under consideration. With the exception of metabolite 6 and metabolite 12, whose LogBB>0.3 values indicate that these two chemicals might surely cross the blood-brain barrier and persist in adequate concentrations inside the brain, the other values defined of LogBB are almost all intermediate. None of the test compounds violated any Lipinski's regulations *(Table B 11)*.

Results of PKB inhibitors

The PKB enzyme inhibitor trifluoriacetate hydrate salt has no metabolites. Because this substance can cross the blood-brain barrier and does not violate any of Lipinski's rule of 5, the results of the studies done allows us to consider this inhibitor as a potential candidate for further research. Since the LogBB value is similarly intermediate, the inhibitor might still be included in the study under consideration *(Table B 12)*.

Results of PKC inhibitors

The GF-109203X inhibitor and its metabolites *(Figure A 33)* are not useful for inhibiting the PKC enzyme beyond the blood-brain barrier. Even though the LogBB values are intermediate and do not entirely rule out the potential of discovering the compounds inside the brain, none of the compounds under investigation are able to cross the blood-brain barrier *(Table B 13)*.

Results of TTBK1 inhibitors

The only documented inhibitor of the TTBK1 enzyme, compound TTBK1-IN-2 *(Figure A 34)*, does not have the optimal characteristics for the research currently considered. A low BBB Filter value for the inhibitor and nearly all of its metabolites shows that these substances cannot cross the blood-brain barrier. All test compounds had intermediate LogBB values *(Table B 14)*. However, the enzyme TTBK1 is of particular interest because of his almost exclusive presence in the brain, making it an ideal target. Because of this, additional study may will be conducted to discover alternative prospective inhibitors, more likely to function crossing the blood-brain barrier.

Results and future perspectives

As stated earlier, the goal of this study is to find potential inhibitors appropriate for the inactivation of the enzymes responsible for the hyperphosphorylation of the tau protein in order to reduce tau protein aggregation and limit, if not completely prevent, the progression of Alzheimer's disease. All of the compounds were analyzed in detail in the previous sections, outlining their advantages as well as their drawbacks. This enabled the formulation of a short list of inhibitors that may be the most effective as a result of the above considerations. The following are potential inhibitors that might be suitable for additional study:

- KN93 for the enzyme CaMKII
- Olomoucine for the enzyme CDK5
- IC261 for the enzyme CK1and its isoforms

- TBCA for the enzyme CK2
- Aristolactam II for enzymes DYRK1A and DYRK2
- Tideglusib and AR-A014418 for the enzyme GSK3β
- SP600125 for the enzyme JNK
- MW181 for the enzyme P38
- H-89 for the enzyme PKA
- Trifluoriacetate Hydrate Salt for the enzyme PKB

Among the indicated inhibitors, there is no inhibitor of the enzyme TTBK1, yet it is important to emphasize how the significance of this last enzyme it the reason why researchers continue searching for potential inhibitors with improved properties that can help the enzyme to overcome the blood brain barrier. In order to carry out further research on the interaction of microtubules and the tau protein, more studies have been conducted to define and build their structures. In particular, a potential use of these structures on the software MOE through the use of docking might be possible. Following the determination of the microtubule and tau protein structures and the identification of all the structures of the enzymes, the inhibitors and their metabolites, it will be possible to conduct a thorough analysis to determine which of the chosen inhibitors produces the best results for the study's subsequent phases. The specific binding force between microtubules and individual tau phosphorylation sites is a crucial factor to consider for future research due to its potential to help focus the search on the sites that are most stimulated by the existing strong bound, enabling a more focused search of the sites of interest. By combining modeling and binding modes to analyze the fuzzy complex made up of microtubules and the R2 region of the tau protein, the researchers of the study (Marien et al., n.d.) were able to discover that the tau protein develops particularly strong bonds at the level of three serine residues, Ser285, Ser289, and Ser293, with an even greater focus on the second of these, which is at the center of R2. Through studies similar to the one just described it will be possible to carry out more and more specific and useful searches to reach the goal. This study, like many others, is simply a piece of ongoing research that will help scientists move closer and closer to a potential ultimate treatment for one of the most common diseases in the world. In the future, it's possible that additional inhibitors will be found which may be analyzed in a similar way to the one used in this study, in order to find compounds that are even more suitable for the final goal.

Appendix A

Figure A 1 Structures of inhibitor KN93 and its metabolites

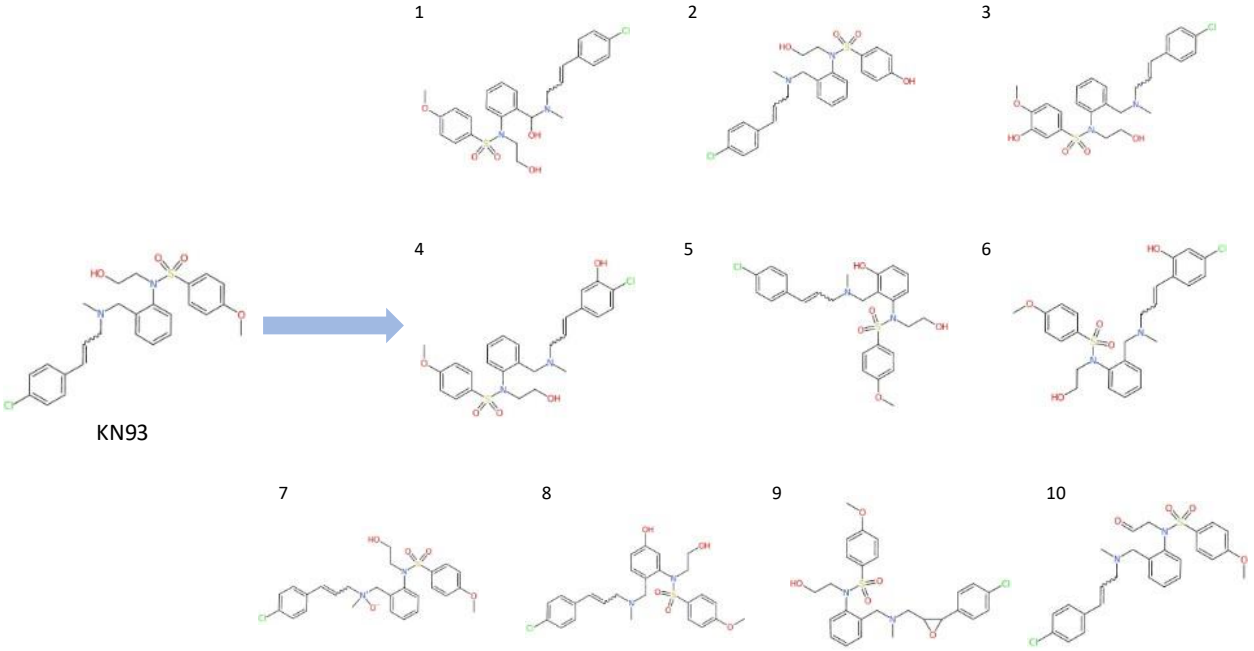

Figure A 2 Structures of inhibitor (R)-roscovitine and its metabolites

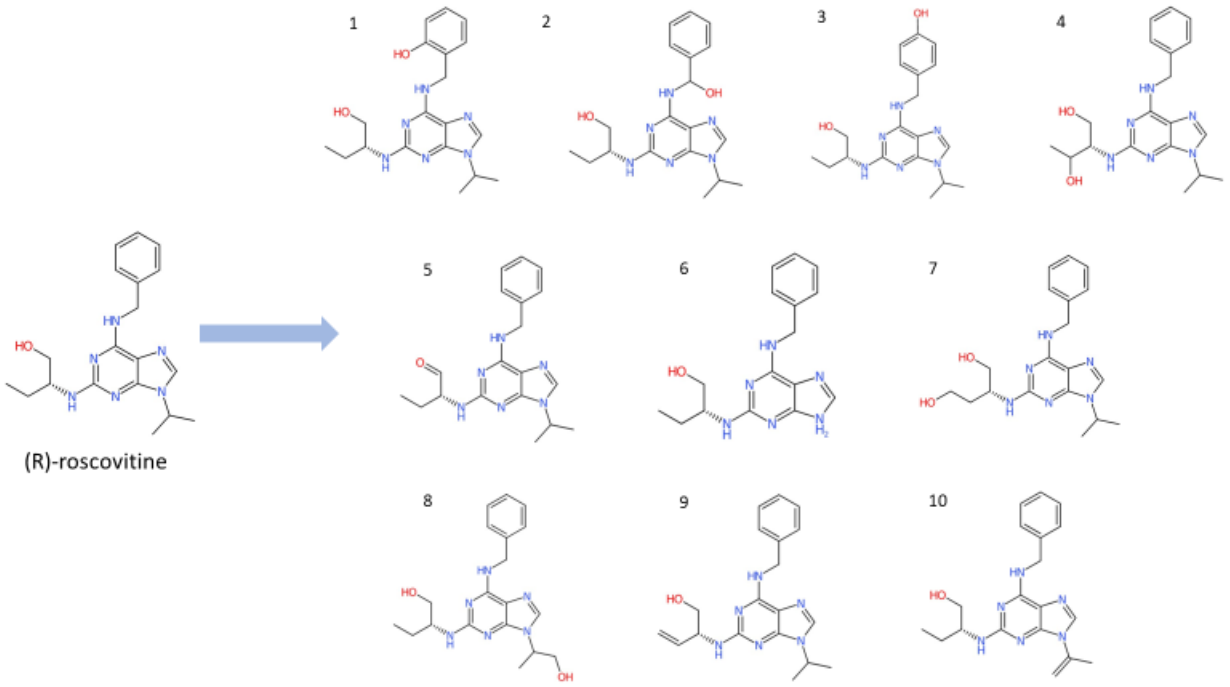

Figure A 3 Structures of inhibitor (R)-CR8 and its metabolites

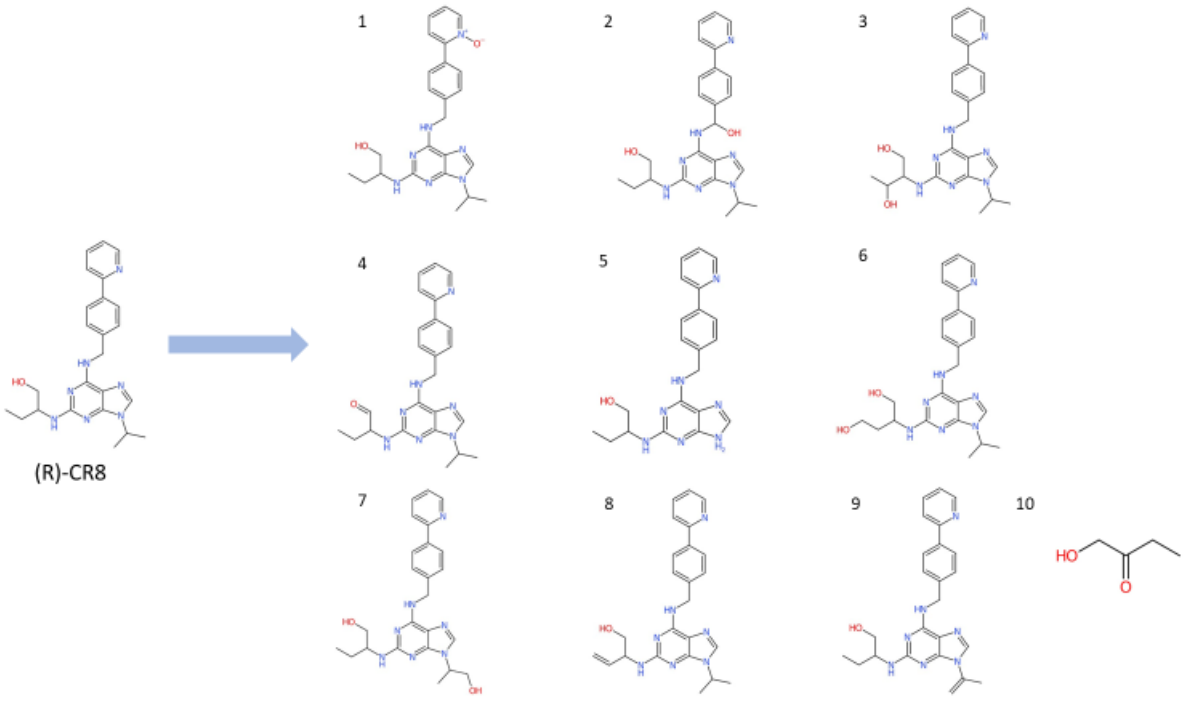

Figure A 4 Structures of inhibitor Olomoucine and its metabolites

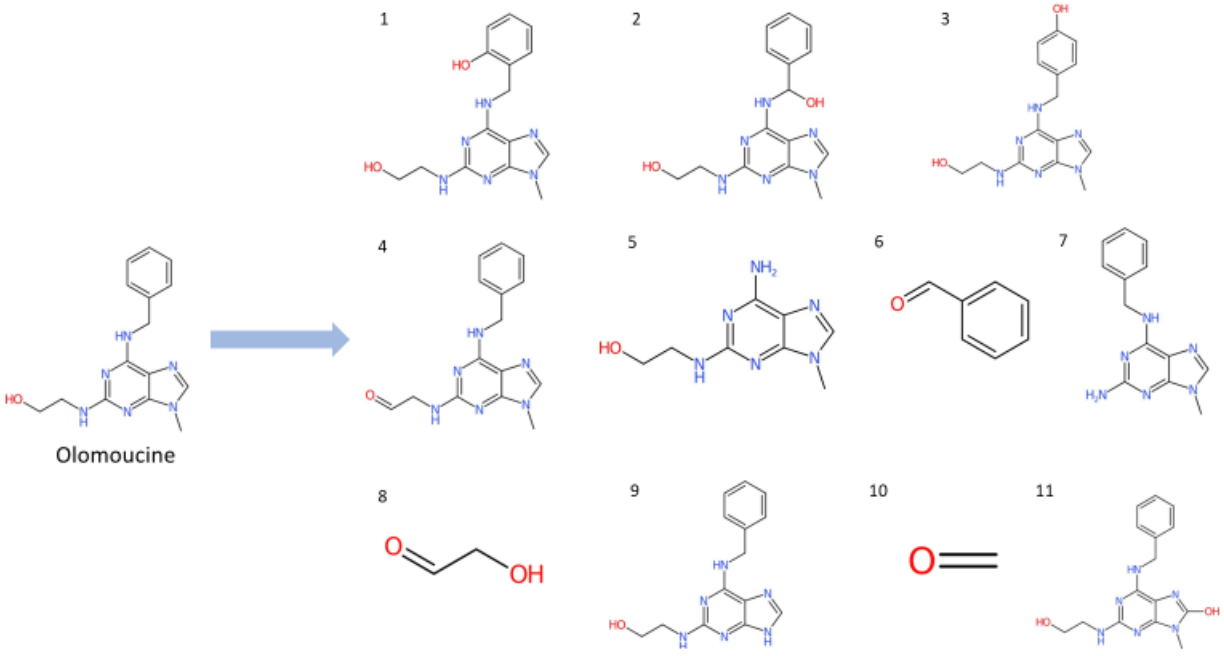

Figure A 5 Structures of inhibitor Butyrolactone I and its metabolites

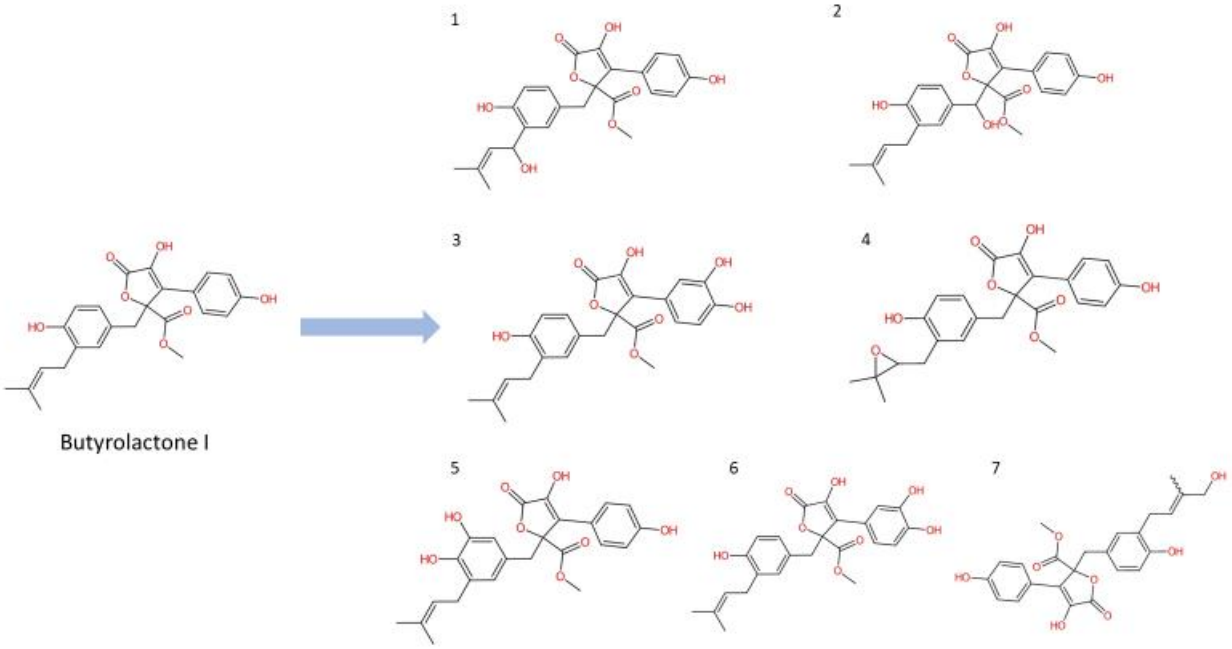

Figure A 6 Structures of inhibitor Hymenialdisine and its metabolites

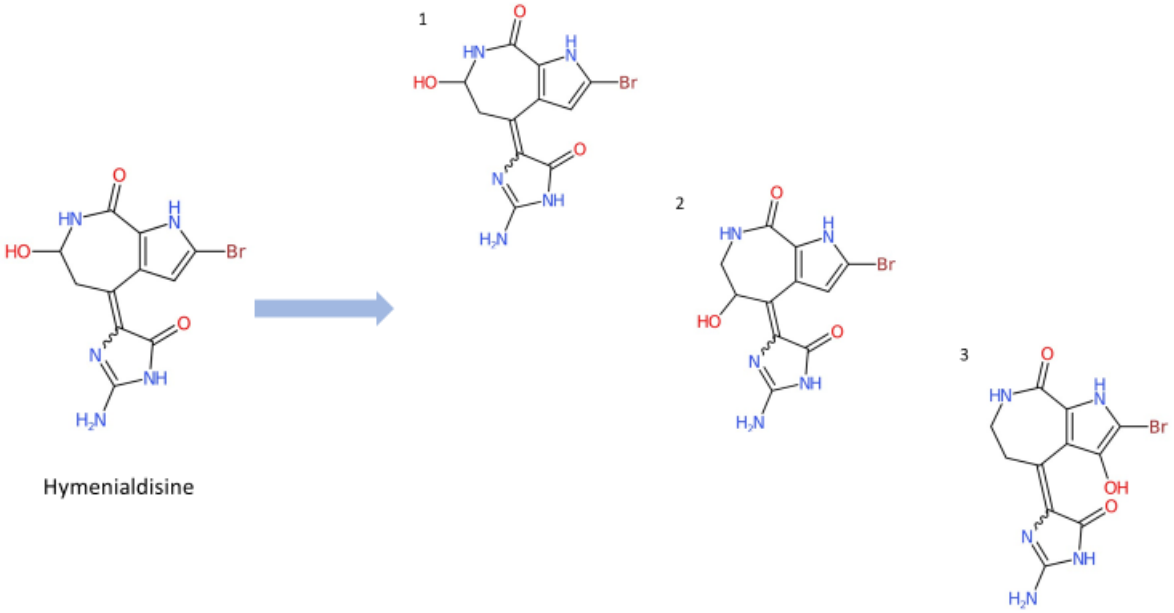

Figure A 7 Structures of inhibitor IC261 and its metabolites

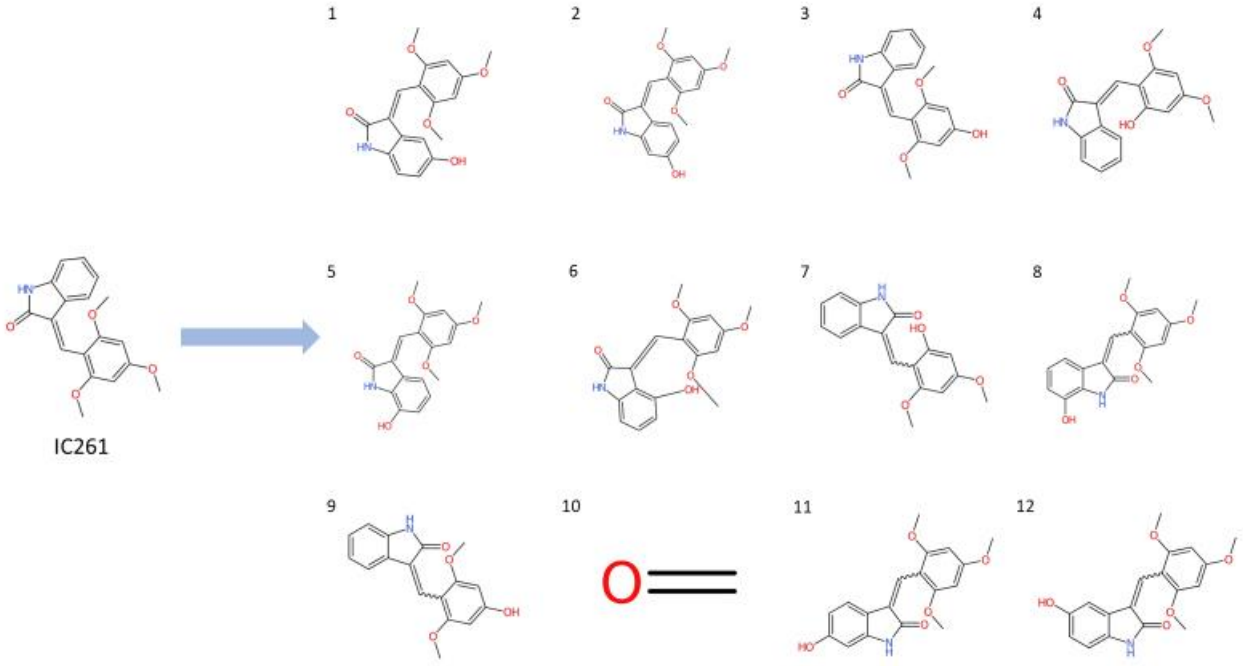

Figure A 8 Structures of inhibitor TBCA and its metabolites

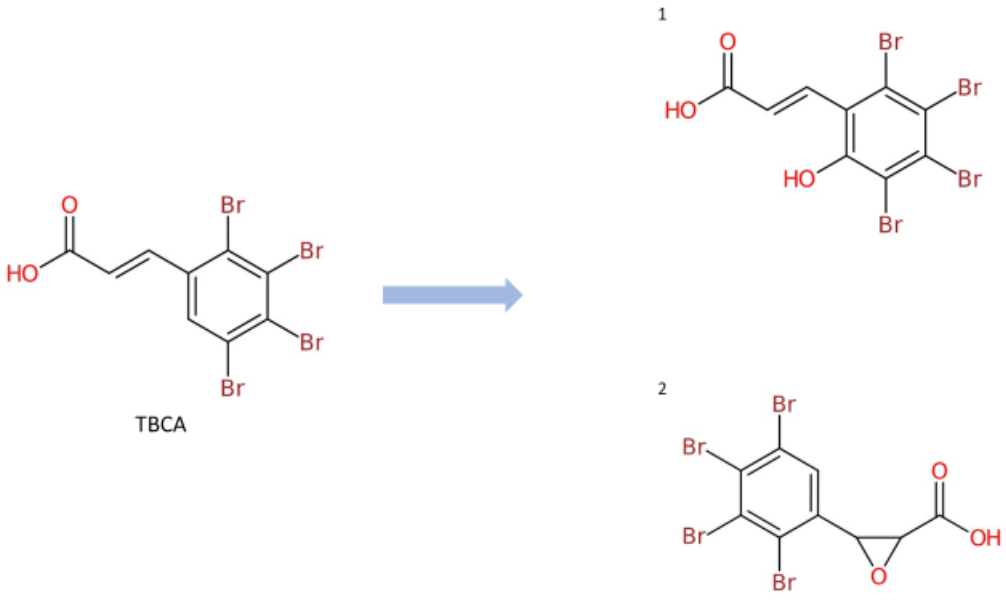

Figure A 9 Structures of inhibitor Pyrazolo 1,5-b and its metabolites

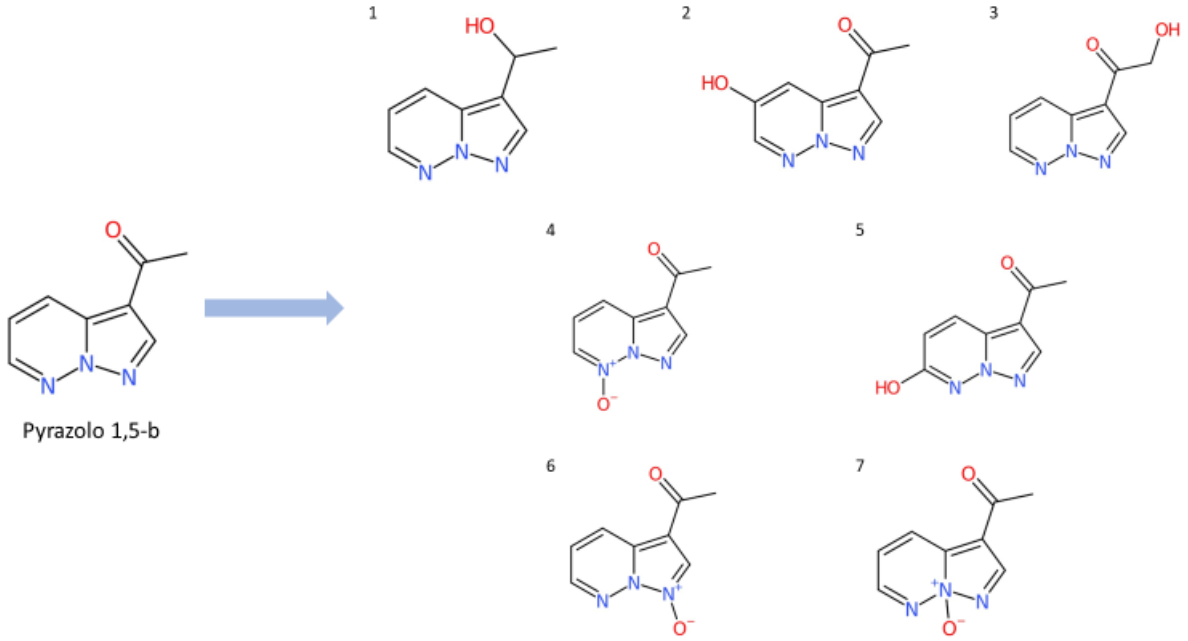

Figure A 10 Structures of inhibitor Aristolactam BII and its metabolites

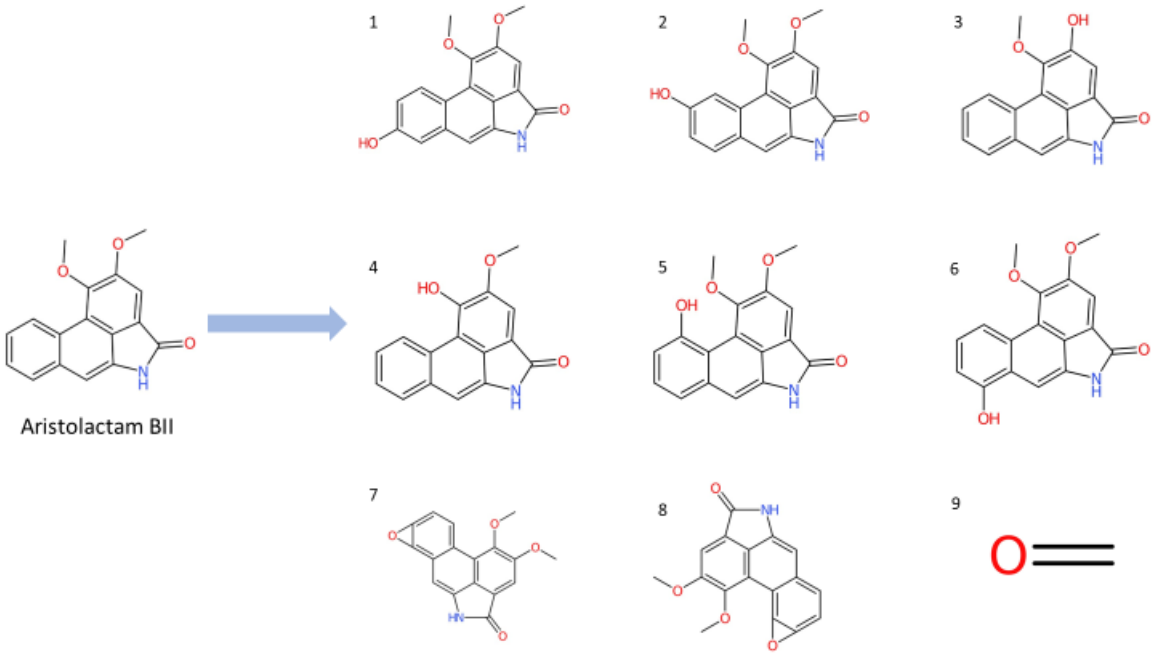

Figure A 11 Structures of inhibitor ZDWX-25 and its metabolites

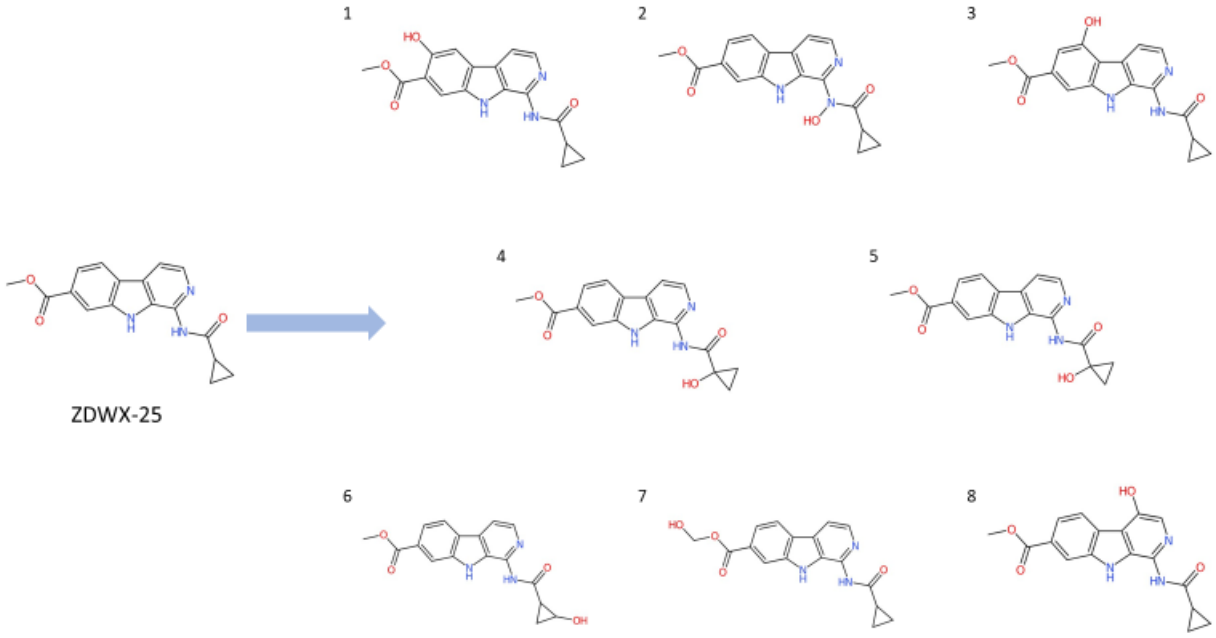

Figure A 12 Structures of inhibitor FR-180204 and its metabolites

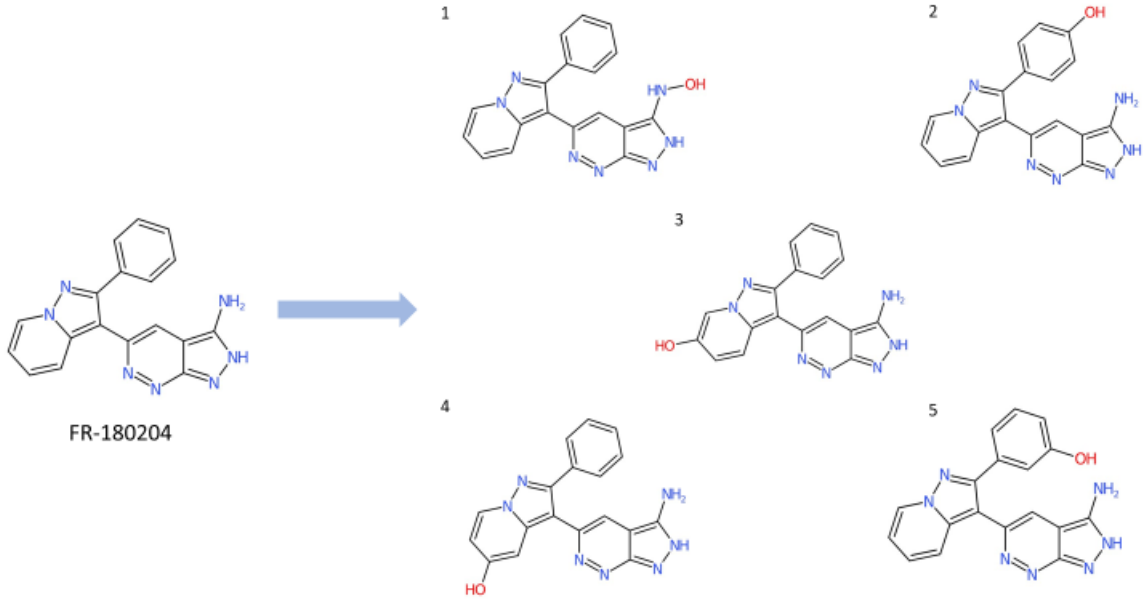

Figure A 13 Structures of inhibitor PD980059 and its metabolites

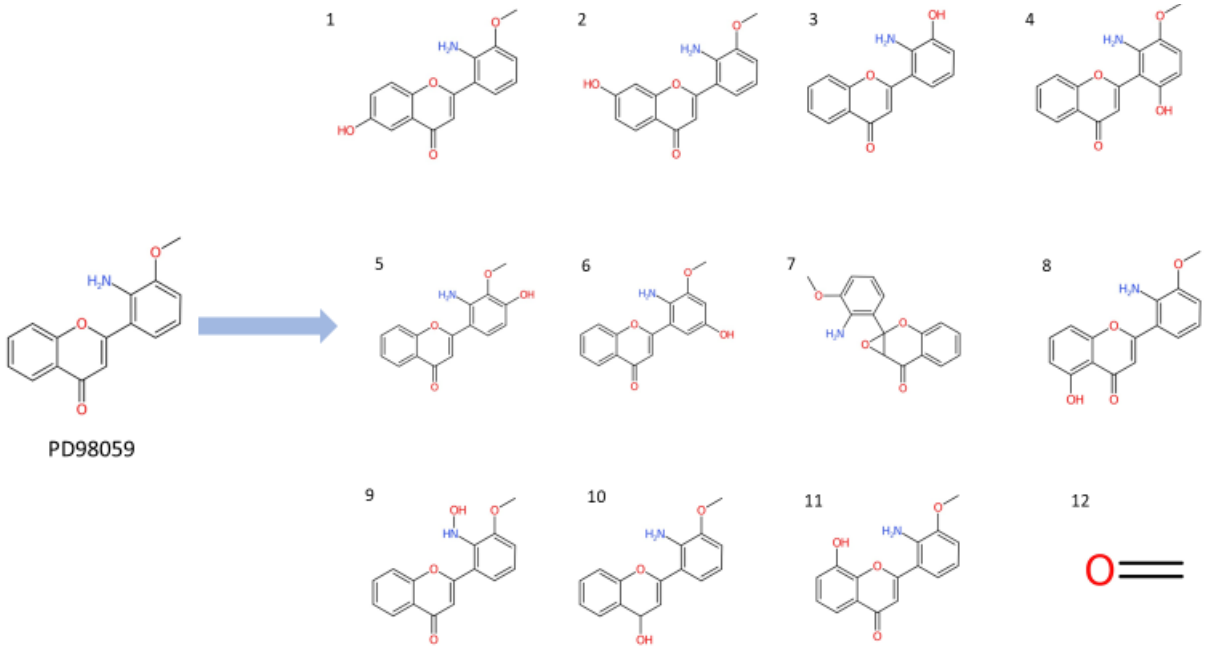

Figure A 14 Structures of inhibitor U0126 and its metabolites

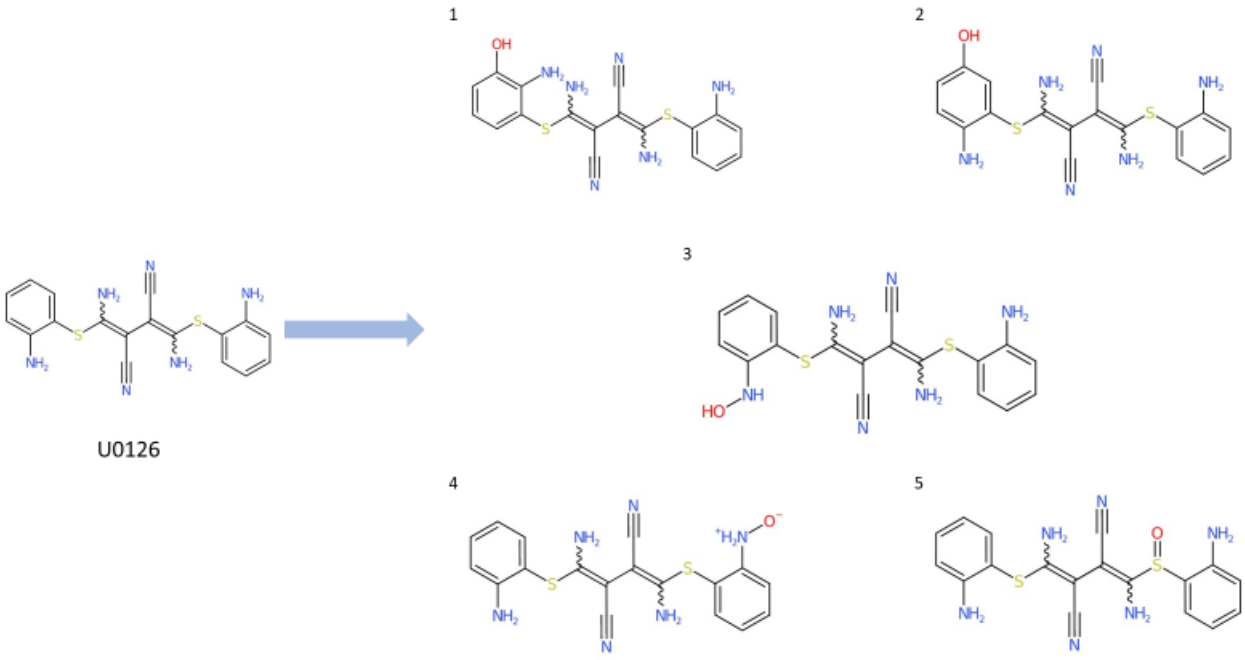

Figure A 15 Structure of inhibitor Tideglusib and its metabolites

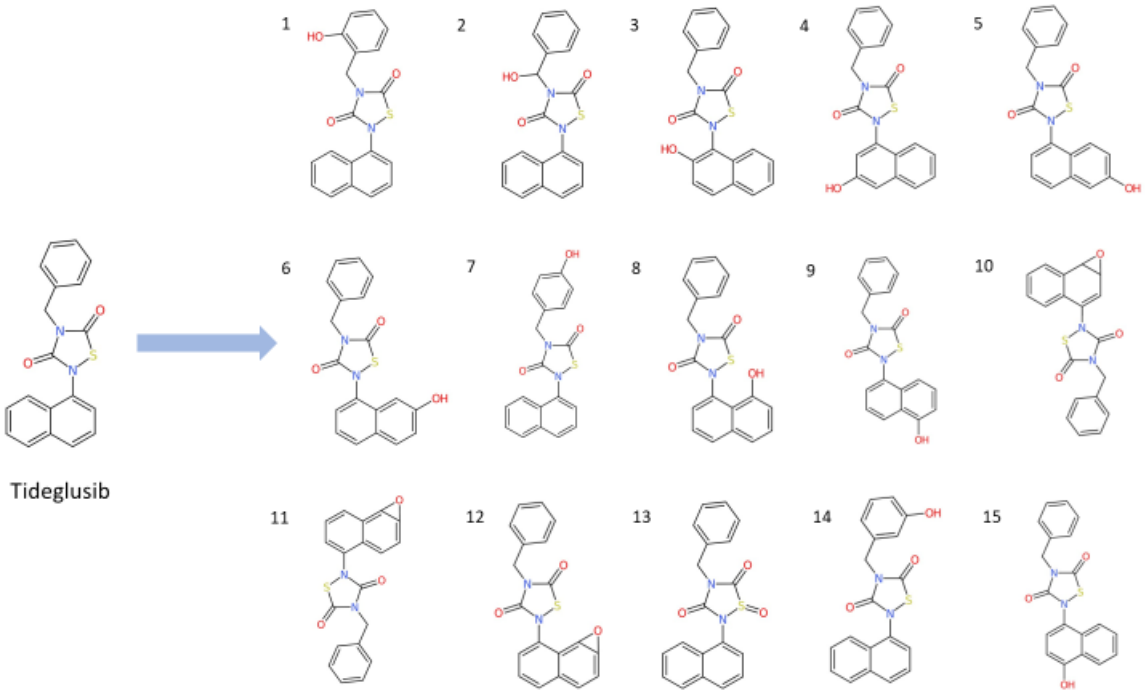

Figure A 16 Structures of inhibitors Valproate and its metabolites

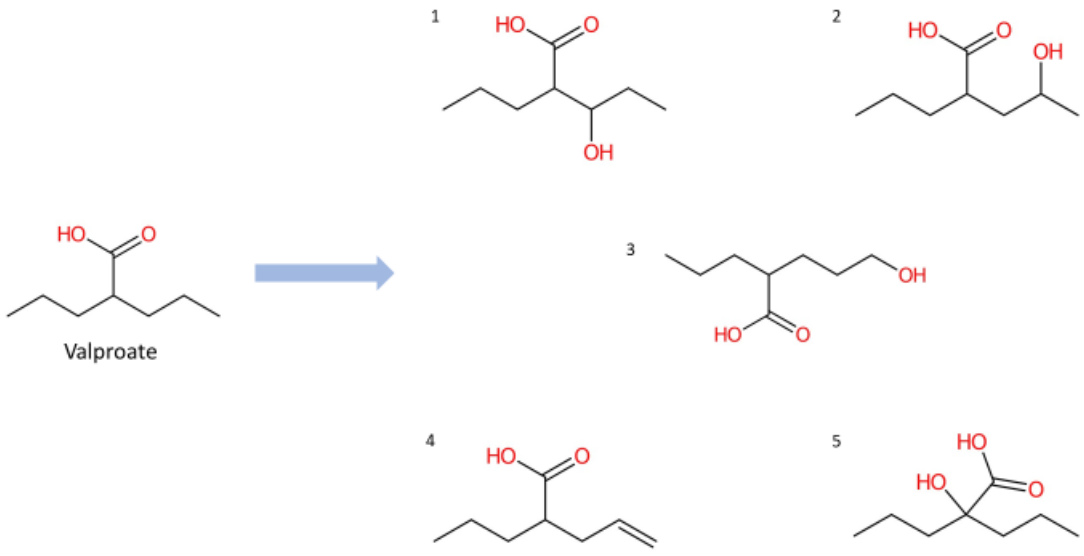

Figure A 17 Structures of inhibitor ARN25068 and its metabolites

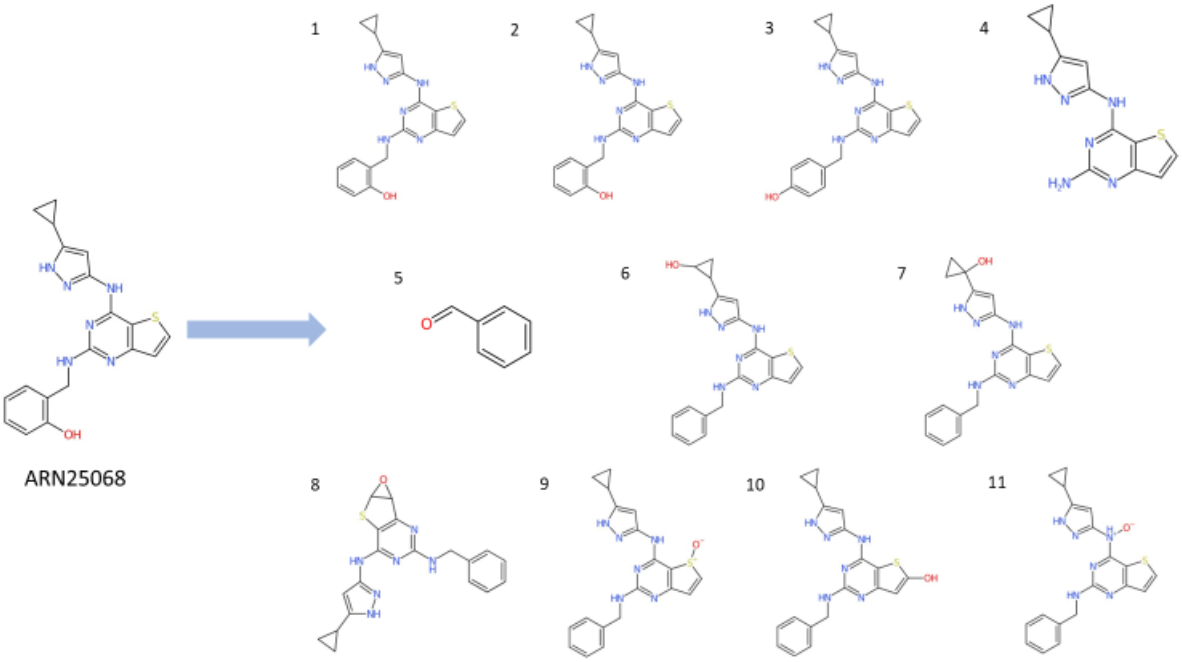

Figure A 18 Structures of inhibitor AR-A014418 and its metabolites

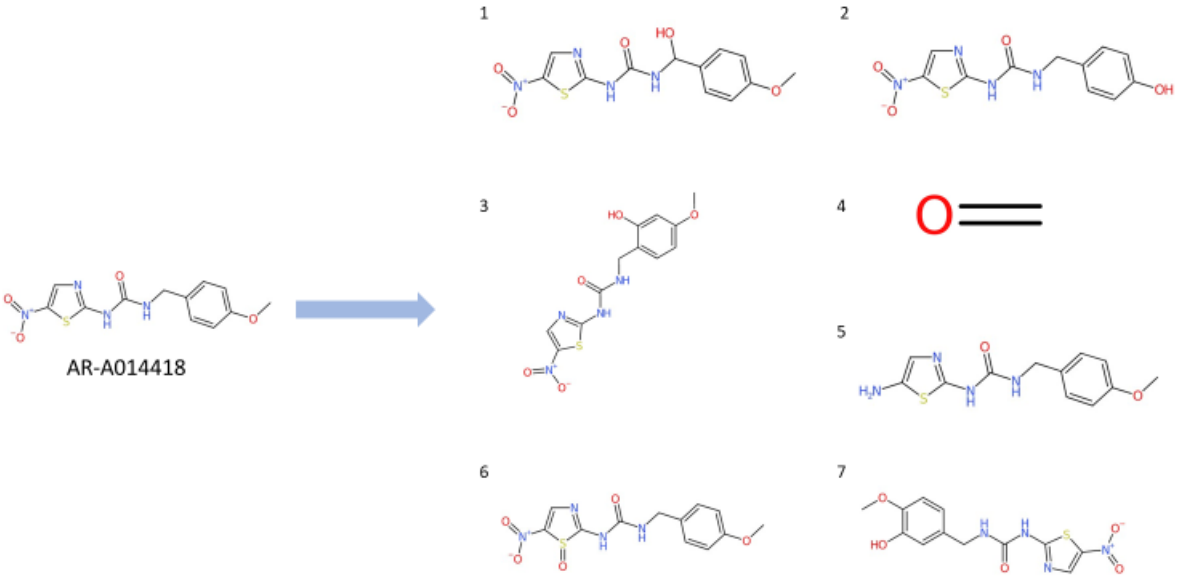

Figure A 19 Structures of SB-216763 and its metabolites

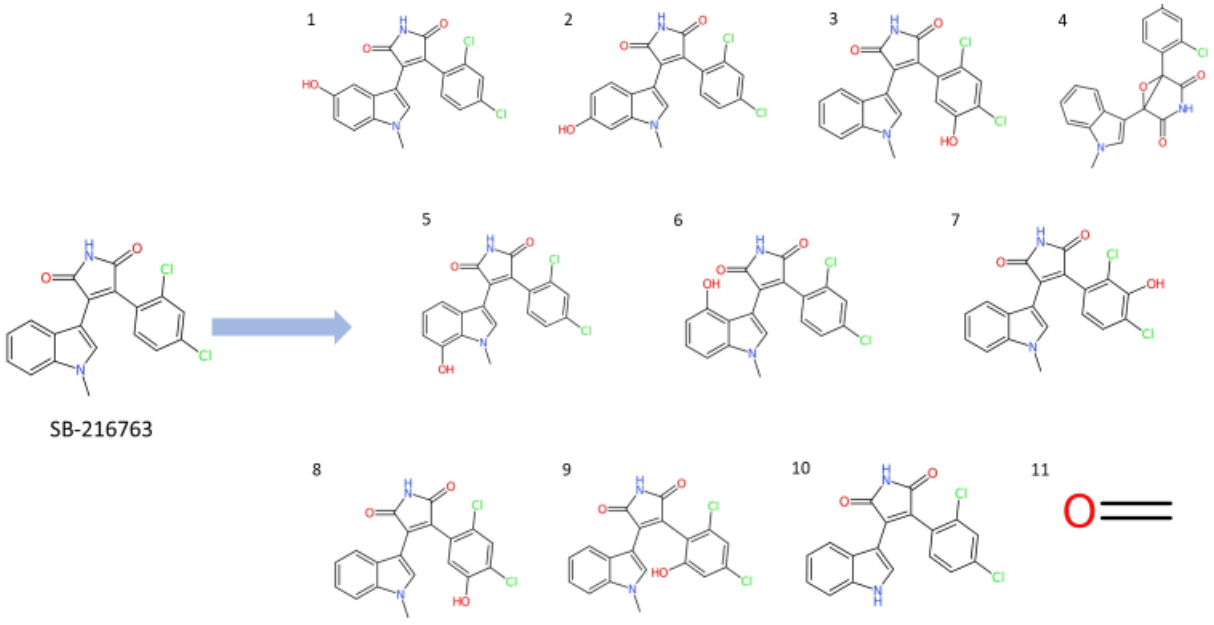

Figure A 20 Structures of inhibitor SB-415286 and its metabolites

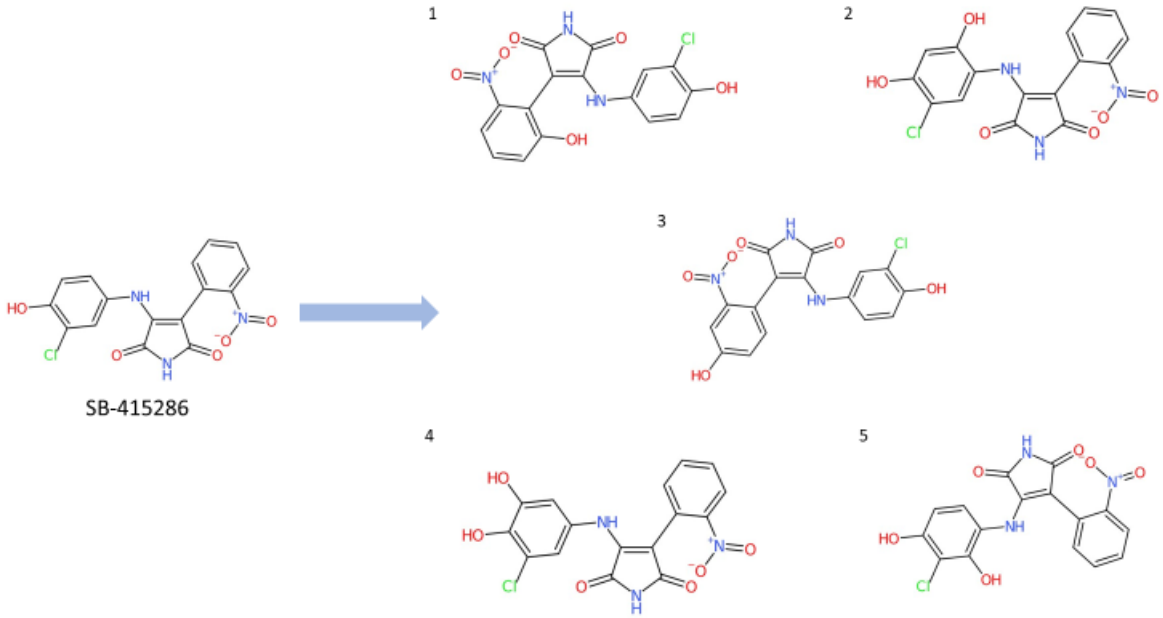

Figure A 21 Structures of inhibitor 6-BIO and its metabolites

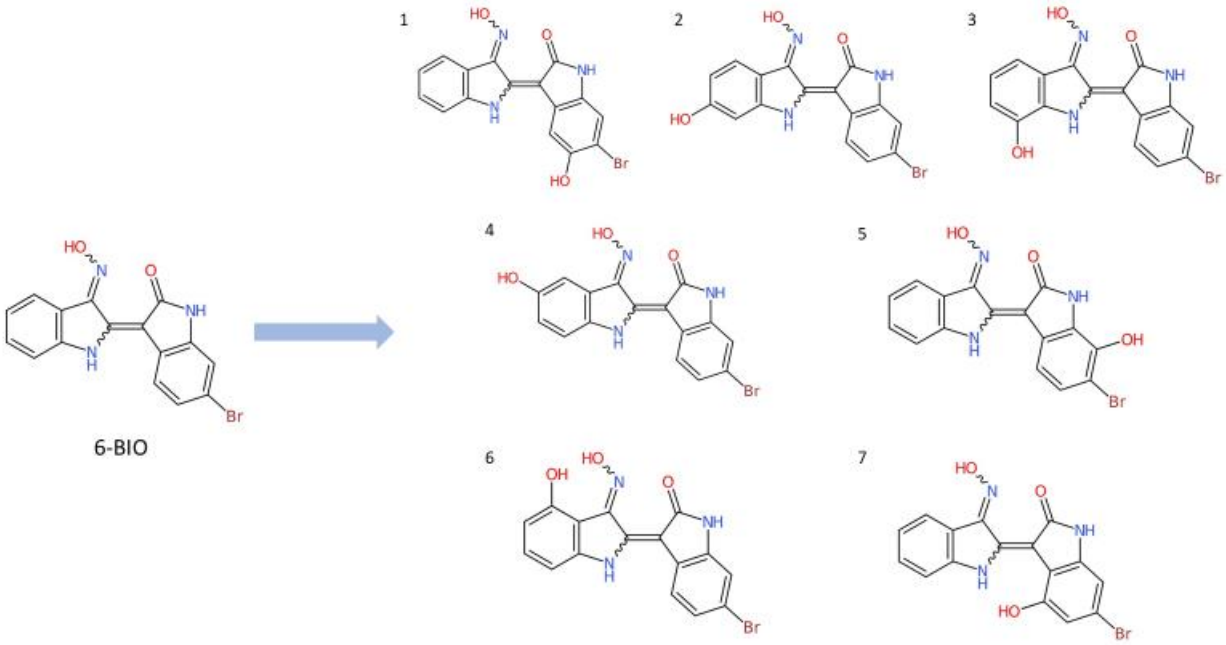

Figure A 22 Structures of inhibitor 6-BIBEO and its metabolites

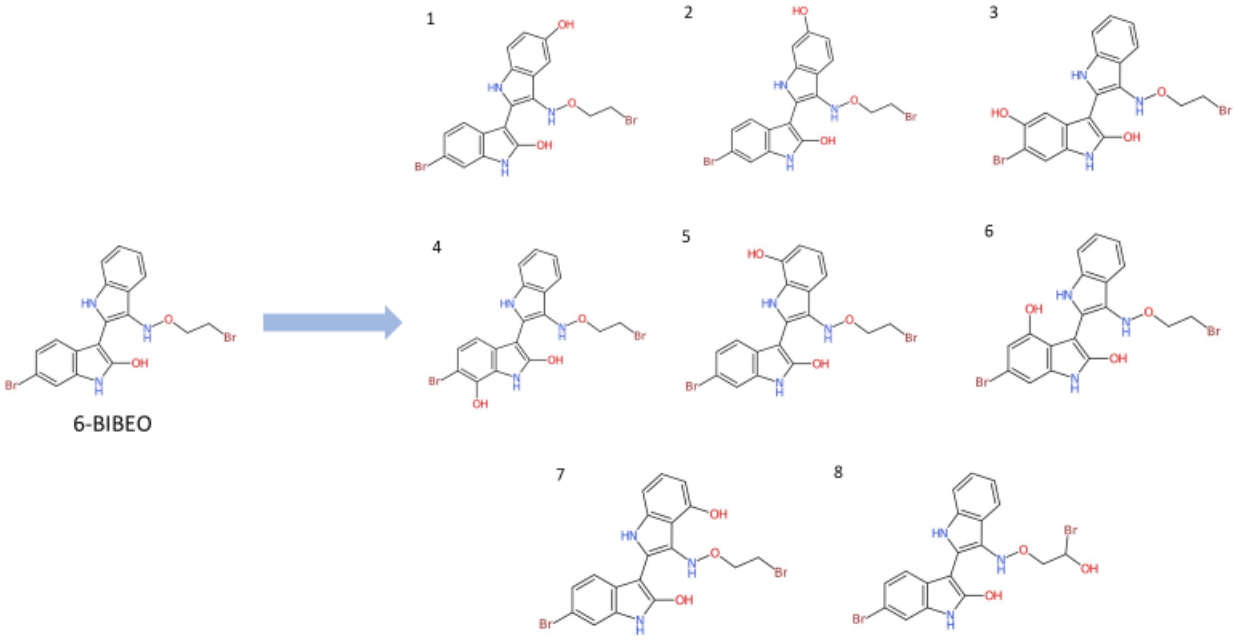

Figure A 23 Structures of inhibitor 6-BIDECO and its metabolites

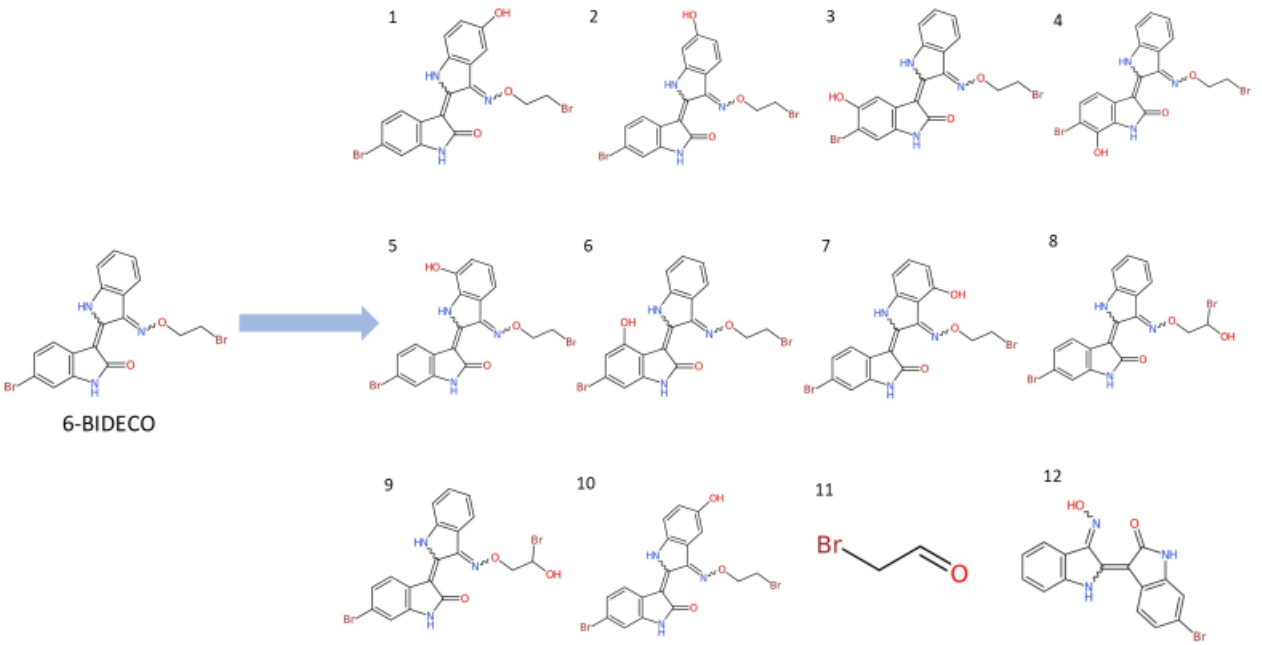

Figure A 24 Structures of inhibitor 6-BIMYEO and its metabolites

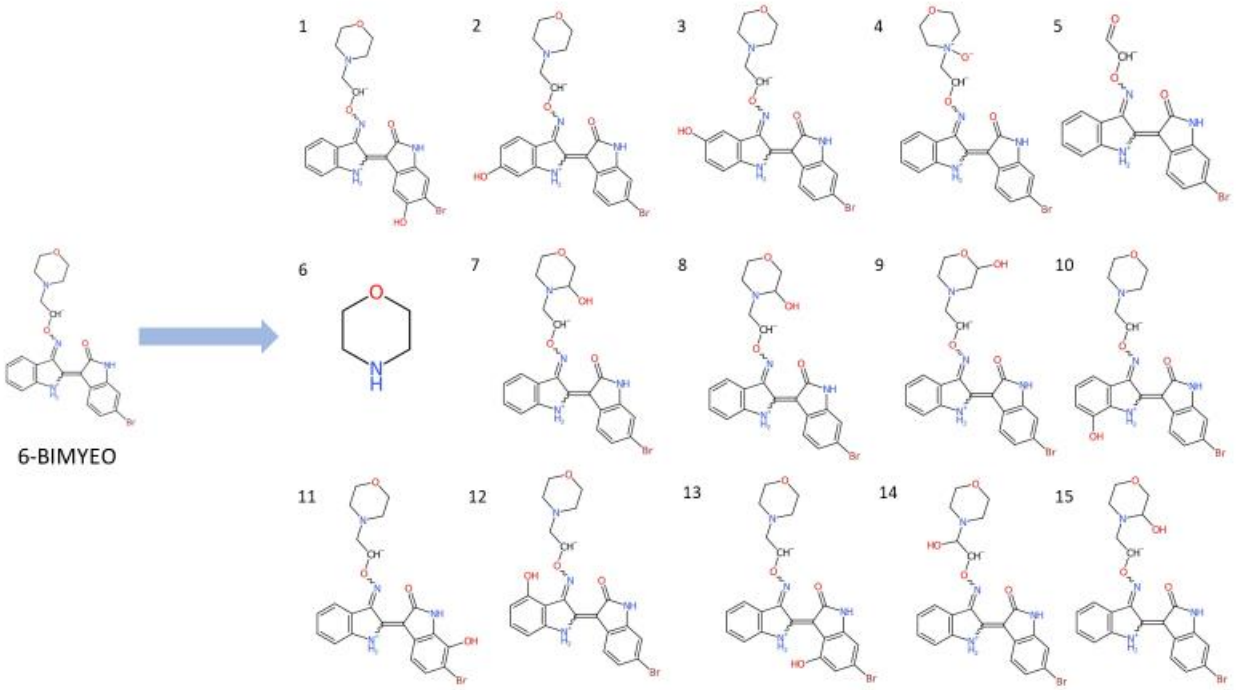

Figure A 25 Structures of inhibitor SP600125 and its inhibitors

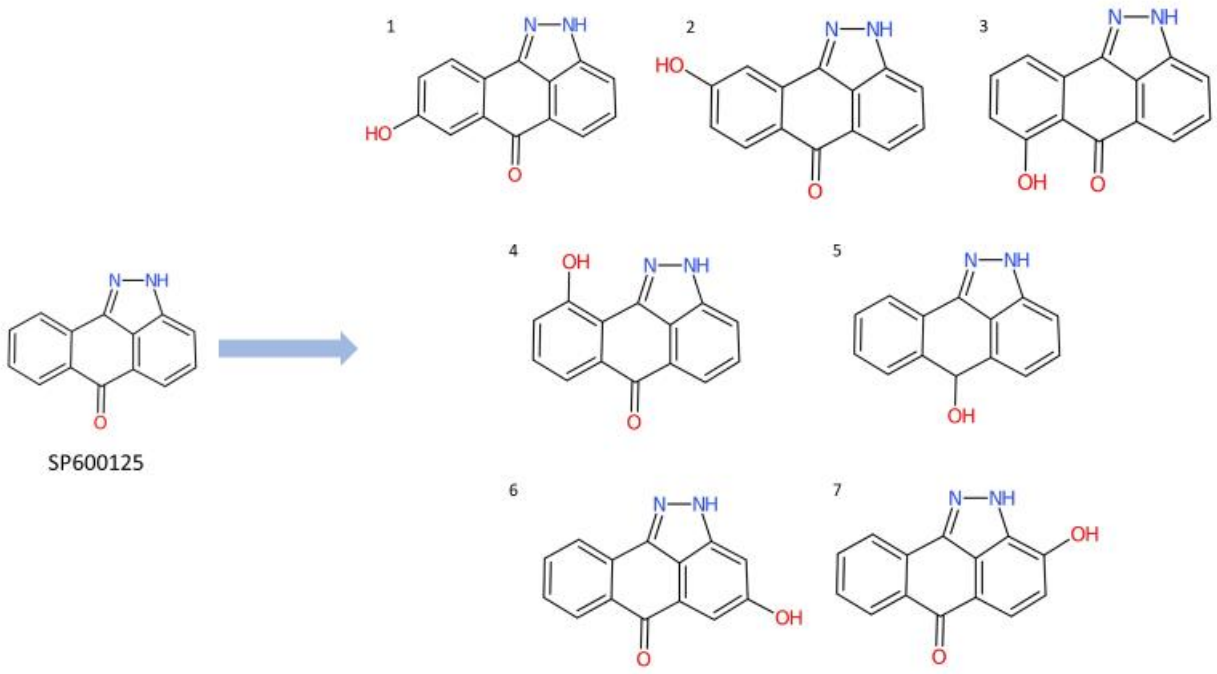

Figure A 26 Structures of inhibitor AS601245 and its metabolites

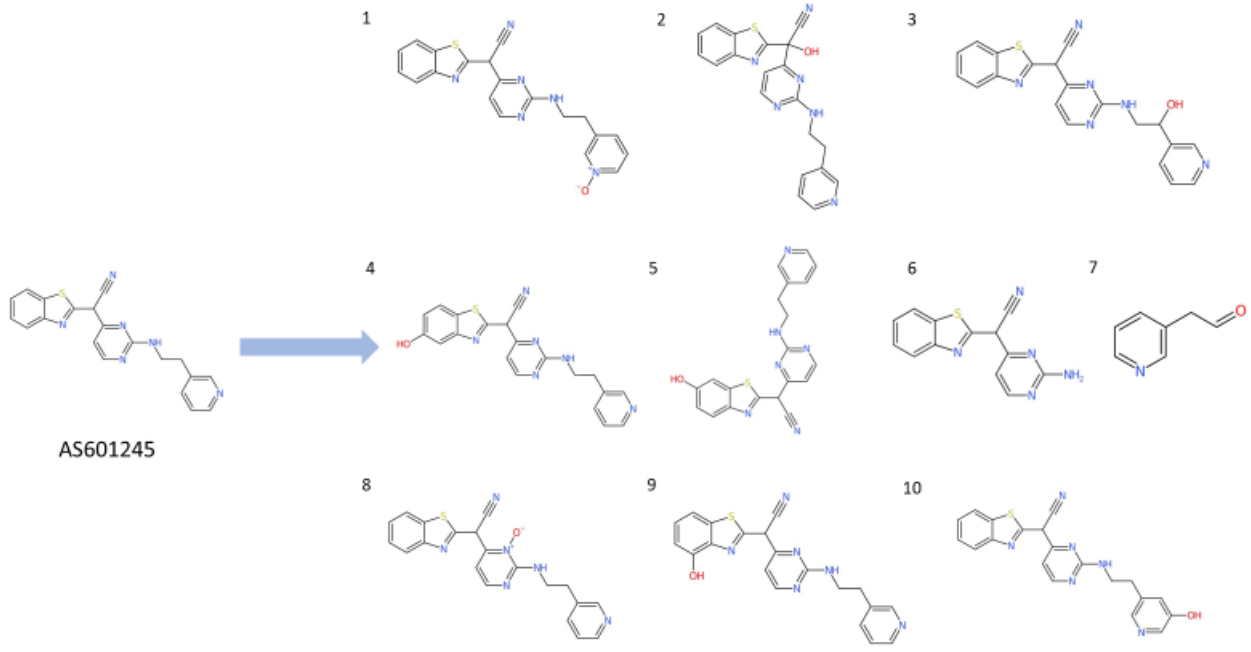

Figure A 27 Structures of inhibitor SB-239063 and its metabolites

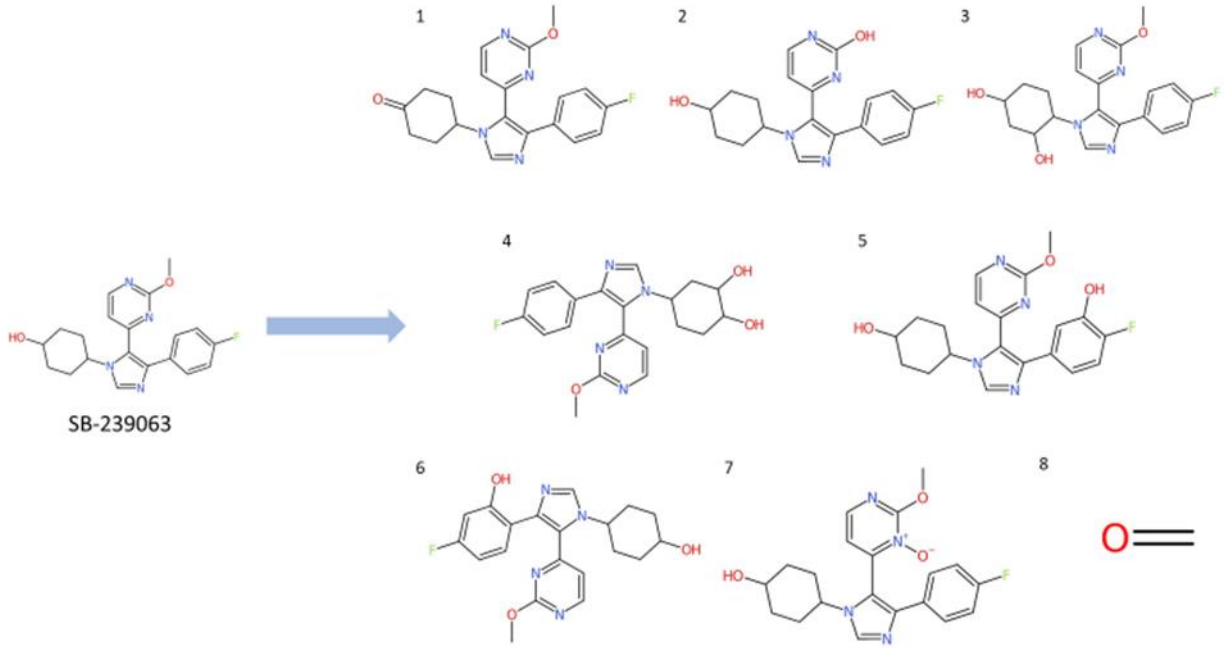

Figure A 28 Structures of inhibitor SB-203580 and its metabolites

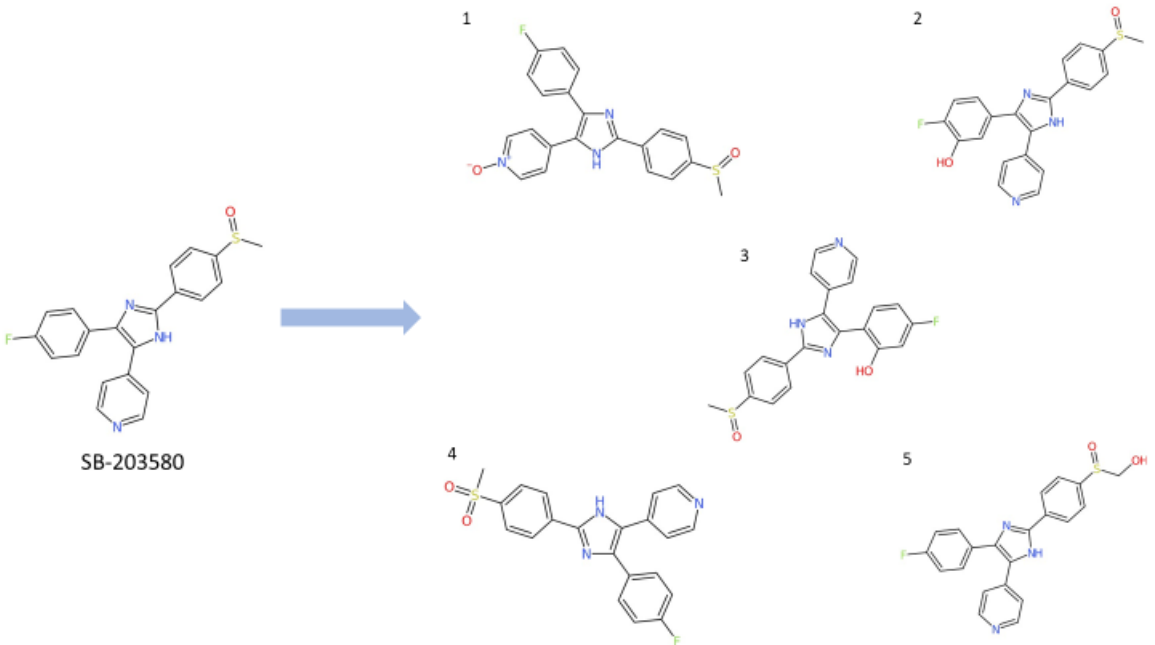

Figure A 29 Structures of inhibitor BIRB-796 and its metabolites

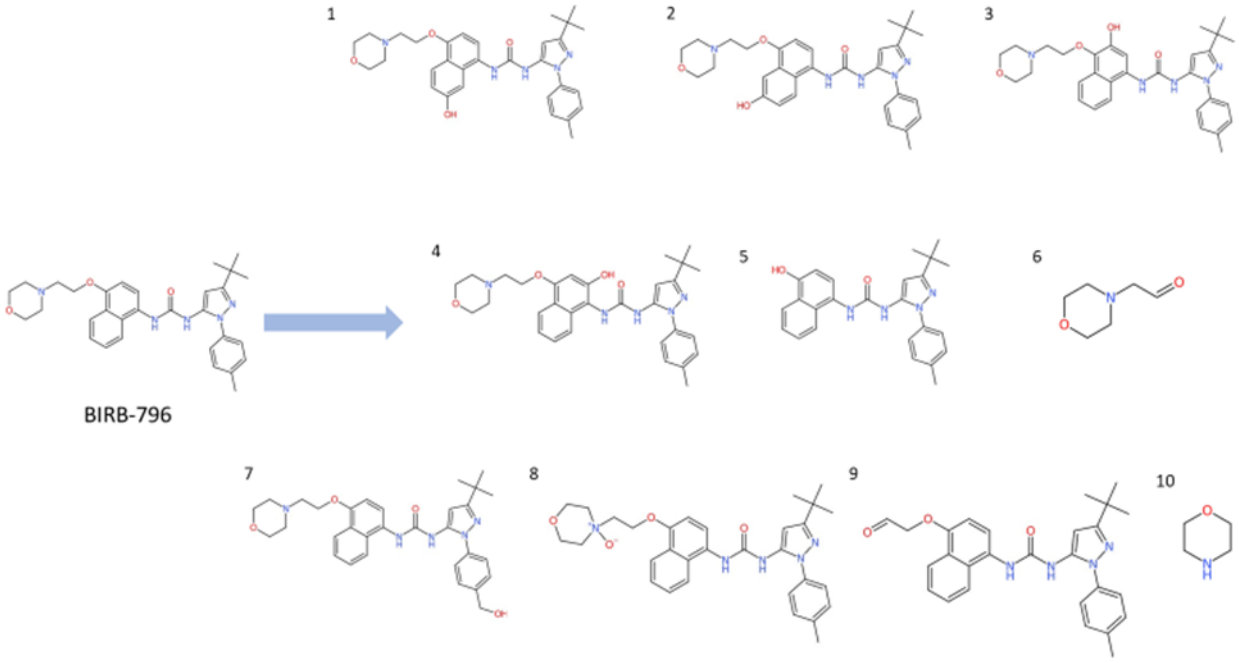

Figure A 30 Structures of inhibitor Trolox and its metabolites

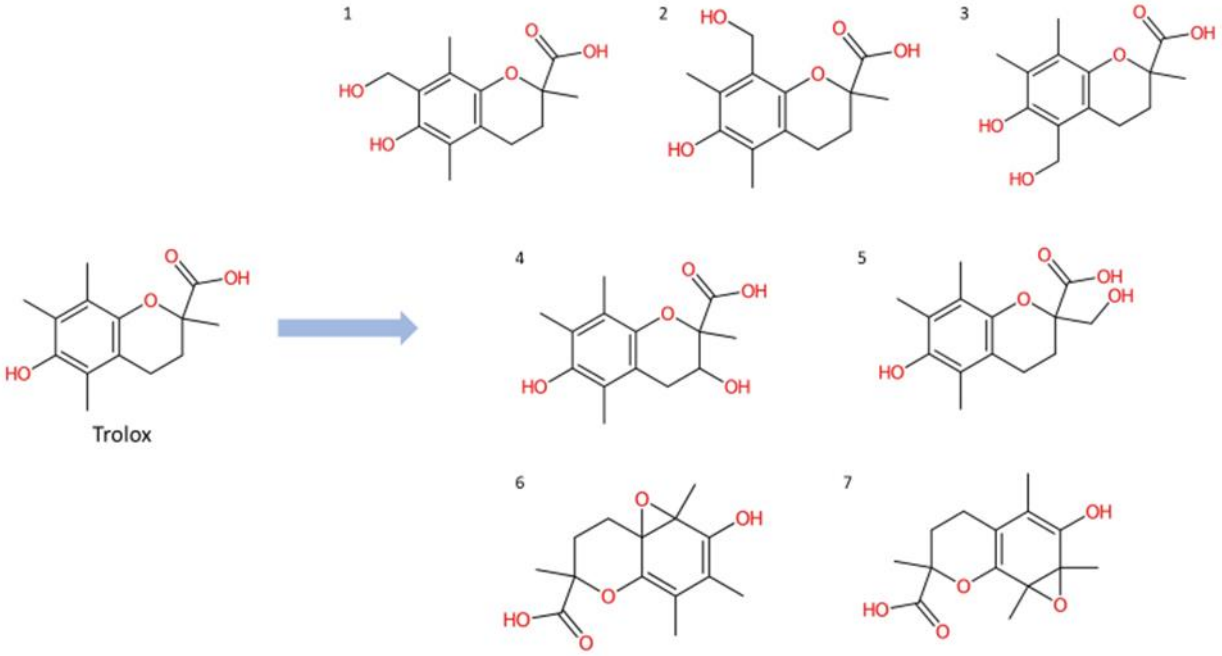

Figure A 31 Structures of inhibitor MW181 and its metabolites

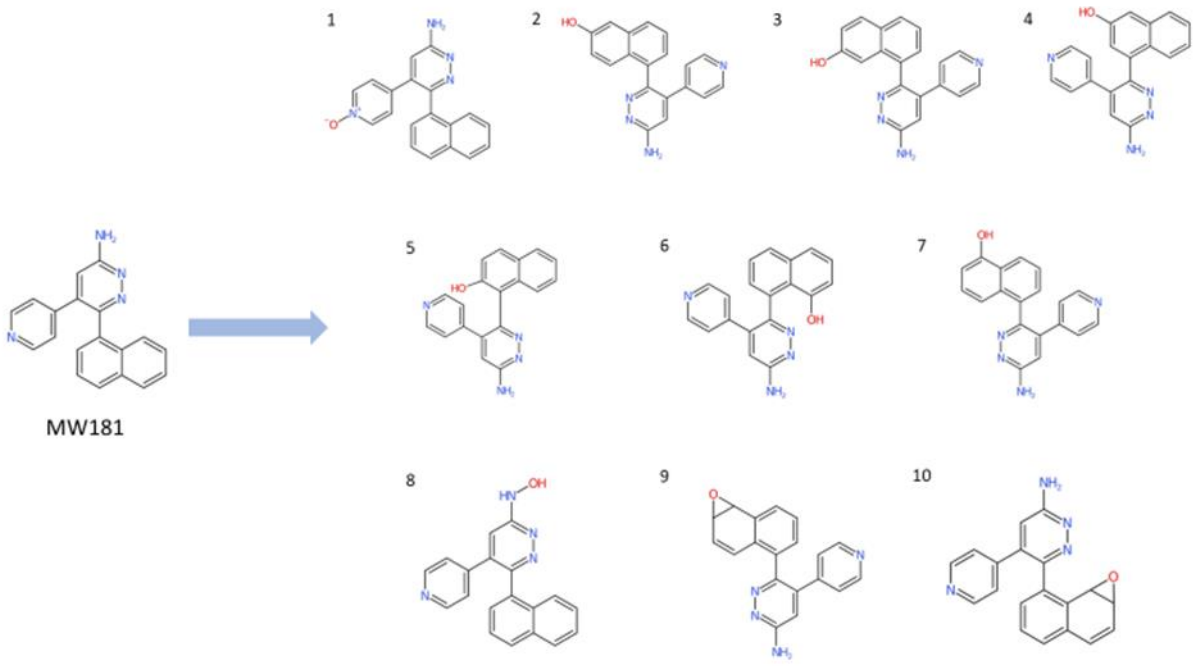

Figure A 32 Structures of inhibitor H-89 and its metabolites

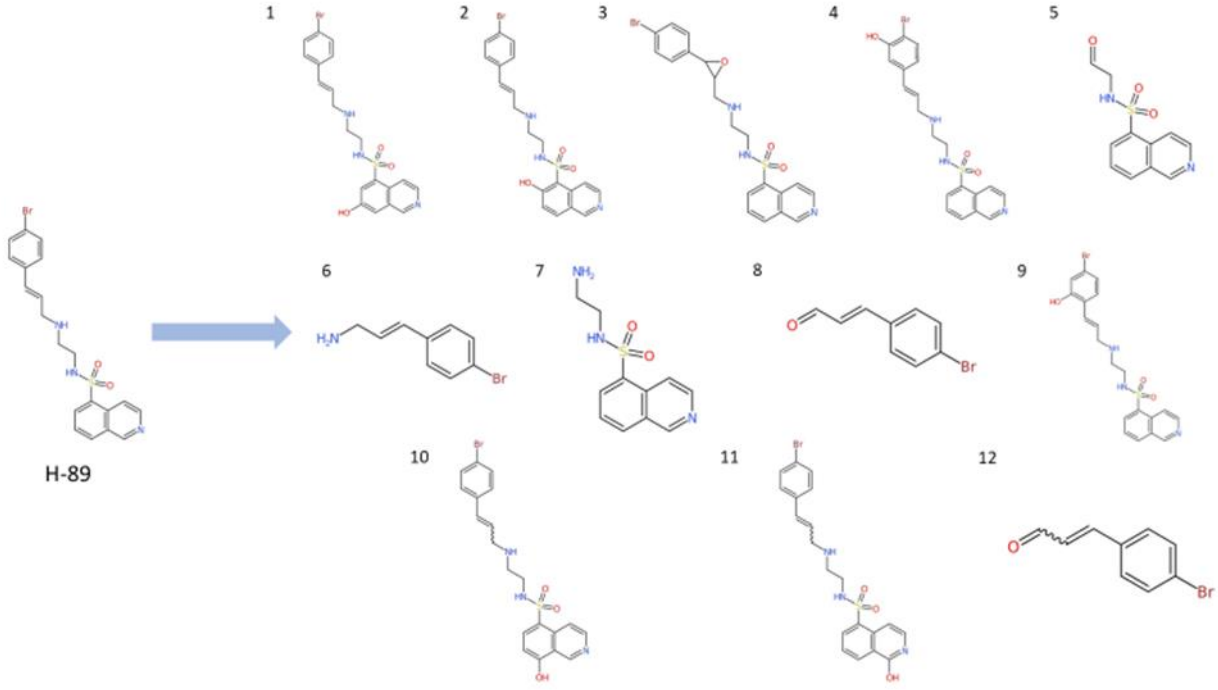

Figure A 33 Structures of inhibitor GF-109203X and its metabolites

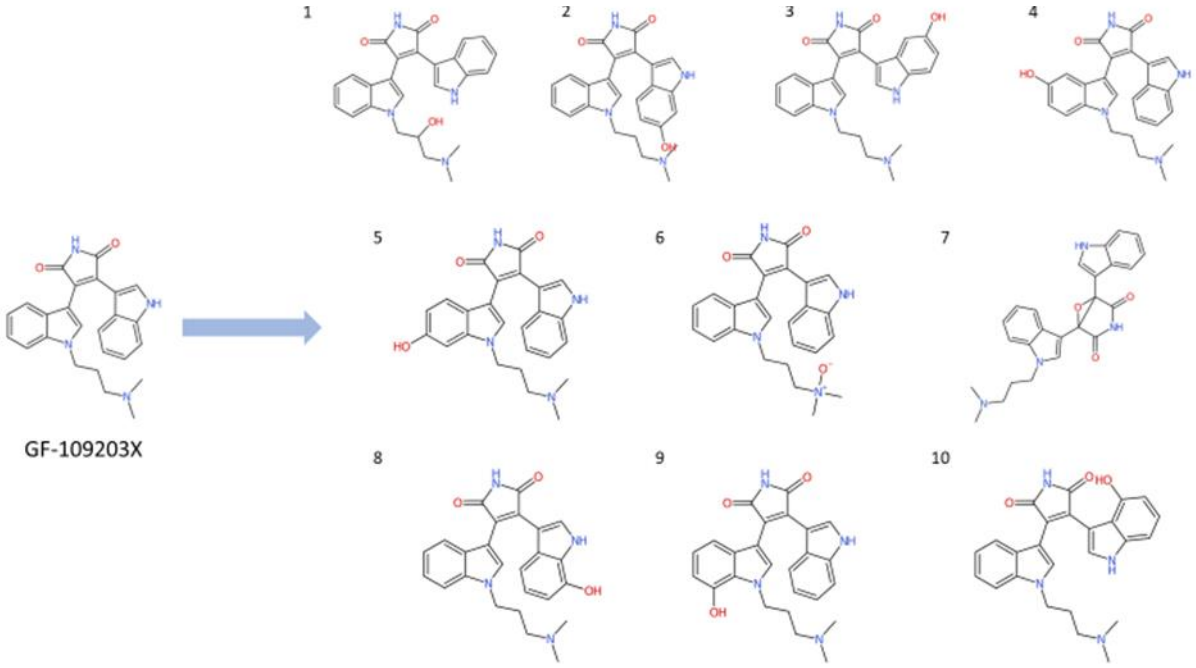

Figure A 34 Structures of inhibitor TTBK1-IN-2 and its metabolites

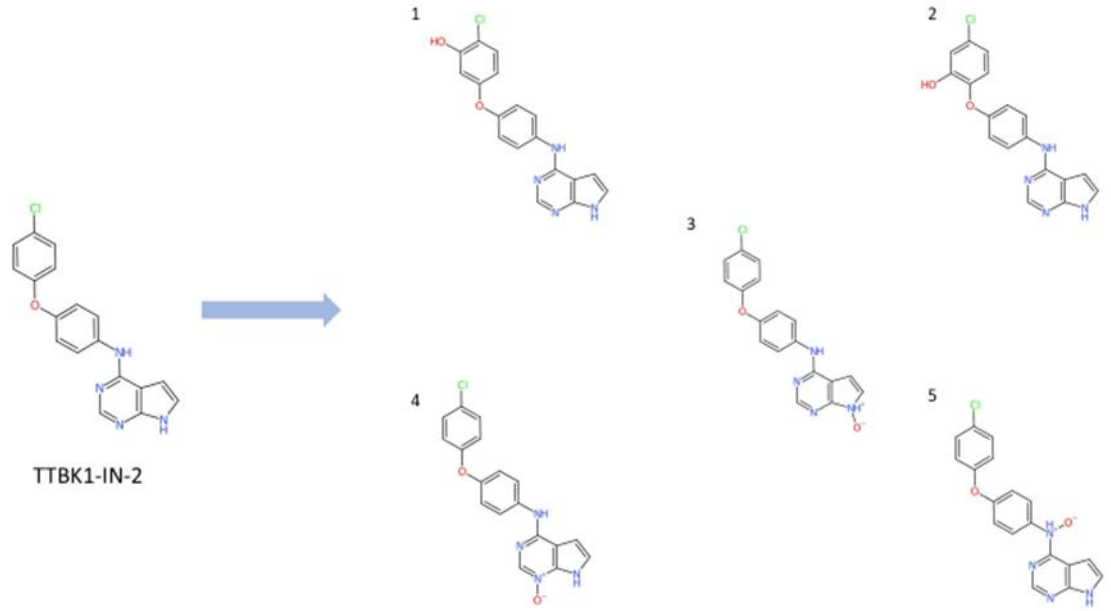

Appendix B

Table B 1 Results of CaMKII inhibitor.

Name	SMILES	AP_FWeight	BBB_Filter	LogBB	RuleOf5	RuleOf5_Code
KN93	CN(CC=CC1=CC=C(C=C1)Cl)CC2=CC=CC=C2N(CCO)S(=O)(=O)C3=CC=C(C=C3)OC	501,048	Low (39%)	0,064	1	Mw
MET1	CN(CC=CC1=CC=C(C=C1)Cl)C(C2=CC=CC=C2N(CCO)S(=O)(=O)C3=CC=C(C=C3)OC)O	517,047	Low (59%)	-0,289	1	Mw
MET2	CN(CC=CC1=CC=C(C=C1)Cl)CC2=CC=CC=C2N(CCO)S(=O)(=O)C3=CC=C(C=C3)O	487,021	Low (55%)	0,004	0	
MET3	CN(CC=CC1=CC=C(C=C1)Cl)CC2=CC=CC=C2N(CCO)S(=O)(=O)C3=CC=C(C(=C3)O)OC	517,047	Low (59%)	-0,127	1	Mw
MET4	CN(CC=CC1=CC=C(C(=C1)O)Cl)CC2=CC=CC=C2N(CCO)S(=O)(=O)C3=CC=C(C=C3)OC	517,047	Low (66%)	-0,271	1	Mw
MET5	CN(CC=CC1=CC=C(C=C1)Cl)CC2=C(C=CC=C2N(CCO)S(=O)(=O)C3=CC=C(C=C3)OC)O	517,047	Low (66%)	-0,286	1	Mw
MET6	CN(CC=CC1=C(C=C(C=C1)Cl)O)CC2=CC=CC=C2N(CCO)S(=O)(=O)C3=CC=C(C=C3)OC	517,047	Low (66%)	-0,229	1	Mw
MET7	C[N+](CC=CC1=CC=C(C=C1)Cl)(CC2=CC=CC=C2N(CCO)S(=O)(=O)C3=CC=C(C=C3)OC)[O-]	517,047	High	-0,931	1	Mw
MET8	CN(CC=CC1=CC=C(C=C1)Cl)CC2=CC=C(C=C2N(CCO)S(=O)(=O)C3=CC=C(C=C3)OC)O	517,047	Low (66%)	-0,133	1	Mw
MET9	CN(CC1C(C2=CC=C(C=C2)Cl)O1)CC3=CC=CC=C3N(CCO)S(=O)(=O)C4=CC=C(C=C4)OC	517,047	High (70%)	-0,573	1	Mw
MET10	CN(CC=CC1=CC=C(C=C1)Cl)CC2=CC=CC=C2N(CC=O)S(=O)(=O)C3=CC=C(C=C3)OC	499,032	High (76%)	0,047	0	

Table B 2 Results of CDK5 inhibitors.

Name	SMILES	AP_FWeight	BBB_Filter	LogBB	RuleOf5	RuleOf5_Code
(R)-roscovitine	CC[C@H](CO)NC1=NC(=C2C(=N1)N(C=N2)C(C)C)NCC3=CC=CC=C3	354,458	Low (74%)	-0,203	0	
MET1	CC[C@H](CO)NC1=NC(=C2C(=N1)N(C=N2)C(C)C)NCC3=C(C=CC=C3)O	370,457	Low (90%)	-0,289	0	
MET2	CC[C@H](CO)NC1=NC(=C2C(=N1)N(C=N2)C(C)C)NC(C3=CC=CC=C3)O	370,457	Low (90%)	-0,184	0	
MET3	CC[C@H](CO)NC1=NC(=C2C(=N1)N(C=N2)C(C)C)NCC3=CC=C(C=C3)O	370,457	Low (90%)	-0,394	0	
MET4	CC([C@H](CO)NC1=NC(=C2C(=N1)N(C=N2)C(C)C)NCC3=CC=CC=C3)O	370,457	Low (90%)	-0,52	0	
MET5	CC[C@H](C=O)NC1=NC(=C2C(=N1)N(C=N2)C(C)C)NCC3=CC=CC=C3	352,442	High (88%)	-0,181	0	
MET6	CC[C@H](CO)NC1=NC(=C2C(=N1)[NH2]C=N2)NCC3=CC=CC=C3	313,385	Low (90%)	-0,773	0	
MET7	C(C[C@H](CO)NC1=NC(=C2C(=N1)N(C=N2)C(C)C)NCC3=CC=CC=C3)O	370,457	Low (84%)	-0,455	0	
MET8	CC[C@H](CO)NC1=NC(=C2C(=N1)N(C=N2)C(C)CO)NCC3=CC=CC=C3	370,457	Low (90%)	-0,603	0	
MET9	C=C[C@H](CO)NC1=NC(=C2C(=N1)N(C=N2)C(C)C)NCC3=CC=CC=C3	352,442	High (70%)	-0,318	0	
MET10	CC[C@H](CO)NC1=NC(=C2C(=N1)N(C=N2)C(=C)C)NCC3=CC=CC=C3	352,442	High (70%)	-0,205	0	
(R)-CR8	CCC(CO)NC1=NC(=C2C(=N1)N(C=N2)C(C)C)NCC3=CC=C(C=C3)C4=CC=CC=N4	431,544	Low (90%)	-0,363	0	
MET1	CCC(CO)NC1=NC(=C2C(=N1)N(C=N2)C(C)C)NCC3=CC=C(C=C3)C4=CC=CC=[N+]4[O-]	447,543	Low (97%)	-0,857	0	
MET2	CCC(CO)NC1=NC(=C2C(=N1)N(C=N2)C(C)C)NC(C3=CC=C(C=C3)C4=CC=CC=N4)O	447,543	Low (97%)	-0,335	0	
MET3	CC(C(CO)NC1=NC(=C2C(=N1)N(C=N2)C(C)C)NCC3=CC=C(C=C3)C4=CC=CC=N4)O	447,543	Low (97%)	-0,662	0	
MET4	CCC(C=O)NC1=NC(=C2C(=N1)N(C=N2)C(C)C)NCC3=CC=C(C=C3)C4=CC=CC=N4	429,528	Low (66%)	-0,349	0	
MET5	CCC(CO)NC1=NC(=C2C(=N1)[NH2]C=N2)NCC3=CC=C(C=C3)C4=CC=CC=N4	390,471	Low (97%)	-0,84	0	
MET6	C(CC(CO)NC1=NC(=C2C(=N1)N(C=N2)C(C)C)NCC3=CC=C(C=C3)C4=CC=CC=N4)O	447,543	Low (90%)	-0,59	0	
MET7	CCC(CO)NC1=NC(=C2C(=N1)N(C=N2)C(C)CO)NCC3=CC=C(C=C3)C4=CC=CC=N4	447,543	Low (90%)	-0,768	0	
MET8	C=CC(CO)NC1=NC(=C2C(=N1)N(C=N2)C(C)C)NCC3=CC=C(C=C3)C4=CC=CC=N4	429,528	Low (70%)	-0,481	0	
MET9	CCC(CO)NC1=NC(=C2C(=N1)N(C=N2)C(=C)C)NCC3=CC=C(C=C3)C4=CC=CC=N4	429,528	Low (70%)	-0,375	0	
MET10	C(CC)(CO)=O	88,107	High (96%)	-0,115	0	
Olomoucine	CN1C=NC2=C(N=C(N=C21)NCCO)NCC3=CC=CC=C3	298,35	Low (74%)	-0,615	0	
MET1	CN1C=NC2=C(N=C(N=C21)NCCO)NCC3=C(C=CC=C3)O	314,349	Low (79%)	-0,7	0	
MET2	CN1C=NC2=C(N=C(N=C21)NCCO)NC(C3=CC=CC=C3)O	314,349	Low (84%)	-0,589	0	
MET3	CN1C=NC2=C(N=C(N=C21)NCCO)NCC3=CC=C(C=C3)O	314,349	Low (84%)	-0,799	0	
MET4	CN1C=NC2=C(N=C(N=C21)NCC=O)NCC3=CC=CC=C3	296,334	High (79%)	-0,591	0	
MET5	CN1C=NC2=C(N=C(N=C21)NCCO)N	208,224	High (84%)	-0,881	0	
MET6	C1=CC=C(C=C1)C=O	106,125	High (99%)	0,23	0	
MET7	CN1C=NC2=C(N=C(N=C21)N)NCC3=CC=CC=C3	254,296	High (88%)	-0,667	0	
MET8	C(C=O)O	60,053	High (96%)	-0,157	0	
MET9	C1=NC2=C(N=C(N=C2N1)NCCO)NCC3=CC=CC=C3	284,323	Low (90%)	-0,822	0	
MET10	O=C	30,026	High (99%)	0,125	0	
MET11	CN1C=2C(N=C1O)=C(N=C(N2)NCCO)NCC3=CC=CC=C3	314,349	Low (84%)	-0,706	0	
Butyrolactone I	CC(=CCC1=C(C=CC(=C1)CC2(C(=C(C(=O)O2)O)C3=CC=C(C=C3)O)C(=O)OC)O)C	424,453	Low (97%)	-0,702	0	
MET1	CC(=CC(C1=C(C=CC(=C1)CC2(C(=C(C(=O)O2)O)C3=CC=C(C=C3)O)C(=O)OC)O)O)C	440,453	Low (97%)	-0,863	0	
MET2	CC(=CCC1=C(C=CC(=C1)C(C2(C(=C(C(=O)O2)O)C3=CC=C(C=C3)O)C(=O)OC)O)O)C	440,453	Low (97%)	-0,759	0	
MET3	CC(=CCC1=C(C=CC(=C1)CC2(C(=C(C(=O)O2)O)C3=CC=C(C(=C3)O)O)C(=O)OC)O)C	440,453	Low (97%)	-0,757	0	
MET4	CC1(C(CC2=C(C=CC(=C2)CC3(C(=C(C(=O)O3)O)C4=CC=C(C=C4)O)C(=O)OC)O)O1)C	440,453	Low (97%)	-0,83	0	
MET5	CC(=CCC1=C(C(=CC(=C1)CC2(C(=C(C(=O)O2)O)C3=CC=C(C=C3)O)C(=O)OC)O)O)C	440,453	Low (97%)	-0,691	0	
MET6	CC(=CCC1=C(C=CC(=C1)CC2(C(=C(C(=O)O2)O)C3=CC=C(C(=C3)O)O)C(=O)OC)O)C	440,453	Low (97%)	-0,757	0	
MET7	C(=CCC1=C(C=CC(=C1)CC2(C(=C(C(=O)O2)O)C3=CC=C(C=C3)O)C(=O)OC)O)(C)CO	440,453	Low (97%)	-0,977	0	
Hymenialdisine	C1CNC(=O)C2=C(C1=C3C(=O)NC(=N3)N)C=C(N2)Br	324,143	Low (55%)	-0,441	0	
MET1	C1C(NC(=O)C2=C(C1=C3C(=O)NC(=N3)N)C=C(N2)Br)O	340,143	Low (84%)	-0,619	1	Hb
MET2	C1(CNC(=O)C2=C(C1=C3C(=O)NC(=N3)N)C=C(N2)Br)O	340,143	Low (84%)	-0,597	1	Hb
MET3	C1CNC(=O)C2=C(C1=C3C(=O)NC(=N3)N)C(=C(N2)Br)O	340,143	Low (84%)	-0,879	1	Hb

Table B 3 Results of CK1α-1δ-1ε-2 inhibitors.

Name	SMILES	AP_FWeight	BBB_Filter	LogBB	RuleOf5	RuleOf5_Code
IC261	COC1=CC(=C(C(=C1)OC)/C=C/2\C3=CC=CC=C3NC2=O)OC	311,34	High (99%)	-0,188	0	
MET1	COC1=CC(=C(C(=C1)OC)/C=C/2\C3=CC(=CC=C3NC2=O)O)OC	327,339	High (86%)	-0,354	0	
MET2	COC1=CC(=C(C(=C1)OC)/C=C/2\C3=CC=C(C=C3NC2=O)O)OC	327,339	High (79%)	-0,328	0	
MET3	OC1=CC(=C(C(=C1)OC)/C=C/2\C3=CC=CC=C3NC2=O)OC	297,313	High (88%)	-0,187	0	
MET4	COC1=CC(=C(C(=C1)OC)/C=C/2\C3=CC=CC=C3NC2=O)O	297,313	Low (79%)	-0,589	0	
MET5	COC1=CC(=C(C(=C1)OC)/C=C/2\C3=CC=CC(=C3NC2=O)O)OC	327,339	High (79%)	-0,312	0	
MET6	COC1=CC(=C(C(=C1)OC)/C=C/2\C3=C(C=CC=C3NC2=O)O)OC	327,339	High (73%)	-0,424	0	
MET7	COC1=CC(=C(C(=C1)O)C=C2C3=CC=CC=C3NC2=O)OC	297,313	Low (79%)	-0,589	0	
MET8	COC1=CC(=C(C(=C1)OC)C=C2C3=CC=CC(=C3NC2=O)O)OC	327,339	High (79%)	-0,312	0	
MET9	C1(=CC(=C(C(=C1)OC)C=C2C3=CC=CC=C3NC2=O)OC)O	297,313	High (88%)	-0,187	0	
MET10	O=C	30,026	High (99%)	0,125	0	
MET11	COC1=CC(=C(C(=C1)OC)C=C2C3=CC=C(C=C3NC2=O)O)OC	327,339	High (79%)	-0,328	0	
MET12	COC1=CC(=C(C(=C1)OC)C=C2C3=CC(=CC=C3NC2=O)O)OC	327,339	High (86%)	-0,354	0	
TBCA	C1=C(C(=C(C(=C1Br)Br)Br)Br)/C=C/C(=O)O	463,767	High (84%)	-0,267	1	LP
MET1	C1(=C(C(=C(C(=C1Br)Br)Br)Br)/C=C/C(=O)O)O	479,766	High (67%)	-0,208	0	
MET2	C1=C(C(=C(C(=C1Br)Br)Br)Br)C2C(C(=O)O)O2	479,766	High (77%)	-0,761	0	

Table B 4 Results of DYRK1A/2 inhibitors.

Name	SMILES	AP_FWeight	BBB_Filter	LogBB	RuleOf5	RuleOf5_Code
Harmine	CC1=NC=CC2=C1NC3=C2C=CC(=C3)OC	212,253	High (96%)	-0,032	0	
Pyrazolo 1,5-b	CC(=O)C1=C2C=CC=NN2N=C1	161,164	High (99%)	0,04	0	
MET1	CC(O)C1=C2C=CC=NN2N=C1	163,18	High (94%)	-0,217	0	
MET2	CC(=O)C1=C2C=C(C=NN2N=C1)O	177,163	High (76%)	-0,54	0	
MET3	C(=O)(C1=C2C=CC=NN2N=C1)CO	177,163	High (86%)	-0,208	0	
MET4	CC(=O)C1=C2C=CC=[N+](N2N=C1)[O-]	177,163	High (99%)	0,061	0	
MET5	CC(=O)C1=C2C=CC(=NN2N=C1)O	177,163	Low (48%)	-0,863	0	
MET6	CC(=O)C1=C2C=CC=NN2[N+](=C1)[O-]	177,163	High (99%)	-0,025	0	
MET7	CC(=O)C1=C2C=CC=N[N+]2(N=C1)[O-]	177,163	High	-0,649	0	
Aristolactam BII	COC1=C(C2=C3C(=C1)C(=O)NC3=CC4=CC=CC=C42)OC	279,297	High (96%)	0,422	0	
MET1	COC1=C(C2=C3C(=C1)C(=O)NC3=CC4=CC(=CC=C42)O)OC	295,297	High (88%)	0,25	0	
MET2	COC1=C(C2=C3C(=C1)C(=O)NC3=CC4=CC=C(C=C42)O)OC	295,297	High (82%)	0,179	0	
MET3	OC1=C(C2=C3C(=C1)C(=O)NC3=CC4=CC=CC=C42)OC	265,27	High (91%)	0,31	0	
MET4	COC1=C(C2=C3C(=C1)C(=O)NC3=CC4=CC=CC=C42)O	265,27	High (91%)	0,326	0	
MET5	COC1=C(C2=C3C(=C1)C(=O)NC3=CC4=CC=CC(=C42)O)OC	295,297	High (86%)	0,229	0	
MET6	COC1=C(C2=C3C(=C1)C(=O)NC3=CC4=C(C=CC=C42)O)OC	295,297	High (79%)	0,095	0	
MET7	COC1=C(C2=C3C(=C1)C(=O)NC3=CC4=C5C(=CC=C42)O5)OC	293,281	High (94%)	-0,233	0	
MET8	COC1=C(C2=C3C(=C1)C(=O)NC3=CC4=CC=C5C(=C42)O5)OC	293,281	High (94%)	-0,13	0	
MET9	O=C	30,026	High (99%)	0,125	0	
ZDWX-25	COC(=O)C1=CC2=C(C=C1)C3=C(N2)C(=NC=C3)NC(=O)C4CC4	309,327	High (84%)	-0,341	0	
MET1	COC(=O)C1=CC2=C(C=C1O)C3=C(N2)C(=NC=C3)NC(=O)C4CC4	325,326	Low (55%)	-0,472	0	
MET2	COC(=O)C1=CC2=C(C=C1)C3=C(N2)C(=NC=C3)N(C(=O)C4CC4)O	325,326	Low (70%)	-1,076	0	
MET3	COC(=O)C1=CC2=C(C(=C1)O)C3=C(N2)C(=NC=C3)NC(=O)C4CC4	325,326	Low (70%)	-0,344	0	
MET4	COC(=O)C1=CC2=C(C=C1)C3=C(N2)C(=NC=C3)NC(=O)C4(CC4)O	325,326	Low (67%)	-0,537	0	
MET5	COC(=O)C1=CC2=C(C=C1)C3=C(N2)C(=NC=C3)NC(=O)C4(CC4)O	325,326	Low (67%)	-0,537	0	
MET6	COC(=O)C1=CC2=C(C=C1)C3=C(N2)C(=NC=C3)NC(=O)C4C(C4)O	325,326	Low (39%)	-0,6	0	
MET7	O(C(=O)C1=CC2=C(C=C1)C3=C(N2)C(=NC=C3)NC(=O)C4CC4)CO	325,326	Low (67%)	-0,747	0	
MET8	COC(=O)C1=CC2=C(C=C1)C3=C(N2)C(=NC=C3O)NC(=O)C4CC4	325,326	Low (48%)	-0,526	0	

Table B 5 Results of ERK1-2 inhibitors.

Name	SMILES	AP_FWeight	BBB_Filter	LogBB	RuleOf5	RuleOf5_Code
FR-180204	C1=CC=C(C=C1)C2=NN3C=CC=CC3=C2C4=CC5=C(NN=C5N=N4)N	327,35	Low (55%)	-0,881	0	
MET1	C1=CC=C(C=C1)C2=NN3C=CC=CC3=C2C4=CC5=C(NN=C5N=N4)NO	343,35	Low (79%)	-0,661	0	
MET2	C=1C=C(C=CC1O)C2=NN3C=CC=CC3=C2C4=CC5=C(NN=C5N=N4)N	343,35	Low (84%)	-0,959	0	
MET3	C1=CC=C(C=C1)C2=NN3C=C(C=CC3=C2C4=CC5=C(NN=C5N=N4)N)O	343,35	Low (97%)	-1,053	0	
MET4	C1=CC=C(C=C1)C2=NN3C=CC(=CC3=C2C4=CC5=C(NN=C5N=N4)N)O	343,35	Low (84%)	-0,967	0	
MET5	C=1C=CC(=CC1O)C2=NN3C=CC=CC3=C2C4=CC5=C(NN=C5N=N4)N	343,35	Low (90%)	-1,013	0	
PD98059	COC1=CC=CC(=C1N)C2=CC(=O)C3=CC=CC=C3O2	267,286	High (94%)	-0,277	0	
MET1	COC1=CC=CC(=C1N)C2=CC(=O)C3=CC(=CC=C3O2)O	283,286	Low (70%)	-0,558	0	
MET2	COC1=CC=CC(=C1N)C2=CC(=O)C3=CC=C(C=C3O2)O	283,286	High (81%)	-0,422	0	
MET3	OC1=CC=CC(=C1N)C2=CC(=O)C3=CC=CC=C3O2	253,259	High (79%)	-0,322	0	
MET4	COC1=CC=C(C(=C1N)C2=CC(=O)C3=CC=CC=C3O2)O	283,286	High (84%)	-0,286	0	
MET5	COC1=C(C=CC(=C1N)C2=CC(=O)C3=CC=CC=C3O2)O	283,286	High (84%)	-0,293	0	
MET6	COC1=CC(=CC(=C1N)C2=CC(=O)C3=CC=CC=C3O2)O	283,286	High (77%)	-0,635	0	
MET7	COC1=CC=CC(=C1N)C23C(C(=O)C4=CC=CC=C4O2)O3	283,286	High (99%)	-0,069	0	
MET8	COC1=CC=CC(=C1N)C2=CC(=O)C3=C(C=CC=C3O2)O	283,286	High (77%)	-0,436	0	
MET9	COC1=CC=CC(=C1NO)C2=CC(=O)C3=CC=CC=C3O2	283,286	High (81%)	-0,259	0	
MET10	COC1=CC=CC(=C1N)C2=CC(O)C3=CC=CC=C3O2	269,302	High (99%)	-0,094	0	
MET11	COC1=CC=CC(=C1N)C2=CC(=O)C3=CC=CC(=C3O2)O	283,286	Low (71%)	-0,486	0	
MET12	O=C	30,026	High (99%)	0,125	0	
U0126	C1=CC=C(C(=C1)N)SC(=C(C#N)C(=C(N)SC2=CC=CC=C2N)C#N)N	380,496	Low	-1,283	1	Hb
MET1	C1=CC=C(C(=C1)N)SC(=C(C#N)C(=C(N)SC2=CC=CC(=C2N)O)C#N)N	396,495	Low	-1,134	1	Hb
MET2	C1=C(C=C(C(=C1)N)SC(=C(C#N)C(=C(N)SC2=CC=CC=C2N)C#N)N)O	396,495	Low	-1,226	1	Hb
MET3	C1=CC=C(C(=C1)N)SC(=C(C#N)C(=C(N)SC2=CC=CC=C2NO)C#N)N	396,495	Low	-1,023	1	Hb
MET4	C1=CC=C(C(=C1)[NH2+][O-])SC(=C(C#N)C(=C(N)SC2=CC=CC=C2N)C#N)N	396,495	Low	-1,142	1	Hb
MET5	C1=CC=C(C(=C1)N)S(C(=C(C#N)C(=C(N)SC2=CC=CC=C2N)C#N)N)=O	396,495	Low	-1,49	1	Hb

Table B 6 Results of GSK3β inhibitors.

Name	SMILES	AP_FWeight	BBB_Filter	LogBB	RuleOf5	RuleOf5_Code
Lithium	[Li]	6,939	High	-0,053	0	
Hydrogen Sulfide	OS(=O)[O-]	81,07	Low	-0,471	0	
Tideglusib	C1=CC=C(C=C1)CN2C(=O)N(SC2=O)C3=CC=CC4=CC=CC=C43	334,399	High (99%)	0,295	0	
MET01	C1=CC(=C(C=C1)CN2C(=O)N(SC2=O)C3=CC=CC4=CC=CC=C43)O	350,398	High (91%)	0,139	0	
MET02	C1=CC=C(C=C1)C(N2C(=O)N(SC2=O)C3=CC=CC4=CC=CC=C43)O	350,398	High (89%)	0,051	0	
MET03	C1=CC=C(C=C1)CN2C(=O)N(SC2=O)C3=C(C=CC4=CC=CC=C43)O	350,398	High (84%)	0,062	0	
MET04	C1=CC=C(C=C1)CN2C(=O)N(SC2=O)C3=CC(=CC4=CC=CC=C43)O	350,398	High (91%)	0,086	0	
MET05	C1=CC=C(C=C1)CN2C(=O)N(SC2=O)C3=CC=CC4=CC(=CC=C43)O	350,398	High (91%)	0,105	0	
MET06	C1=CC=C(C=C1)CN2C(=O)N(SC2=O)C3=CC=CC4=CC=C(C=C43)O	350,398	High (91%)	-0,054	0	
MET07	C1(=CC=C(C=C1)CN2C(=O)N(SC2=O)C3=CC=CC4=CC=CC=C43)O	350,398	High (91%)	0,09	0	
MET08	C1=CC=C(C=C1)CN2C(=O)N(SC2=O)C3=CC=CC4=CC=CC(=C43)O	350,398	High (89%)	0,051	0	
MET09	C1=CC=C(C=C1)CN2C(=O)N(SC2=O)C3=CC=CC4=C(C=CC=C43)O	350,398	High (89%)	-0,084	0	
MET10	C1=CC=C(C=C1)CN2C(=O)N(SC2=O)C3=CC4C(C5=CC=CC=C53)O4	350,398	High (99%)	-0,003	0	
MET11	C1=CC=C(C=C1)CN2C(=O)N(SC2=O)C3=CC=CC4=C5C(=CC=C43)O5	348,382	High (99%)	0,002	0	
MET12	C1=CC=C(C=C1)CN2C(=O)N(SC2=O)C3=CC=CC4=CC=C5C(=C43)O5	348,382	High (99%)	0,031	0	
MET13	C1=CC=C(C=C1)CN2C(=O)N(C3=CC=CC4=CC=CC=C34)S(C2=O)=O	350,398	High	0,11	0	
MET14	C=1C=CC(=CC1O)CN2C(=O)N(SC2=O)C3=CC=CC4=CC=CC=C34	350,398	High (91%)	-0,054	0	
MET15	C1=CC=C(C=C1)CN2C(=O)N(SC2=O)C3=CC=C(C4=CC=CC=C34)O	350,398	High (91%)	-0,061	0	
Valproate	CCCC(CCC)C(=O)O	144,215	Low (67%)	-0,59	0	
MET1	CCC(C(CCC)C(=O)O)O	160,215	Low (66%)	-0,907	0	
MET2	CC(CC(CCC)C(=O)O)O	160,215	Low (70%)	-0,942	0	
MET3	C(CCC(CCC)C(=O)O)O	160,215	Low (66%)	-0,917	0	
MET4	C=CCC(CCC)C(=O)O	142,199	High (79%)	-0,691	0	
MET5	CCCC(CCC)(C(=O)O)O	160,215	Low (66%)	-0,807	0	
ARN25068	C1CC1C2=CC(=NN2)NC3=NC(=NC4=C3SC=C4)NCC5=CC=CC=C5	362,459	Low (67%)	-0,423	0	
MET1	C1CC1C2=CC(=NN2)NC3=NC(=NC4=C3SC=C4)NCC5=C(C=CC=C5)O	378,458	Low (74%)	-0,409	0	
MET2	C1CC1C2=CC(=NN2)NC3=NC(=NC4=C3SC=C4)NC(C5=CC=CC=C5)O	378,458	Low (84%)	-0,457	0	
MET3	C1CC1C2=CC(=NN2)NC3=NC(=NC4=C3SC=C4)NCC5=CC=C(C=C5)O	378,458	Low (74%)	-0,562	0	
MET4	C1CC1C2=CC(=NN2)NC3=NC(=NC4=C3SC=C4)N	272,333	High (76%)	-0,593	0	
MET5	C1=CC=C(C=C1)C=O	106,125	High (99%)	0,23	0	
MET6	C1(CC1C2=CC(=NN2)NC3=NC(=NC4=C3SC=C4)NCC5=CC=CC=C5)O	378,458	Low (79%)	-0,637	0	
MET7	C1CC1(C2=CC(=NN2)NC3=NC(=NC4=C3SC=C4)NCC5=CC=CC=C5)O	378,458	Low (79%)	-0,723	0	
MET8	C1CC1C2=CC(=NN2)NC3=NC(=NC4=C3SC5C4O5)NCC6=CC=CC=C6	378,458	Low (59%)	-0,843	0	
MET9	C1CC1C2=CC(=NN2)NC3=NC(=NC4=C3[S+](C=C4)[O-])NCC5=CC=CC=C5	378,458	High (74%)	-0,706	0	
MET10	C1CC1C2=CC(=NN2)NC3=NC(=NC4=C3SC(=C4)O)NCC5=CC=CC=C5	378,458	Low (84%)	-0,566	0	
MET11	C1CC1C2=CC(=NN2)[NH+](C3=NC(=NC4=C3SC=C4)NCC5=CC=CC=C5)[O-]	378,458	High	0,092	0	

Table B 7 Results of GSK3β inhibitors.

Name	SMILES	AP_FWeight	BBB_Filter	LogBB	RuleOf5	RuleOf5_Code
AR-A014418	COC1=CC=C(C=C1)CNC(=O)NC2=NC=C(S2)[N+](=O)[O-]	308,317	High (96%)	-0,141	0	
MET1	COC1=CC=C(C=C1)C(NC(=O)NC2=NC=C(S2)[N+](=O)[O-])O	324,317	High (73%)	-0,21	0	
MET2	OC1=CC=C(C=C1)CNC(=O)NC2=NC=C(S2)[N+](=O)[O-]	294,29	High (81%)	-0,213	0	
MET3	COC1=CC=C(C(=C1)O)CNC(=O)NC2=NC=C(S2)[N+](=O)[O-]	324,317	Low (42%)	-0,304	0	
MET4	O=C	30,026	High (99%)	0,125	0	
MET5	COC1=CC=C(C=C1)CNC(=O)NC2=NC=C(S2)N	278,334	High (96%)	-0,475	0	
MET6	COC1=CC=C(C=C1)CNC(=O)NC2=NC=C([N+](=O)[O-])S2=	*	*	*	*	
MET7	COC=1C=CC(=CC1O)CNC(=O)NC2=NC=C(S2)[N+](=O)[O-]	324,317	High (79%)	-0,39	0	
SB-216763	CN1C=C(C2=CC=CC=C21)C3=C(C(=O)NC3=O)C4=C(C=C(C=C4)Cl)Cl	371,225	Low (52%)	-0,149	0	
MET1	CN1C=C(C2=CC(=CC=C21)O)C3=C(C(=O)NC3=O)C4=C(C=C(C=C4)Cl)Cl	387,224	Low (79%)	-0,303	0	
MET2	CN1C=C(C2=CC=C(C=C21)O)C3=C(C(=O)NC3=O)C4=C(C=C(C=C4)Cl)Cl	387,224	Low (84%)	-0,322	0	
MET3	CN1C=C(C2=CC=CC=C21)C3=C(C(=O)NC3=O)C4=C(C=C(C(=C4)O)Cl)Cl	387,224	Low (84%)	-0,255	0	
MET4	CN1C=C(C2=CC=CC=C21)C34C(C(=O)NC3=O)(C5=C(C=C(C=C5)Cl)Cl)O4	387,224	Low (67%)	-0,609	0	
MET5	CN1C=C(C2=CC=CC(=C21)O)C3=C(C(=O)NC3=O)C4=C(C=C(C=C4)Cl)Cl	387,224	Low (79%)	-0,307	0	
MET6	CN1C=C(C2=C(C=CC=C21)O)C3=C(C(=O)NC3=O)C4=C(C=C(C=C4)Cl)Cl	387,224	Low (74%)	-0,335	0	
MET7	CN1C=C(C2=CC=CC=C21)C3=C(C(=O)NC3=O)C4=C(C(=C(C=C4)Cl)O)Cl	387,224	Low (79%)	-0,234	0	
MET8	CN1C=C(C2=CC=CC=C21)C3=C(C(=O)NC3=O)C4=C(C=C(C(=C4)O)Cl)Cl	387,224	Low (84%)	-0,255	0	
MET9	CN1C=C(C2=CC=CC=C21)C3=C(C(=O)NC3=O)C4=C(C=C(C=C4O)Cl)Cl	387,224	Low (84%)	-0,247	0	
MET10	C1=C(C2=CC=CC=C2N1)C3=C(C(=O)NC3=O)C4=C(C=C(C=C4)Cl)Cl	357,198	Low (48%)	-0,29	0	
MET11	O=C	30,026	High (99%)	0,125	0	
SB-415286	C1=CC=C(C(=C1)C2=C(C(=O)NC2=O)NC3=CC(=C(C=C3)O)Cl)[N+](=O)[O-]	359,727	Low (84%)	-0,575	0	
MET1	C1=CC=C(C(=C1O)C2=C(C(=O)NC2=O)NC3=CC(=C(C=C3)O)Cl)[N+](=O)[O-]	375,727	Low (84%)	-0,583	0	
MET2	C1=CC=C(C(=C1)C2=C(C(=O)NC2=O)NC3=CC(=C(C=C3O)O)Cl)[N+](=O)[O-]	375,727	Low (84%)	-0,507	0	
MET3	C1=C(C=C(C(=C1)C2=C(C(=O)NC2=O)NC3=CC(=C(C=C3)O)Cl)[N+](=O)[O-])O	375,727	Low (90%)	-0,631	0	
MET4	C1=CC=C(C(=C1)C2=C(C(=O)NC2=O)NC3=CC(=C(C(=C3)O)O)Cl)[N+](=O)[O-]	375,727	Low (90%)	-0,549	0	
MET5	C1=CC=C(C(=C1)C2=C(C(=O)NC2=O)NC3=C(C(=C(C=C3)O)Cl)O)[N+](=O)[O-]	375,727	Low (84%)	-0,468	0	
6-BIO	Brc1cc2NC(=O)C(=C3C(=NO)c4c(N3)cccc4)c2cc1	356,185	Low (70%)	-0,086	0	
MET1	BrC1=CC=2NC(=O)C(=C3C(=NO)C4=C(N3)C=CC=C4)C2C=C1O	372,185	Low (97%)	-0,362	0	
MET2	BrC1=CC=2NC(=O)C(=C3C(=NO)C4=C(N3)C=C(C=C4)O)C2C=C1	372,185	Low (97%)	-0,258	0	
MET3	BrC1=CC=2NC(=O)C(=C3C(=NO)C4=C(N3)C=CC(=C4)O)C2C=C1	372,185	Low (97%)	-0,292	0	
MET4	BrC1=CC=2NC(=O)C(=C3C(=NO)C4=C(N3)C(=CC=C4)O)C2C=C1	372,185	Low (97%)	-0,397	0	
MET5	BrC1=C(C=2NC(=O)C(=C3C(=NO)C4=C(N3)C=CC=C4)C2C=C1)O	372,185	Low (97%)	-0,594	0	
MET6	BrC1=CC=2NC(=O)C(=C3C(=NO)C4=C(N3)C=CC=C4O)C2C=C1	372,185	Low (97%)	-0,452	0	
MET7	BrC1=CC=2NC(=O)C(=C3C(=NO)C4=C(N3)C=CC=C4)C2C(=C1)O	372,185	Low (97%)	-0,46	0	

Table B 8 Results of GSK3β inhibitors.

Name	SMILES	AP_FWeight	BBB_Filter	LogBB	RuleOf5	RuleOf5_Code
6-BIBEO	BrCCONc1c(-c2c(O)[nH]c3c2ccc(Br)c3)[nH]c2c1cccc2	465,156	Low	-0,132	0	
MET1	BrCCONC1=C(C2=C(O)NC3=C2C=CC(Br)=C3)NC4=C1C=C(C=C4)O	481,156	Low (62%)	-0,314	0	
MET2	BrCCONC1=C(C2=C(O)NC3=C2C=CC(Br)=C3)NC4=C1C=CC(=C4)O	481,156	Low (66%)	-0,273	0	
MET3	BrCCONC1=C(C2=C(O)NC3=C2C=C(C(Br)=C3)O)NC4=C1C=CC=C4	481,156	Low (70%)	-0,265	0	
MET4	BrCCONC1=C(C2=C(O)NC3=C2C=CC(Br)=C3O)NC4=C1C=CC=C4	481,156	Low (79%)	-0,308	0	
MET5	BrCCONC1=C(C2=C(O)NC3=C2C=CC(Br)=C3)NC4=C1C=CC=C4O	481,156	Low (70%)	-0,338	0	
MET6	BrCCONC1=C(C2=C(O)NC3=C2C(=CC(Br)=C3)O)NC4=C1C=CC=C4	481,156	Low (70%)	-0,319	0	
MET7	BrCCONC1=C(C2=C(O)NC3=C2C=CC(Br)=C3)NC4=C1C(=CC=C4)O	481,156	Low (66%)	-0,277	0	
MET8	BrC(CONC1=C(C2=C(O)NC3=C2C=CC(Br)=C3)NC4=C1C=CC=C4)O	481,156	Low (62%)	-0,366	0	
6-BIDECO	BrCCON=C1C(=C2C(=O)Nc3c2ccc(Br)c3)Nc2c1cccc2	463,14	Low (42%)	0,143	0	
MET1	BrCCON=C1C(=C2C(=O)NC3=C2C=CC(Br)=C3)NC4=C1C=C(C=C4)O	479,14	Low (97%)	-0,062	0	
MET2	BrCCON=C1C(=C2C(=O)NC3=C2C=CC(Br)=C3)NC4=C1C=CC(=C4)O	479,14	Low (97%)	-0,044	0	
MET3	BrCCON=C1C(=C2C(=O)NC3=C2C=C(C(Br)=C3)O)NC4=C1C=CC=C4	479,14	Low (97%)	-0,102	0	
MET4	BrCCON=C1C(=C2C(=O)NC3=C2C=CC(Br)=C3O)NC4=C1C=CC=C4	479,14	Low (90%)	-0,423	0	
MET5	BrCCON=C1C(=C2C(=O)NC3=C2C=CC(Br)=C3)NC4=C1C=CC=C4O	479,14	Low (97%)	-0,215	0	
MET6	BrCCON=C1C(=C2C(=O)NC3=C2C(=CC(Br)=C3)O)NC4=C1C=CC=C4	479,14	Low (97%)	-0,222	0	
MET7	BrCCON=C1C(=C2C(=O)NC3=C2C=CC(Br)=C3)NC4=C1C(=CC=C4)O	479,14	Low (97%)	-0,335	0	
MET8	BrC(CON=C1C(=C2C(=O)NC3=C2C=CC(Br)=C3)NC4=C1C=CC=C4)O	479,14	Low (84%)	-0,149	0	
MET9	BrC(CON=C1C(=C2C(=O)NC3=C2C=CC(Br)=C3)NC4=C1C=CC=C4)O	479,14	Low (84%)	-0,149	0	
MET10	BrCCON=C1C(=C2C(=O)NC3=C2C=CC(Br)=C3)NC4=C1C=C(C=C4)O	479,14	Low (97%)	-0,062	0	
MET11	C(CBr)=O	122,955	High (99%)	0,039	0	
MET12	BrC1=CC=2NC(=O)C(=C3C(=NO)C4=C(N3)C=CC=C4)C2C=C1	356,185	Low (70%)	-0,086	0	
6-BIMYEO	Brc1cc2NC(=O)C(=C3C(=NO[C-]CN4CCOCC4)c4c([N+]3)cccc4)c2cc1	466,322	Low	-0,063	0	
MET1	BrC1=CC=2NC(=O)C(=C3C(=NO[CH-]CN4CCOCC4)C5=C([NH2+]3)C=CC=C5)C2C=C1O	485,345	Low	-0,209	0	
MET2	BrC1=CC=2NC(=O)C(=C3C(=NO[CH-]CN4CCOCC4)C5=C([NH2+]3)C=C(C=C5)O)C2C=C1	485,345	Low	-0,193	0	
MET3	BrC1=CC=2NC(=O)C(=C3C(=NO[CH-]CN4CCOCC4)C5=C([NH2+]3)C=CC(=C5)O)C2C=C1	485,345	Low	-0,237	0	
MET4	BrC1=CC=2NC(=O)C(=C3C(=NO[CH-]C[N+]4(CCOCC4)[O-])C5=C([NH2+]3)C=CC=C5)C2C=C1	485,345	Low	-1,028	0	
MET5	BrC1=CC=2NC(=O)C(=C3C(=NO[CH-]C=O)C4=C([NH2+]3)C=CC=C4)C2C=C1	398,223	Low	-0,654	0	
MET6	N1CCOCC1	87,122	High (94%)	0,231	0	
MET7	BrC1=CC=2NC(=O)C(=C3C(=NO[CH-]CN4C(COCC4)O)C5=C([NH2+]3)C=CC=C5)C2C=C1	485,345	Low	-0,579	0	
MET8	BrC1=CC=2NC(=O)C(=C3C(=NO[CH-]CN4C(COCC4)O)C5=C([NH2+]3)C=CC=C5)C2C=C1	485,345	Low	-0,579	0	
MET9	BrC1=CC=2NC(=O)C(=C3C(=NO[CH-]CN4CC(OCC4)O)C5=C([NH2+]3)C=CC=C5)C2C=C1	485,345	Low	-0,564	0	
MET10	BrC1=CC=2NC(=O)C(=C3C(=NO[CH-]CN4CCOCC4)C5=C([NH2+]3)C(=CC=C5)O)C2C=C1	485,345	Low	-0,264	0	
MET11	BrC1=C(C=2NC(=O)C(=C3C(=NO[CH-]CN4CCOCC4)C5=C([NH2+]3)C=CC=C5)C2C=C1)O	485,345	Low	-0,178	0	
MET12	BrC1=CC=2NC(=O)C(=C3C(=NO[CH-]CN4CCOCC4)C5=C([NH2+]3)C=CC=C5O)C2C=C1	485,345	Low	-0,262	0	
MET13	BrC1=CC=2NC(=O)C(=C3C(=NO[CH-]CN4CCOCC4)C5=C([NH2+]3)C=CC=C5)C2C(=C1)O	485,345	Low	-0,243	0	
MET14	BrC1=CC=2NC(=O)C(=C3C(=NO[CH-]C(N4CCOCC4)O)C5=C([NH2+]3)C=CC=C5)C2C=C1	485,345	Low	-0,536	0	
MET15	BrC1=CC=2NC(=O)C(=C3C(=NO[CH-]CN4C(COCC4)O)C5=C([NH2+]3)C=CC=C5)C2C=C1	485,345	Low	-0,579	0	

Table B 9 Results of JNK inhibitors.

Name	SMILES	AP_FWeight	BBB_Filter	LogBB	RuleOf5	RuleOf5_Code
SP600125	C1=CC=C2C(=C1)C3=NNC4=CC=CC(=C43)C2=O	220,232	High (91%)	-0,017	0	
MET1	O=C1C2=C3C(=NNC3=CC=C2)C=4C1=CC(=CC4)O	236,231	Low (52%)	-0,149	0	
MET2	O=C1C2=C3C(=NNC3=CC=C2)C=4C1=CC=C(C4)O	236,231	Low (52%)	-0,155	0	
MET3	O=C1C2=C3C(=NNC3=CC=C2)C=4C1=C(C=CC4)O	236,231	High (68%)	0,022	0	
MET4	O=C1C2=C3C(=NNC3=CC=C2)C=4C1=CC=CC4O	236,231	High (70%)	-0,00007801	0	
MET5	OC1C2=C3C(=NNC3=CC=C2)C=4C1=CC=CC4	222,248	High (88%)	-0,333	0	
MET6	O=C1C2=C3C(=NNC3=CC(=C2)O)C=4C1=CC=CC4	236,231	Low (55%)	-0,176	0	
MET7	O=C1C2=C3C(=NNC3=C(C=C2)O)C=4C1=CC=CC4	236,231	Low (70%)	-0,602	0	
AS601245	C1=CC=C2C(=C1)N=C(S2)C(C#N)C3=NC(=NC=C3)NCCC4=CN=CC=C4	372,454	High (88%)	-1,073	0	
MET1	C1=CC=C2C(=C1)N=C(S2)C(C#N)C3=NC(=NC=C3)NCCC4=C[N+](=CC=C4)[O-]	388,453	High (88%)	-1,192	0	
MET2	C1=CC=C2C(=C1)N=C(S2)C(C#N)(C3=NC(=NC=C3)NCCC4=CN=CC=C4)O	388,453	High (73%)	-1,131	0	
MET3	C1=CC=C2C(=C1)N=C(S2)C(C#N)C3=NC(=NC=C3)NCC(C4=CN=CC=C4)O	388,453	Low (45%)	-1,282	0	
MET4	C1(=CC=C2C(=C1)N=C(S2)C(C#N)C3=NC(=NC=C3)NCCC4=CN=CC=C4)O	388,453	Low (52%)	-1,228	0	
MET5	C1=C(C=C2C(=C1)N=C(S2)C(C#N)C3=NC(=NC=C3)NCCC4=CN=CC=C4)O	388,453	Low (55%)	-1,223	0	
MET6	C1=CC=C2C(=C1)N=C(S2)C(C#N)C3=NC(=NC=C3)N	267,314	High (96%)	-0,752	0	
MET7	C(CC1=CN=CC=C1)=O	121,14	High (99%)	-0,34	0	
MET8	C1=CC=C2C(=C1)N=C(S2)C(C#N)C3=[N+](C(=NC=C3)NCCC4=CN=CC=C4)[O-]	388,453	High (91%)	-1,097	0	
MET9	C1=CC=C2C(N=C(S2)C(C#N)C3=NC(=NC=C3)NCCC4=CN=CC=C4)=C1O	388,453	Low (48%)	-1,252	0	
MET10	C1=CC=C2C(=C1)N=C(S2)C(C#N)C3=NC(=NC=C3)NCCC4=CN=CC(=C4)O	388,453	Low (45%)	-1,098	0	

Table B 10 Results of P38 inhibitors.

Name	SMILES	AP_FWeight	BBB_Filter	LogBB	RuleOf5	RuleOf5_Code
SB-239063	COC1=NC=CC(=N1)C2=C(N=CN2C3CCC(CC3)O)C4=CC=C(C=C4)F	368,413	High (81%)	-0,057	0	
MET1	COC1=NC=CC(=N1)C2=C(N=CN2C3CCC(CC3)=O)C4=CC=C(C=C4)F	366,397	High (91%)	-0,074	0	
MET2	OC1=NC=CC(=N1)C2=C(N=CN2C3CCC(CC3)O)C4=CC=C(C=C4)F	354,386	Low (55%)	-0,152	0	
MET3	COC1=NC=CC(=N1)C2=C(N=CN2C3C(CC(CC3)O)O)C4=CC=C(C=C4)F	384,413	Low (42%)	-0,221	0	
MET4	COC1=NC=CC(=N1)C2=C(N=CN2C3CC(C(CC3)O)O)C4=CC=C(C=C4)F	384,413	Low (55%)	-0,328	0	
MET5	COC1=NC=CC(=N1)C2=C(N=CN2C3CCC(CC3)O)C4=CC(=C(C=C4)F)O	384,413	Low (70%)	-0,218	0	
MET6	COC1=NC=CC(=N1)C2=C(N=CN2C3CCC(CC3)O)C4=C(C=C(C=C4)F)O	384,413	Low (45%)	-0,078	0	
MET7	COC1=NC=CC(=[N+]1[O-])C2=C(N=CN2C3CCC(CC3)O)C4=CC=C(C=C4)F	384,413	High (88%)	-0,096	0	
MET8	O=C	30,026	High (99%)	0,125	0	
SB-203580	CS(=O)C1=CC=C(C=C1)C2=NC(=C(N2)C3=CC=NC=C3)C4=CC=C(C=C4)F	377,443	Low (42%)	-0,515	0	
MET1	CS(=O)C1=CC=C(C=C1)C2=NC(=C(N2)C3=CC=[N+](C=C3)[O-])C4=CC=C(C=C4)F	393,442	Low (48%)	-0,771	0	
MET2	CS(=O)C1=CC=C(C=C1)C2=NC(=C(N2)C3=CC=NC=C3)C4=CC(=C(C=C4)F)O	393,442	Low (79%)	-0,527	0	
MET3	CS(=O)C1=CC=C(C=C1)C2=NC(=C(N2)C3=CC=NC=C3)C4=C(C=C(C=C4)F)O	393,442	Low (66%)	-0,472	0	
MET4	CS(C1=CC=C(C=C1)C2=NC(=C(N2)C3=CC=NC=C3)C4=CC=C(C=C4)F)(=O)=O	393,442	Low (67%)	-0,593	0	
MET5	S(=O)(C1=CC=C(C=C1)C2=NC(=C(N2)C3=CC=NC=C3)C4=CC=C(C=C4)F)CO	393,442	Low (70%)	-0,806	0	
BIRB-796	CC1=CC=C(C=C1)N2C(=CC(=N2)C(C)(C)C)NC(=O)NC3=CC=C(C4=CC=CC=C43)OCCN5CCOCC5	527,671	Low (48%)	-0,385	2	Mw; LP
MET1	O=C(NC1=CC(C(C)(C)C)=NN1C2=CC=C(C)C=C2)NC3=C4C=C(C=CC4=C(OCCN5CCOCC5)C=C3)O	543,67	Low (97%)	-0,62	1	Mw
MET2	O=C(NC1=CC(C(C)(C)C)=NN1C2=CC=C(C)C=C2)NC3=C4C=CC(=CC4=C(OCCN5CCOCC5)C=C3)O	543,67	Low (97%)	-0,488	1	Mw
MET3	O=C(NC1=CC(C(C)(C)C)=NN1C2=CC=C(C)C=C2)NC3=C4C=CC=CC4=C(OCCN5CCOCC5)C(=C3)O	543,67	Low (97%)	-0,377	1	Mw
MET4	O=C(NC1=CC(C(C)(C)C)=NN1C2=CC=C(C)C=C2)NC3=C4C=CC=CC4=C(OCCN5CCOCC5)C=C3O	543,67	Low (97%)	-0,568	1	Mw
MET5	O=C(NC1=CC(C(C)(C)C)=NN1C2=CC=C(C)C=C2)NC3=C4C=CC=CC4=C(O)C=C3	414,51	Low (62%)	-0,427	1	LP
MET6	C(CN1CCOCC1)=O	129,16	High (99%)	-0,292	0	
MET7	O=C(NC1=CC(C(C)(C)C)=NN1C2=CC=C(CO)C=C2)NC3=C4C=CC=CC4=C(OCCN5CCOCC5)C=C3	543,67	Low (66%)	-0,633	1	Mw
MET8	O=C(NC1=CC(C(C)(C)C)=NN1C2=CC=C(C)C=C2)NC3=C4C=CC=CC4=C(OCC[N+]5(CCOCC5)[O-])C=C3	543,67	Low (39%)	-0,786	1	Mw
MET9	O=C(NC1=CC(C(C)(C)C)=NN1C2=CC=C(C)C=C2)NC3=C4C=CC=CC4=C(OCC=O)C=C3	456,548	Low (67%)	-0,771	0	
MET10	N1CCOCC1	87,122	High (94%)	0,231	0	
Ginosenoside Rg1	CC(=CCCC(C)(C1CCC2(C1C(CC3C2(CC(C4C3(CCC(C4(C)C)O)O)C)OC5C(C(C(C(O5)CO)O)O)O)C)O)OC6C(C(C(C(O6)CO)O)O)O)C	801,032	Low (97%)	-1,5	3	Hb; Mw; NO
Trolox	CC1=C(C2=C(CCC(O2)(C)C(=O)O)C(=C1O)C)C	250,296	Low (97%)	-1,042	0	
MET1	C(C1=C(C2=C(CCC(O2)(C)C(=O)O)C(=C1O)C)C)O	266,296	Low (97%)	-1,202	0	
MET2	CC1=C(C2=C(CCC(O2)(C)C(=O)O)C(=C1O)C)CO	266,296	Low (97%)	-1,177	0	
MET3	CC1=C(C2=C(CCC(O2)(C)C(=O)O)C(=C1O)CO)C	266,296	Low (97%)	-1,207	0	
MET4	CC1=C(C2=C(CC(C(O2)(C)C(=O)O)O)C(=C1O)C)C	266,296	Low (97%)	-1,119	0	
MET5	CC1=C(C2=C(CCC(O2)(CO)C(=O)O)C(=C1O)C)C	266,296	Low (97%)	-1,216	0	
MET6	CC=1C(=C2C3(CCC(O2)(C)C(=O)O)C(C1O)(C)O3)C	266,296	Low (90%)	-1,007	0	
MET7	CC12C(C3=C(CCC(O3)(C)C(=O)O)C(=C1O)C)(C)O2	266,296	Low (90%)	-1,013	0	
MW181	Nc1nnc(c(-c2ccncc2)c1)-c1c2c(ccc1)cccc2	298,349	High (81%)	-0,304	0	
MET1	NC1=NN=C(C(C2=CC=[N+](C=C2)[O-])=C1)C3=C4C(=CC=C3)C=CC=C4	314,349	High (86%)	-0,482	0	
MET2	NC1=NN=C(C(C2=CC=NC=C2)=C1)C3=C4C(=CC=C3)C=C(C=C4)O	314,349	Low (62%)	-0,446	0	
MET3	NC1=NN=C(C(C2=CC=NC=C2)=C1)C3=C4C(=CC=C3)C=CC(=C4)O	314,349	Low (55%)	-0,458	0	
MET4	NC1=NN=C(C(C2=CC=NC=C2)=C1)C3=C4C(=CC(=C3)O)C=CC=C4	314,349	Low (48%)	-0,401	0	
MET5	NC1=NN=C(C(C2=CC=NC=C2)=C1)C3=C4C(=CC=C3O)C=CC=C4	314,349	Low (59%)	-0,315	0	
MET6	NC1=NN=C(C(C2=CC=NC=C2)=C1)C3=C4C(=CC=C3)C=CC=C4O	314,349	Low (52%)	-0,39	0	
MET7	NC1=NN=C(C(C2=CC=NC=C2)=C1)C3=C4C(=CC=C3)C(=CC=C4)O	314,349	Low (52%)	-0,453	0	
MET8	N(C1=NN=C(C(C2=CC=NC=C2)=C1)C3=C4C(=CC=C3)C=CC=C4)O	314,349	High (70%)	-0,031	0	
MET9	NC1=NN=C(C(C2=CC=NC=C2)=C1)C3=C4C(=CC=C3)C5C(C=C4)O5	314,349	High (94%)	-0,761	0	
MET10	NC1=NN=C(C(C2=CC=NC=C2)=C1)C3=C4C(=CC=C3)C=CC5C4O5	314,349	High (94%)	-0,75	0	

Table B 11 Results of PKA inhibitor.

Name	SMILES	AP_FWeight	BBB_Filter	LogBB	RuleOf5	RuleOf5_Code
H-89	C1=CC2=C(C=CN=C2)C(=C1)S(=O)(=O)NCCNC/C=C/C3=CC=C(C=C3)Br	446,373	High (94%)	-0,136	0	
MET1	C1(=CC2=C(C=CN=C2)C(=C1)S(=O)(=O)NCCNC/C=C/C3=CC=C(C=C3)Br)O	462,373	Low (67%)	-0,319	0	
MET2	C1=CC2=C(C=CN=C2)C(=C1O)S(=O)(=O)NCCNC/C=C/C3=CC=C(C=C3)Br	462,373	High (73%)	-0,274	0	
MET3	C1=CC2=C(C=CN=C2)C(=C1)S(=O)(=O)NCCNCC3C(C4=CC=C(C=C4)Br)O3	462,373	High (84%)	-0,437	0	
MET4	C1=CC2=C(C=CN=C2)C(=C1)S(=O)(=O)NCCNC/C=C/C3=CC(=C(C=C3)Br)O	462,373	High (68%)	-0,401	0	
MET5	C1=CC2=C(C=CN=C2)C(=C1)S(=O)(=O)NCC=O	250,277	High (99%)	-0,63	0	
MET6	NC/C=C/C1=CC=C(C=C1)Br	212,095	High (99%)	0,335	0	
MET7	C1=CC2=C(C=CN=C2)C(=C1)S(=O)(=O)NCCN	251,309	High (96%)	-0,698	0	
MET8	C(/C=C/C1=CC=C(C=C1)Br)=O	211,064	High (99%)	0,371	0	
MET9	C1=CC2=C(C=CN=C2)C(=C1)S(=O)(=O)NCCNC/C=C/C3=C(C=C(C=C3)Br)O	462,373	High (68%)	-0,246	0	
MET10	C=1C=C(C2=C(C=NC=C2)C1O)S(=O)(=O)NCCNCC=CC3=CC=C(C=C3)Br	462,373	Low (66%)	-0,476	0	
MET11	C1=CC2=C(C=CN=C2O)C(=C1)S(=O)(=O)NCCNCC=CC3=CC=C(C=C3)Br	462,373	High (68%)	-0,116	0	
MET12	C(=CC1=CC=C(C=C1)Br)C=O	211,064	High (99%)	0,371	0	

Table B 12 Results of PKB inhibitor.

Name	SMILES	AP_FWeight	BBB_Filter	LogBB	RuleOf5	RuleOf5_Code
Trifluoroacetate hydrate salt	[Li+].C(=O)(C(F)(F)F)[O-].O	137,971	High (94%)	-0,585	0	

Table B 13 Results of PKC inhibitor.

Name	SMILES	AP_FWeight	BBB_Filter	LogBB	RuleOf5	RuleOf5_Code
GF-109203X	CN(C)CCCN1C=C(C2=CC=CC=C21)C3=C(C(=O)NC3=O)C4=CNC5=CC=CC=C54	412,494	Low (74%)	-0,009	0	
MET1	CN(C)CC(CN1C=C(C2=CC=CC=C21)C3=C(C(=O)NC3=O)C4=CNC5=CC=CC=C54)O	428,494	Low (84%)	-0,242	0	
MET2	CN(C)CCCN1C=C(C2=CC=CC=C21)C3=C(C(=O)NC3=O)C4=CNC5=CC(=CC=C54)O	428,494	Low (90%)	-0,137	0	
MET3	CN(C)CCCN1C=C(C2=CC=CC=C21)C3=C(C(=O)NC3=O)C4=CNC5=CC=C(C=C54)O	428,494	Low (84%)	-0,238	0	
MET4	CN(C)CCCN1C=C(C2=CC(=CC=C21)O)C3=C(C(=O)NC3=O)C4=CNC5=CC=CC=C54	428,494	Low (84%)	-0,195	0	
MET5	CN(C)CCCN1C=C(C2=CC=C(C=C21)O)C3=C(C(=O)NC3=O)C4=CNC5=CC=CC=C54	428,494	Low (84%)	-0,157	0	
MET6	C[N+](C)(CCCN1C=C(C2=CC=CC=C21)C3=C(C(=O)NC3=O)C4=CNC5=CC=CC=C54)[O-]	428,494	Low (62%)	-0,569	0	
MET7	CN(C)CCCN1C=C(C2=CC=CC=C21)C34C(C(=O)NC3=O)(C5=CNC6=CC=CC=C65)O4	428,494	Low (62%)	-0,451	0	
MET8	CN(C)CCCN1C=C(C2=CC=CC=C21)C3=C(C(=O)NC3=O)C4=CNC5=C(C=CC=C54)O	428,494	Low (84%)	-0,226	0	
MET9	CN(C)CCCN1C=C(C2=CC=CC(=C21)O)C3=C(C(=O)NC3=O)C4=CNC5=CC=CC=C54	428,494	Low (84%)	-0,234	0	
MET10	CN(C)CCCN1C=C(C2=CC=CC=C21)C3=C(C(=O)NC3=O)C4=CNC5=CC=CC(=C54)O	428,494	Low (84%)	-0,158	0	

Table B 14 Results of TTBK1 inhibitor.

Name	SMILES	AP_FWeight	BBB_Filter	LogBB	RuleOf5	RuleOf5_Code
TTBK1-IN-2	C1=CC(=CC=C1NC2=NC=NC3=C2C=CN3)OC4=CC=C(C=C4)Cl	336,783	Low (45%)	-0,171	0	
MET1	C1=CC(=CC=C1NC2=NC=NC3=C2C=CN3)OC4=CC(=C(C=C4)Cl)O	352,782	Low (79%)	-0,509	0	
MET2	C1=CC(=CC=C1NC2=NC=NC3=C2C=CN3)OC4=C(C=C(C=C4)Cl)O	352,782	Low (84%)	-0,253	0	
MET3	C1=CC(=CC=C1NC2=NC=NC3=C2C=C[NH+]3[O-])OC4=CC=C(C=C4)Cl	352,782	High (73%)	-0,858	0	
MET4	C1=CC(=CC=C1NC2=NC=[N+](C3=C2C=CN3)[O-])OC4=CC=C(C=C4)Cl	352,782	Low (39%)	-0,471	0	
MET5	C1=CC(=CC=C1[NH+](C2=NC=NC3=C2C=CN3)[O-])OC4=CC=C(C=C4)Cl	352,782	Low (48%)	-0,457	0	

Bibliography

Bao, C., Bajrami, B., Marcotte, D. J., Chodaparambil, J. V., Kerns, H. M., Henderson, J., Wei, R., Gao, B., & Dillon, G. M. (2021). Mechanisms of Regulation and Diverse Activities of Tau-Tubulin Kinase (TTBK) Isoforms. *Cellular and Molecular Neurobiology*, *41*(4), 669–685. https://doi.org/10.1007/s10571-020-00875-6

Calabrò, M., Rinaldi, C., Santoro, G., & Crisafulli, C. (2021). The biological pathways of Alzheimer disease: a review. *AIMS Neuroscience*, *8*(1), 86–132. https://doi.org/10.3934/Neuroscience.2021005

Carpenter, T. S., Kirshner, D. A., Lau, E. Y., Wong, S. E., Nilmeier, J. P., & Lightstone, F. C. (2014). A Method to Predict Blood-Brain Barrier Permeability of Drug-Like Compounds Using Molecular Dynamics Simulations. *Biophysical Journal*, *107*(3), 630–641. https://doi.org/10.1016/j.bpj.2014.06.024

Cehlar, O., Bagarova, O., Hornakova, L., & Skrabana, R. (2021). The structure of the unstructured: mosaic of tau protein linear motobtained by high-resolution techniques and molecular simulation. *General Physiology and Biophysics*, *40*(6), 479–493. https://doi.org/10.4149/gpb_2021031

Demuro, S., Sauvey, C., Tripathi, S. K., Di Martino, R. M. C., Shi, D., Ortega, J. A., Russo, D., Balboni, B., Giabbai, B., Storici, P., Girotto, S., Abagyan, R., & Cavalli, A. (2022). ARN25068, a versatile starting point towards triple GSK-3β/FYN/DYRK1A inhibitors to tackle tau-related neurological disorders. *European Journal of Medicinal Chemistry*, *229*. https://doi.org/10.1016/j.ejmech.2021.114054

Djoumbou-Feunang, Y., Fiamoncini, J., Gil-de-la-Fuente, A., Greiner, R., Manach, C., & Wishart, D. S. (2019). BioTransformer: A comprehensive computational tool for small molecule metabolism prediction and metabolite identification. *Journal of Cheminformatics*, *11*(1). https://doi.org/10.1186/s13321-018-0324-5

Giovinazzo, D., Bursac, B., Sbodio, J. I., Nalluru, S., Vignane, T., Snowman, A. M., Albacarys, L. M., Sedlak, T. W., Torregrossa, R., Whiteman, M., Filipovic, M. R., Snyder, S. H., & Paul, B. D. (n.d.). *Hydrogen sulfide is neuroprotective in Alzheimer's disease by sulfhydrating GSK3β and inhibiting Tau hyperphosphorylation*. https://doi.org/10.1073/pnas.2017225118/-/DCSupplemental

Kolarova, M., García-Sierra, F., Bartos, A., Ricny, J., & Ripova, D. (2012). Structure and pathology of tau protein in Alzheimer disease. In *International Journal of Alzheimer's Disease*. https://doi.org/10.1155/2012/731526

Limorenko, G., & Lashuel, H. A. (2022). Revisiting the grammar of Tau aggregation and pathology formation: How new insights from brain pathology are shaping how we study and target Tauopathies. In *Chemical Society Reviews* (Vol. 51, Issue 2, pp. 513–565). Royal Society of Chemistry. https://doi.org/10.1039/d1cs00127b

Lund, H., Cowburn, R. F., Gustafsson, E., Strömberg, K., Svensson, A., Dahllund, L., Malinowsky, D., & Sunnemark, D. (2013). Tau-tubulin kinase 1 expression, phosphorylation and co-

localization with phospho-ser422 tau in the Alzheimer's disease brain. *Brain Pathology*, *23*(4), 378–389. https://doi.org/10.1111/bpa.12001

Marien, J., Prévost, C., & Sacquin-Mora, S. (n.d.). *It takes tau to tango: Investigating the fuzzy interaction between the R2-repeat domain and tubulin C-terminal tails*. https://doi.org/10.1101/2023.02.09.527845

Martin, L., Latypova, X., Wilson, C. M., Magnaudeix, A., Perrin, M. L., Yardin, C., & Terro, F. (2013). Tau protein kinases: Involvement in Alzheimer's disease. In *Ageing Research Reviews* (Vol. 12, Issue 1, pp. 289–309). https://doi.org/10.1016/j.arr.2012.06.003

Muehlbacher, M., Spitzer, G. M., Liedl, K. R., & Kornhuber, J. (2011). Qualitative prediction of blood-brain barrier permeability on a large and refined dataset. *Journal of Computer-Aided Molecular Design*, *25*(12), 1095–1106. https://doi.org/10.1007/s10822-011-9478-1

Muralidar, S., Ambi, S. V., Sekaran, S., Thirumalai, D., & Palaniappan, B. (2020). Role of tau protein in Alzheimer's disease: The prime pathological player. In *International Journal of Biological Macromolecules* (Vol. 163, pp. 1599–1617). Elsevier B.V. https://doi.org/10.1016/j.ijbiomac.2020.07.327

Ricci, M., Cimini, A., Camedda, R., Chiaravalloti, A., & Schillaci, O. (2021). Tau biomarkers in dementia: Positron emission tomography radiopharmaceuticals in Tauopathy assessment and future perspective. In *International Journal of Molecular Sciences* (Vol. 22, Issue 23). MDPI. https://doi.org/10.3390/ijms222313002

Rogowski, K., Hached, K., Crozet, C., & van der Laan, S. (2021). Tubulin modifying enzymes as target for the treatment oftau-related diseases. In *Pharmacology and Therapeutics* (Vol. 218). Elsevier Inc. https://doi.org/10.1016/j.pharmthera.2020.107681

Song, L., Wells, E. A., & Robinson, A. S. (2021). Critical molecular and cellular contributors to tau pathology. In *Biomedicines* (Vol. 9, Issue 2, pp. 1–28). MDPI AG. https://doi.org/10.3390/biomedicines9020190

Stefanoska, K., Gajwani, M., Tan, A. R. P., Ahel, H. I., Asih, P. R., Volkerling, A., Poljak, A., & Ittner, A. (2022). Alzheimer's disease: Ablating single master site abolishes tau hyperphosphorylation. In *Sci. Adv* (Vol. 8). https://www.science.org

Tan, B., Aslan-Gülpınar, E., Dursun, N., & Süer, C. (2021). N-methyl-d-aspartate receptor blockade reduces plasticity-related tau expression and phosphorylation of tau at Ser416 residue but not Thr231 residue. *Experimental Brain Research*, *239*(5), 1627–1637. https://doi.org/10.1007/s00221-021-06090-z

Vilar, S., Chakrabarti, M., & Costanzi, S. (2010). Prediction of passive blood-brain partitioning: Straightforward and effective classification models based on in silico derived physicochemical descriptors. *Journal of Molecular Graphics and Modelling*, *28*(8), 899–903. https://doi.org/10.1016/j.jmgm.2010.03.010

Wegmann, S., Biernat, J., & Mandelkow, E. (2021). A current view on Tau protein phosphorylation in Alzheimer's disease. In *Current Opinion in Neurobiology* (Vol. 69, pp. 131–138). Elsevier Ltd. https://doi.org/10.1016/j.conb.2021.03.003

Xia, Y., Prokop, S., & Giasson, B. I. (2021). "Don't Phos Over Tau": recent developments in clinical biomarkers and therapies targeting tau phosphorylation in Alzheimer's disease and

other tauopathies. In *Molecular Neurodegeneration* (Vol. 16, Issue 1). BioMed Central Ltd. https://doi.org/10.1186/s13024-021-00460-5

Yadikar, H., Torres, I., Aiello, G., Kurup, M., Yang, Z., Lin, F., Kobeissy, F., Yost, R., & Wang, K. K. (2020). Screening of tau protein kinase inhibitors in a tauopathy-relevant cell-based model of tau hyperphosphorylation and oligomerization. *PLoS ONE*, *15*(7 July). https://doi.org/10.1371/journal.pone.0224952

Zhang, Y., Wu, K. M., Yang, L., Dong, Q., & Yu, J. T. (2022). Tauopathies: new perspectives and challenges. In *Molecular Neurodegeneration* (Vol. 17, Issue 1). BioMed Central Ltd. https://doi.org/10.1186/s13024-022-00533-z